The Pennsylvania State University

The Graduate School

Department of Energy and Mineral Engineering

EVALUATION OF PERFORMANCE OF CYCLIC STEAM INJECTION IN NATURALLY FRACTURED RESERVOIRS – AN ARTIFICIAL NEURAL NETWORK APPLICATION

A Thesis in

Energy and Mineral Engineering

by

Santosh Phani Bhushan Chintalapati

Submitted in Partial Fulfillment
of the Requirements
for the Degree of

Master of Science

December 2011

The thesis of Santosh Phani Bhushan Chintalapati was reviewed and approved* by the following:

Turgay Ertekin
Professor of Petroleum & Natural Gas Engineering
George E. Trimble Chair in Earth and Mineral Sciences
Thesis Advisor

Zuleima T. Karpyn
Associate Professor of Petroleum and Natural Gas Engineering

John Yilin Wang
Assistant Professor of Petroleum and Natural Gas Engineering

R. Larry Grayson
Professor of Energy and Mineral Engineering
Graduate Program Officer of Energy and Mineral Engineering

*Signatures are on file in the Graduate School

ABSTRACT

With increasing demand on oil, it is important to improve the recovery factor of oil reservoirs. Naturally fractured reservoirs constitute a major portion of world's hydrocarbon reserves and are good targets for enhanced oil recovery operation (EOR). Cyclic steam injection is an attractive EOR process for recovering oil from naturally fractured reservoirs. Predicting the performance of different naturally fractured oil reservoirs undergoing cyclic steam injection under varying design parameters is a difficult task. The simulation time and effort required to evaluate such performance for a large number of scenarios is likely to be very high.

Artificial neural networks (ANNs) are mathematical tools designed to map an input domain into an output domain. They are based on observations made in the study of biological systems. Their function is similar to that of a mathematical function. In this work neural network based proxy models are developed for comparative evaluation of cyclic steam injection in various naturally fractured oil reservoirs with constant injection, soaking and production periods. Five different oils with viscosities ranging from 5800 cp to as low as 1 cp at room temperature are used as reservoir fluids in this study and a proxy model is developed for each oil. The proxy models developed are found to be capable of successfully mimicking the reservoir simulation model for above mentioned process within a certain range of input parameters in considerably small computational times.

TABLE OF CONTENTS

LIST OF FIGURES

LIST OF TABLES

ACKNOWLEDGEMENTS

At the outset, I would like to thank Dr. Turgay Ertekin for being a wonderful advisor, mentor and guide during the course of my master's studies at Pennsylvania State University. I also thank him for introducing me to the amazing world of ANN. I would like to thank Dr. Zuleima Karpyn and Dr. John Yilin Wang for accepting to serve as committee members.

I would like to thank doctoral students Yogesh Bansal and Seyhan Emre Gorucu and master's student Luoyi Hua for their valuable suggestions and help during the times of need. I would also like to thank the Department of Energy and Mineral Engineering for providing me with scholarship during the course of my study.

I would like to express gratitude to my friends Phani Kiran Pamidimukkala, Sarath Pavan Ketineni and Sridhar Ranganathan for taking care of me and for providing words of encouragement when I fell ill.

Finally, I would like to thank my mother Seetha Chintalapati and my father Thandava Krishna Chintalapati for their unconditional love and emotional support and for providing me with the best throughout my education.

Chapter 1

Introduction

With increasing demand of consumption of oil, it is important to improve the recovery factor of reservoirs. Recovery factor is the ratio of oil that can be produced with the existing technology to the original oil in place (OOIP). When oil wells are produced under natural oil recovery mechanisms and shut-in after abandonment rate is reached, a major portion of the original oil in place is left unrecovered. The average oil recovery even after performing secondary oil recovery techniques like water drive or gas injection drive is only 35%. Recoveries can be as low as 5% or less for highly viscous oils [Boberg, 1988]. Hence, it is important to implement enhanced oil recovery techniques in depleted and heavy oil reservoirs. Enhanced oil recovery (EOR) is a method of tertiary recovery of oil by injection of fluids not normally present in the reservoir. There are many types of EOR processes, the important ones being: chemical, thermal and miscible recovery methods.

Naturally fractured reservoirs constitute a large portion of hydrocarbon reserves of the world. They contain up to 30% of the world supply of oil and thus represent a significant target for EOR [Reis, 1992]. Naturally fractured reservoirs contain fractures and matrix blocks. The fracture network has higher permeability than matrix and provides flow paths for the oil to flow. It has high permeability but low porosity compared to matrix. The matrix on the other hand acts as a sink or source of oil in the reservoir. It has low permeability and high storativity.

"Injection of high temperature fluids into fractured reservoirs to recover matrix oil has been considered as an effective EOR application and numerous studies have been published providing enough evidence to support this" [Babadagli, 2002]. Steam Injection is an attractive process for recovering oil from fractured reservoirs. It has been shown that more oil can be recovered from heated blocks than unheated blocks [Reis, 1992]. Cyclic steam injection is more attractive than steam flooding in naturally fractured reservoirs because condensed steam breaks through early through the fracture network in a steam drive process. On the other hand, as cyclic steam injection is a single-well process, such problems do not occur. Though initially the water production rate is high, the oil rate peaks and the well can be produced till the abandonment rate is reached. Once a cycle is completed, the process can be repeated till sufficient oil is produced from the reservoir. The payback period is also shorter compared to steam flooding projects. For large reservoirs, a network of such wells can be created to produce oil.

Evaluating the performance of different oil reservoirs undergoing cyclic steam injection under varying design parameters is a difficult task. Also the simulation time required to evaluate the performance of such reservoirs is extensive. In this work, proxy models are developed to evaluate the performance of different naturally fractured oil reservoirs undergoing cyclic steam injection with constant injection, soaking and production periods. Five different oils with viscosities ranging from 5800 cp to as low as 1cp at room temperature are used in this study. Five proxy models are developed, each corresponding to the respective oil.

The proxy models are developed using artificial neural network (ANN) toolbox of MATLAB® [1]. The CMG® [2] STARS™ [3] black oil simulator is used to generate data sets for training the neural network. MATLAB is also used to generate batch files to run CMG STARS. In this work CMG STARS will now be referred as commercial simulator.

The thesis is divided into 7 Chapters and 3 Appendices. Chapter 2 is a survey of literature on naturally fractured reservoirs, cyclic steam injection and artificial neural networks. Chapter 3 gives the statement of the problem. Chapter 4 describes the reservoir model used in this study along with description of how data sets were generated for training the artificial neural networks. Chapter 5 is a summary of results obtained in this study and it also contains discussion of results. Chapter 6 gives the conclusion of this work and recommendations for future work. Chapter 7 contains references used in this study. Appendix A describes the implementation of graphical user interface (GUI) developed in this study. Appendix B contains MATLAB code used to train Artificial Neural Networks. Finally, Appendix C contains MATLAB code used to create batch files.

---

[1]MATLAB: MATrix LABoratory, a numerical computing environment developed by The MathWorks, Inc.,
[2]CMG: Computer Modeling Group
[3]STARS: Steam, Thermal, and Advanced Processes Reservoir Simulator

Chapter 2

Literature Review

This chapter gives a brief description of Naturally Fractured Reservoirs, Cyclic Steam Injection and Artificial Neural Networks.

2.1 Naturally Fractured Reservoirs

Naturally fractured reservoirs contain a large portion of world's oil reserves. It is estimated that they contain 30% of the world supply of oil [Reis, 1992]. It is also estimated that naturally fractured carbonate reservoirs hold well over 100 billion barrels of heavy oil [Shahin, 2006]. Unlike non fractured reservoirs the fractures of naturally fractured reservoirs can provide flow paths having permeabilities higher than that of reservoir matrix. The fracture network has porosity that is an order of magnitude lower than the matrix. Thus fractures control fluid flow whereas matrix acts as sink/source for oil in the reservoir. Several papers have been published to quantify fluid and heat flow in naturally fractured reservoirs. In these papers different models are proposed. All these models divide the reservoir into matrix and fracture continua with a superimposed computational grid. There may be several fracture and matrix elements lumped together in each grid block as shown in Figure **2-1** [STARS user guide, 2008].

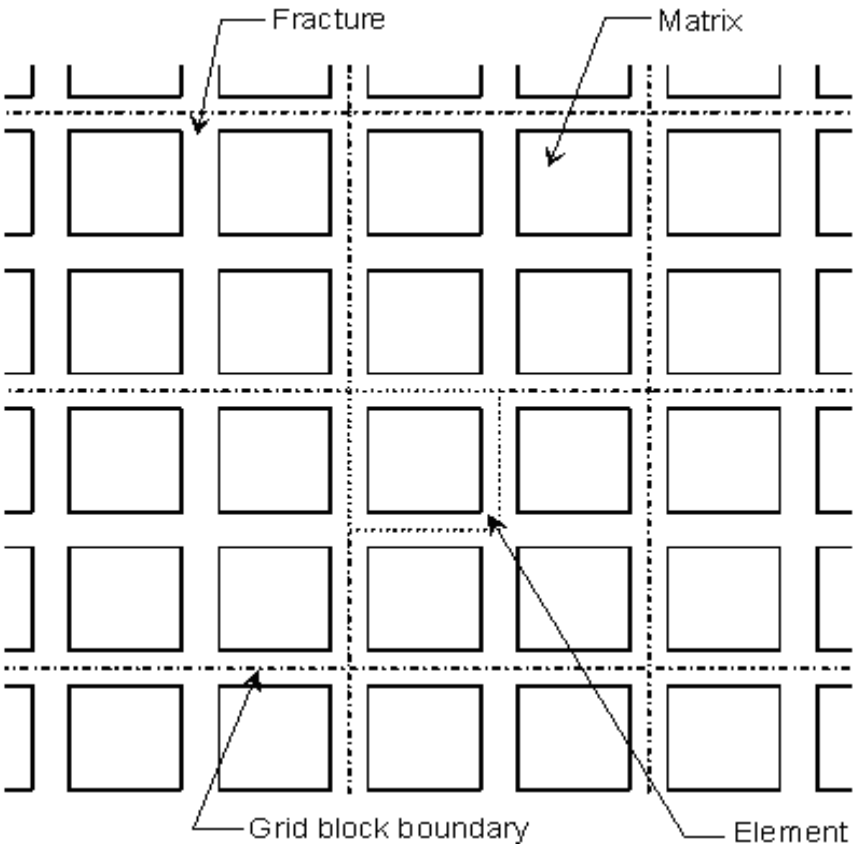

Figure **2-1**: Representation of Fractured Reservoir [STARS user guide, 2008].

The fractured porous media models developed in various papers can be broadly classified into two groups: dual porosity and dual permeability. Dual porosity models are based on the assumption that the fracture network is the primary continuum for fluid flow. The matrix is considered to be a sink or source to the fracture. The models are further sub-divided into standard dual-porosity model, multiple interacting continua model and vertical refinement model. In the work presented here standard dual porosity model is used.

2.1.1 Standard Dual Porosity Model

This is the simplest model to describe the behavior of naturally fractured reservoirs. In this model matrix blocks are isolated and they do not directly communicate with each other. They are only connected through fractures Figure **2-2**. Thus, either fluid or heat can be transferred only to adjoining fracture. As the fracture acts as primary continuum for fluid flow the wells are assumed to be connected to fracture only. Within a grid block fracture and matrix are assumed to be at the same depth [STARS user guide, 2008].

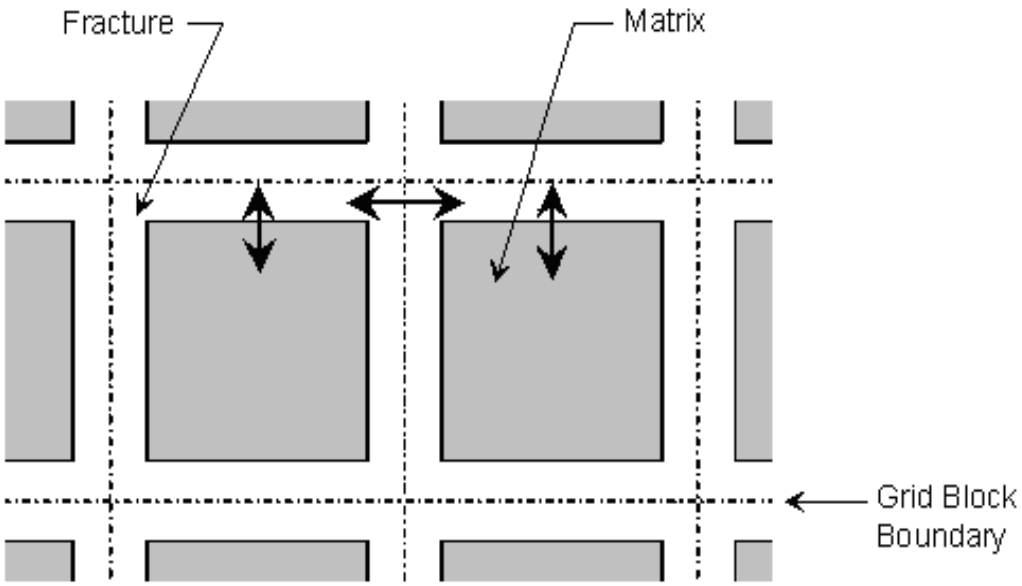

Figure **2-2**: Standard Dual Porosity Model [STARS user guide, 2008].

2.2 Cyclic Steam Injection

Cyclic steam injection is a thermal enhanced oil recovery method in which a well is injected with steam and subsequently put on production after a brief shut-in period. It basically involves three stages (see Figure **2-3)**. During the first stage called injection period, steam is injected into the reservoir for a certain number of days usually 3-4 weeks. In the second stage called soaking period, the well is shut-in allowing the steam to condense and lose its heat to reservoir rock and fluids for few days. The soaking period allows thermal gradients to equalize, but it should not be long enough for the pressure to escape [Lake, 1989]. Finally, during the third stage called production period the well is put on production till the economic rate limit is reached. In this period lot of water is produced initially, but the water cut quickly declines and oil production rate will peak usually higher than the original value [Boberg, 1988]. Cyclic steam injection is different from steam drive in that it is a single well process and the same well acts as both injector and producer.

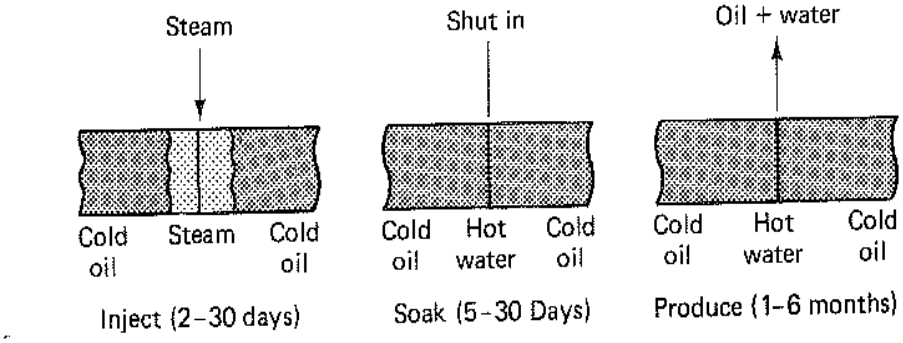

Figure **2-3**: Cyclic Steam Injection [Lake, 1989].

The problem of cyclic steam injection simulation in a single porosity system is discussed by [Aziz et al, 1987]. The paper compares the results of cyclic steam injection problem submitted by six different participants using their simulators. All the participants use the same reservoir fluid and same reservoir properties to study cyclic steam injection in a single porosity reservoir.

A simulator for modeling thermal recovery processes in naturally fractured reservoirs is presented by [Chen et al, 1987]. The rock matrix block is subdivided into a two dimensional (r-z) grid system to study the effects of gravity. According to [Chen et al, 1987], both conductive and convective rate of heat transfer between matrix and fracture plays an important role in oil recovery from naturally fractured reservoirs. Also, the effect of capillary pressure is small and is ignored.

A simulator for studying the effect of various parameters on the performance of cyclic steam injection operations in heavy oil naturally fractured reservoirs is presented by [Briggs, 1989]. The importance of fracture system in conducting heat to rock matrix is highlighted. The paper also shows the importance of steam injection rate and bottom hole pressure in attaining the best operating conditions.

Oil expulsion mechanisms during steam injection in naturally fractured reservoirs are presented by [Reis, 1992]. Thermal expansion of oil and generation of gases from chemical reactions at high temperature are considered to be the most important recovery mechanisms. With these mechanisms it has been found that oil is expelled from blocks as wide as 10 feet within a year. It has also been shown that steam injection is attractive in both light and heavy oil naturally fractured reservoirs. Pilot studies also have been performed to study cyclic steam injection [Li et al, 2010].

2.3 Artificial Neural Network

Artificial neural network (ANN) is a mathematical tool that has been developed based on inspiration from biological neural networks. The objective of a neural network is to map an input into a desired output [Priddy et al, 2005] and it is characterized by [Fausett, 1994]:

1. Its architecture – a pattern of connections between the neurons
2. Its method of assigning the weights for the connections
3. Its activation function or transfer function.

A neural net consists of a large number of small computing engines/elements called neurons. The neuron takes in inputs, processes them, and transmits an output. Each neuron of one layer is connected to neurons of other layers through links, each associated with a weight. Figure **2-4** shows the architecture of a typical artificial neural network.

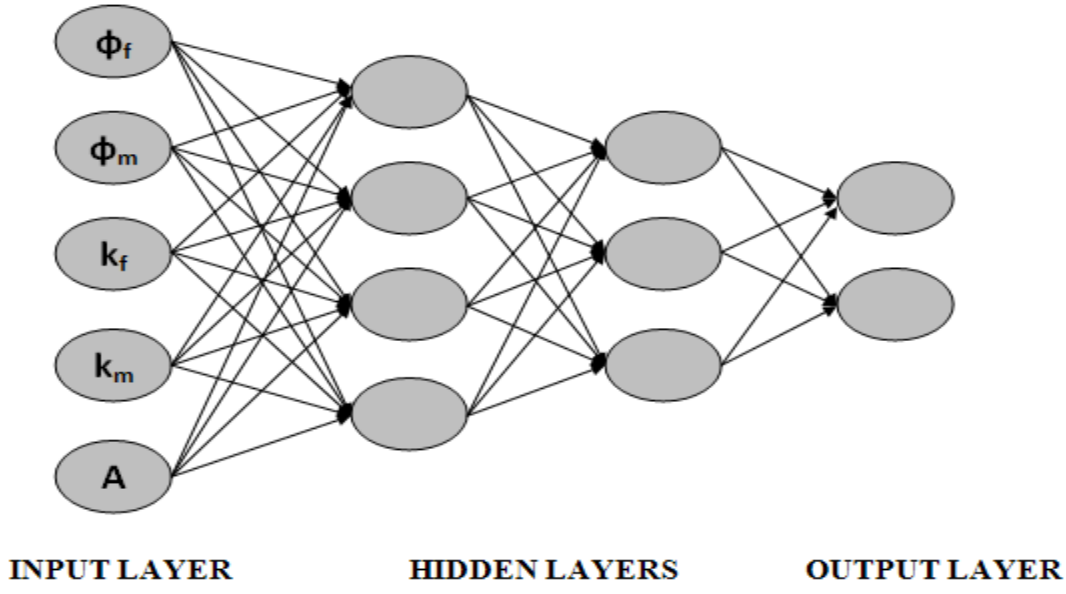

Figure **2-4**: Typical Architecture of an artificial neural network.

Neural networks have a plethora of applications. They are used for speech generation, speech recognition, autonomous vehicle navigation, handwritten digit recognition, image compression etc., [Bose and Liang, 1996]. There have been many recent advances in the application of neural networks in petroleum industry. They have been used for oil spill detection [Browne, 1997], for predicting relative permeability [Guler et al, 2003], for determining optimum production protocols for exploitation of gas/condensate reservoirs [Ayala et al, 2007], for predicting the performance of coalbed methane reservoirs [Srinivasan and Ertekin, 2008], for optimized design of gas cyclic pressure pulsing [Artun et al, 2008], for field development [Doraisamy et al, 2008].

2.3.1 Normalizing data

Normalizing data is one of the most common tools used by ANN developers. In order to minimize bias towards certain input parameters, the developer would want to confine all of them into a same range (usually 0-1 or -1-1) of values. Normalizing data can also speed up training time. It is particularly useful when the inputs are on widely different scales [Priddy et al, 2005]. There are many types of normalizing data. In this work the min-max normalization method has been used. The min-max normalization is done by rescaling the input features or outputs from original values to a new range of values. Mostly the features are rescaled to lie between 0 to1 or between -1 to 1. The rescaling is done using a linear interpolation formula as shown in Equation (2.1) [Priddy et al, 2005]:

$$x_i^{'} = (\max_{target} - \min_{target}) \times \left[\frac{(x_i - \min_{value})}{(\max_{value} - \min_{value})} \right] + \min_{target} \quad (2.1)$$

where,

$x_i^{'}$ = normalized input/output

$\max_{target}$ = maximum normalized value (1 here)

$\min_{target}$ = minimum normalized value (-1 here)

x_i = input/output before normalizing

$\max_{value}$ = maximum input/output value

$\min_{value}$ = minimum input/output value

Min-Max method preserves exactly all relationships in the data without introducing any bias.

2.3.2 Feed Forward Neural Network

A feed forward network typically looks like the one shown in Figure **2-5**.

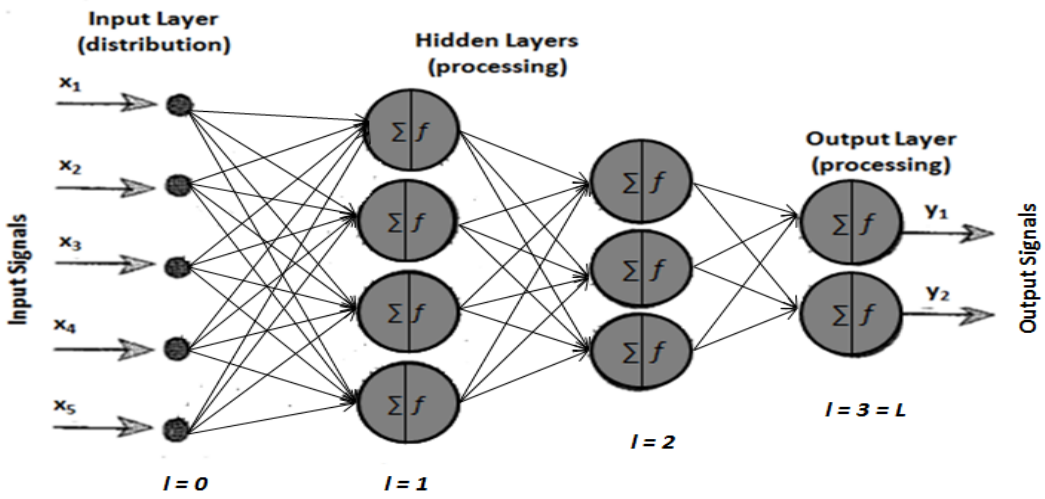

Figure **2-5**: Multilayer Feed Forward Neural Network [Priddy et al, 2005].

The input layer of the network does no processing and is also called the zeroth layer. The outputs of this layer are described by Equation (2.2):

$$o_i^0 = x_i \tag{2.2}$$

where,

$i = 1\ldots..N^0$

N^0 = number of neurons in the input or zeroth layer

x_i = input vector

The input to a neuron in first hidden layer is the summation of product of weights (w_i) between input layer and hidden layer and the input vector. The sum known as net stimulus is denoted by *net*. A bias term θ or w_0 is added to offset the input. The bias can also be viewed as a weight coming from a unitary valued input [Priddy et al, 2005]. This is given by Equation (2.3):

$$net = \sum_{i=1}^{N^0} w_i o_i^0 + w_0 \tag{2.3}$$

The net stimulus is transformed by the neuron's activation or transfer function *f(net)*. The transfer function is used to map non linearity into the network. It also stabilizes the net stimulus. There are many types of transfer functions. They are discussed by [Kulga, 2010]. In this work linear transfer function (*purelin*) and tangent sigmoid (*tansig*) are used. The final output of the neuron is given by:

$$output = f(net) = f(\sum_{i=1}^{N^0} w_i o_i^0 + w_0). \tag{2.4}$$

This is shown in Figure **2-6**.

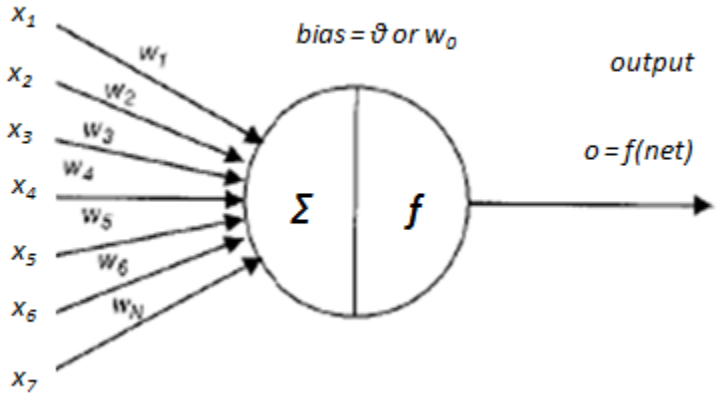

Figure **2-6**: The working process of a neuron [Priddy et al, 2005].

When we extend this concept to multilayer networks, the output of j^{th} neuron in l^{th} layer is given by Equation (2.5):

$$o_j^l = f_j^l(net_j^l) = f_j^l(\sum_{i=1}^{N^{l-1}} w_{ji}^l o_i^{l-1} + w_{j0}^l). \tag{2.5}$$

The outputs of the final layer or L^{th} layer are given by Equation (2.6):

$$y_j = o_j^L \tag{2.6}$$

The whole process described above can be visualized in Figures **2-5** & **2-6**.

Chapter 3

Problem Statement

The objective of this research is to develop an expert system for evaluating the performance of different naturally fractured reservoirs undergoing cyclic steam injection with constant injection, soaking and production periods. The reservoir properties evaluated in this study are: matrix permeability (k_m), fracture permeability (k_f), matrix porosity (ϕ_m), fracture porosity (ϕ_f), fracture spacing (S_f), thickness of reservoir (h), initial temperature (T_i), initial oil saturation (S_{oi}) and initial pressure (P_i). The design characteristics pertaining to cyclic steam injection are: drainage area (A), steam temperature (T_s), steam quality (Q_s), steam injection rate (q_{inj}) and bottom hole pressure (P_{sf}). The output parameters evaluated in this study are cumulative production of each cycle (Q_i). The number of cycles is fixed to four. This work is divided into the following tasks:

1. Devise a reservoir model in commercial simulation software (CMG) for steam injection process in a single porosity system.
2. Extend the model for a dual porosity system.
3. Extend the dual porosity model for a large number of scenarios by varying the reservoir properties and design characteristics within meaningful ranges.
4. Extract results after simulating the model with large number of scenarios in the commercial simulator.
5. Create data sets containing inputs and outputs.
6. Train an artificial neural network for the generated data sets.
7. Repeat the above six steps for each specific oil.

Five different oils are used in this study. The oils have viscosities ranging from 5800 cp to 1 cp at room temperature. An expert system is developed for each oil. Finally a GUI is designed. The GUI integrates all the five expert systems and mimics the commercial simulator in predicting the performance of different naturally fractured reservoirs undergoing cyclic steam injection with constant injection, soaking and production periods.

The initial objective of this research was to develop an expert system for single oil using only five of the reservoir properties and three of design characteristics mentioned above. After successfully developing an expert system for single oil, the complexity of the system was increased by including additional reservoir properties like thickness of reservoir, initial temperature and initial oil saturation. The number of oils/reservoir fluids was increased to five based on their viscosity. An expert system was developed for each oil. The viscosity of the oil could not be included in the list of reservoir properties because by varying the viscosity randomly with other reservoir properties there was a possibility of generating large number of incorrect reservoir models. Finally, the system was further complicated by including initial pressure in reservoir properties and steam injection rate and bottom hole pressure in design characteristics making the total number of inputs to 14.

Chapter 4

Reservoir Model and Generation of Data Sets

4.1 Reservoir Model

The reservoir model was built based on following assumptions:

1. Two dimensional cylindrical (r-z) grid with 91 blocks in the radial (r) direction and 4 blocks in the vertical (z) direction. The blocks in the radial direction are logarithmically spaced.
2. Single well reservoir, well being placed at the center. The well acts as injector and producer depending on the time of operation.
3. Constant well bore radius of 0.3 ft.
4. Dual porosity system.
5. Thermal conductivity of reservoir, overburden and underburden is 24 Btu/(ft-D-^{0}F).
6. Heat capacity of reservoir, overburden and underburden is 35 Btu/ (ft^3 of rock-^{0}F).
7. Capillary pressures are equal to zero throughout.
8. Skin factor is zero throughout. All layers are open to flow during injection and production.
9. Injection with specified injection rate (q_{inj}).
10. Production with specified bottom hole pressure (P_{sf}).
11. Constant injection period of 30 days/cycle, soaking period of 10 days/cycle and production period of 550 days/cycle. Total number of cycles is fixed at 4.

Many of these assumptions were taken from literature [Aziz et al, 1987]. Figure **4-1** is a snapshot of the reservoir used in this work.

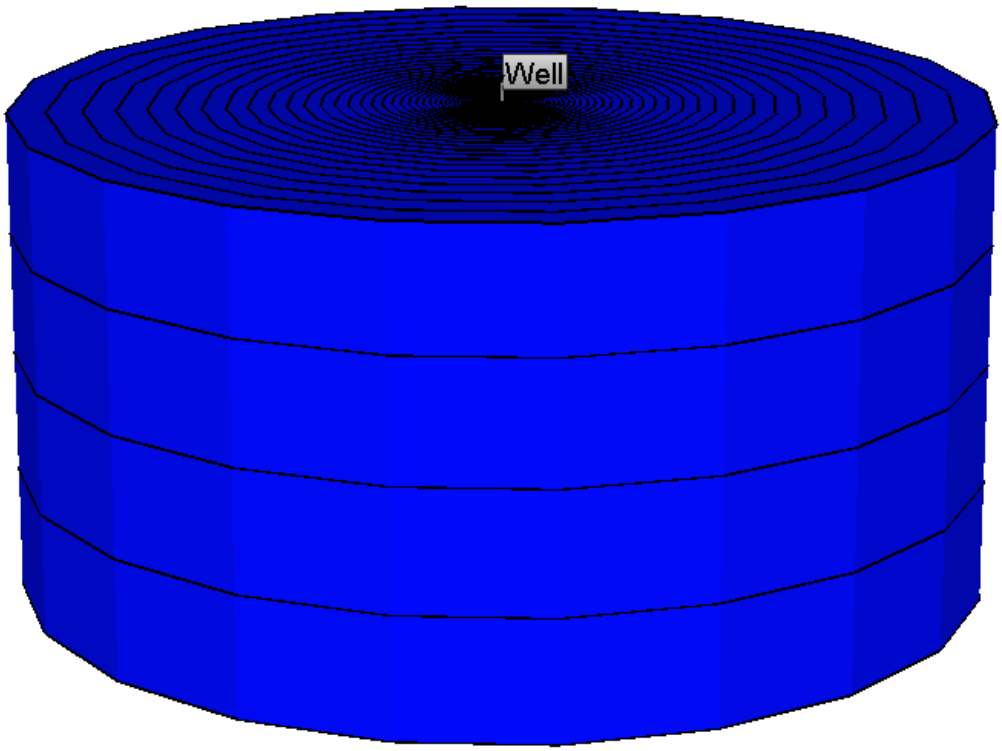

Figure **4-1**: Two dimensional cylindrical grid system with a well at center.

Gridblock sizes are relatively arbitrary for rectangular grid systems. Usually cylindrical grid system follows logarithmic spacing. The pressure points are spaced away from the wellbore in the following way [Ertekin et al, 2001]:

$$\alpha_{\lg} = \left(\frac{r_e}{r_w} \right)^{1/n_r} \tag{4.1}$$

$$r_1 = \left(\frac{r_w \log_e (\alpha_{\lg})}{1 - (1/\alpha_{\lg})} \right) \tag{4.2}$$

and

$$r_{i+1} = \alpha_{\lg} r_i \tag{4.3}$$

where,

r_e = external radius.

r_w = radius of wellbore.

r_{i+1} = radius of i+1th block.

r_i = radius of ith block.

n_r = number of blocks.

The number of blocks in the radial direction is fixed to 91 after performing sensitive analysis on the radius of outermost block r_{nr}. Figure **4-2** is a schematic of logarithmically spaced grid.

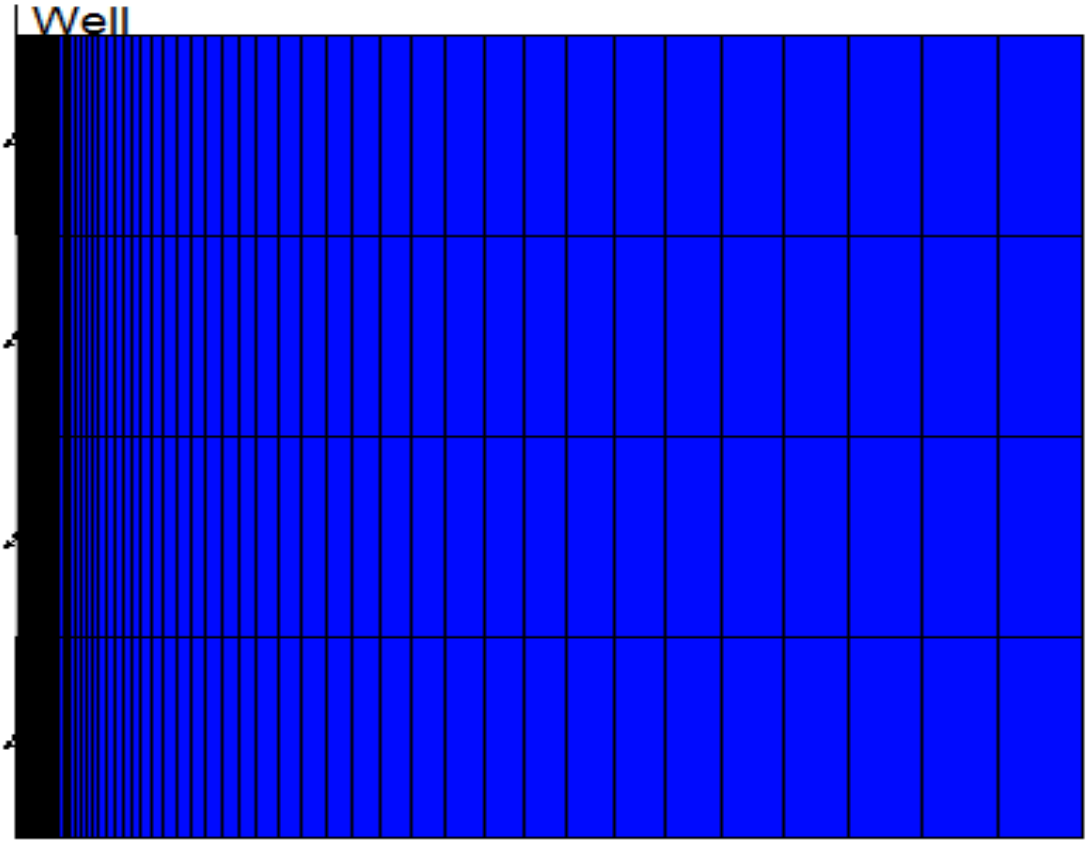

Figure **4-2**: Logarithmic spacing of grids in the radial direction.

4.1.1 Reservoir Fluid

Five different oils are used as reservoir fluids in this study. Oil 1 is heavy oil, oil 2 and oil 5 are black oils, and oil 3 and oil 4 are volatile oils. The data for oil 1 and oil 2 are taken from literature [Aziz et al, 1987; Michael, 1982]. The data for rest of the oils are taken from the template files of the commercial simulator. The properties of these oils are summarized in Table **4-1**.

OIL	TYPE	M.W(LB/LBMOLE)	DENSITY (LB/FT^3)	API^0
Oil 1	Heavy Oil	600	60.67	14
Oil 2	Black Oil	450	56.7	24.2
Oil 3	Volatile Oil	450	57.64	22
Oil 4	Volatile Oil	250	52.3	37.3
Oil 5	Black Oil	200	52.4	37

Table **4-1**: Properties of various reservoir fluids used in the study.

These oils are selected as their viscosities range from as high as 5800 cp to 1 cp at room temperature. The variation of viscosity of these oils with temperature is shown in Tables **4-2, 4-3 & 4-4**.

TEMPERATURE (^0F)	VISCOSITY OF OIL 1 (CP)	VISCOSITY OF OIL 3 (CP)	VISCOSITY OF OIL 4 (CP)
75	5780	10.58	2.328
100	1380	9.06	1.9935
150	187	6.775	1.4905
200	47	5.183	1.1403
250	17.4	4.043	0.8896
300	8.5	3.208	0.7058
350	5.2	2.583	0.5683
500	2.5	1.45	0.32
800	2.4	1.44	0.318

Table **4-2**: Variation of viscosity of oils 1, 3 & 4 with temperature.

TEMPERATURE (^{0}F)	VISCOSITY OF OIL 2 (CP)
80	182
100	91
150	27.3
200	11.4
250	5.46
300	3.46
350	2.46
500	1.13
800	1.11

Table **4-3**: Variation of viscosity of oil 2 with temperature.

TEMPERATURE (^{0}F)	VISCOSITY OF OIL 5 (CP)
70	1.36
80	0.844
90	0.57
100	0.41
200	0.0838
300	0.06
400	0.056
500	0.0553
800	0.054

Table **4-4**: Variation of viscosity of oil 5 with temperature.

4.1.2 Relative Permeability

The capillary pressures are assumed to be zero. The interstitial water saturation S_{iw} is assumed to be equal to irreducible water saturation S_{wir} ($S_{iw} = S_{wir} = 0.25$). The residual oil saturation for water/oil system, is $S_{orw} = 0.15$, and the residual oil saturation for gas/oil system $S_{org} = 0.1$ and the critical gas saturation $S_{gc} = 0.06$. The following relative permeability expressions are used [Aziz et al, 1987]:

For water/oil system,

$$k_{rw} = k_{rwro}\left(\frac{S_w - S_{wir}}{1 - S_{orw} - S_{wir}}\right)^{2.5} \tag{4.4}$$

$$k_{row} = k_{roiw}\left(\frac{1 - S_{orw} - S_w}{1 - S_{orw} - S_{iw}}\right)^{2} \tag{4.5}$$

For gas/oil system,

$$k_{rog} = k_{roiw}\left(\frac{1 - S_{iw} - S_{org} - S_g}{1 - S_{iw} - S_{org}}\right)^{2} \tag{4.6}$$

$$k_{rg} = k_{rgro}\left(\frac{S_g - S_{gc}}{1 - S_{iw} - S_{gc}}\right)^{1.5} \tag{4.7}$$

where,

k_{rw} = relative permeability to water.

k_{row} = relative permeability of oil w.r.t water

k_{rg} = relative permeability to gas

k_{rog} = relative permeability of oil w.r.t gas

S_w = saturation of water

S_g = saturation of gas

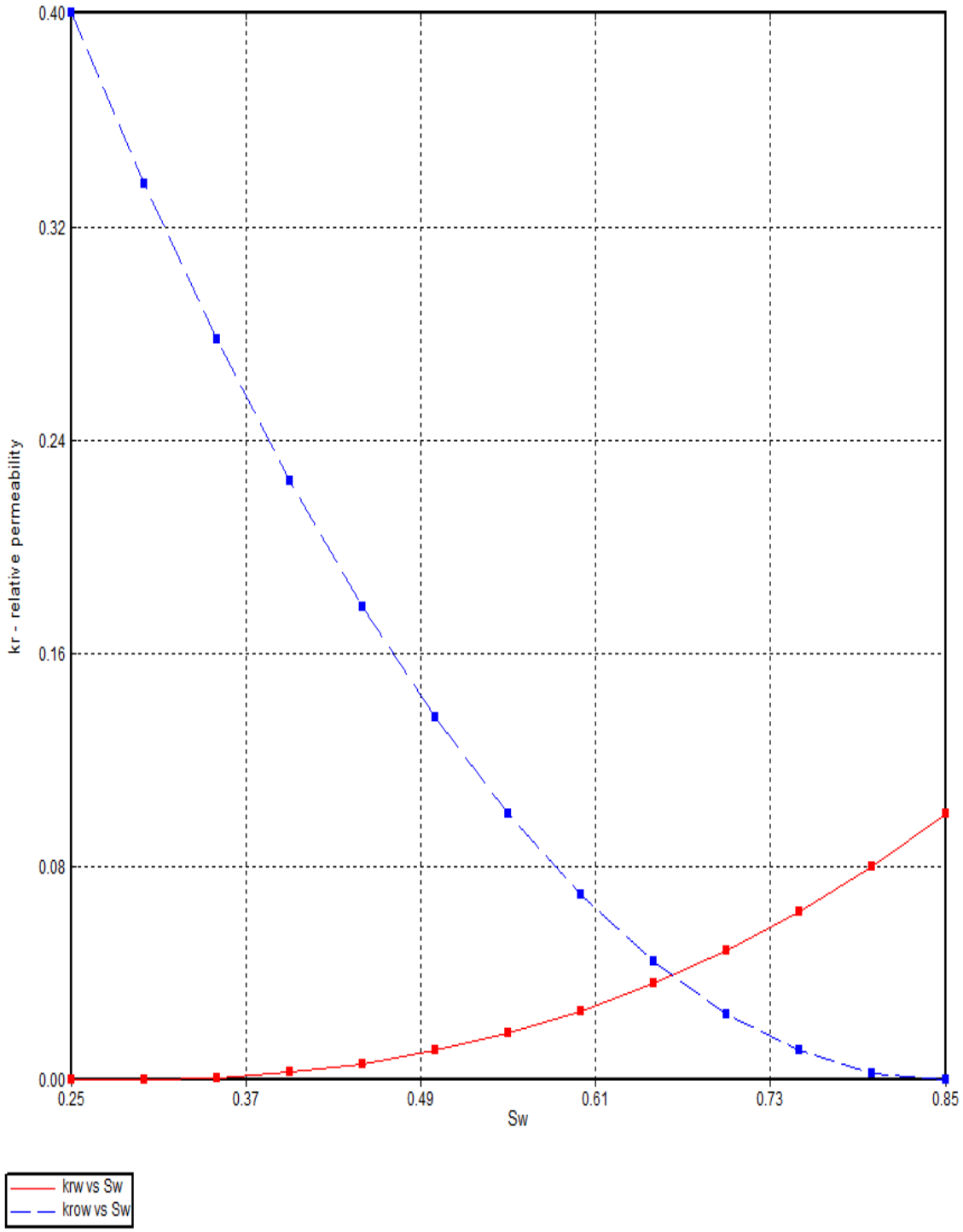

Figure **4-3**: Relative permeability of water/oil system.

$\mathbf{S_W}$	K_{RW}	K_{ROW}
0.25	0	0.4
0.3	0.0002	0.3361
0.35	0.001134	0.2777
0.4	0.003125	0.225
0.45	0.00641	0.1777
0.5	0.01112	0.1361
0.55	0.01768	0.1
0.6	0.02598	0.0694
0.65	0.03628	0.0444
0.7	0.04871	0.025
0.75	0.06339	0.0111
0.8	0.08045	0.00277
0.85	0.1	0

Table **4-5**: Relative permeability values for water/oil system.

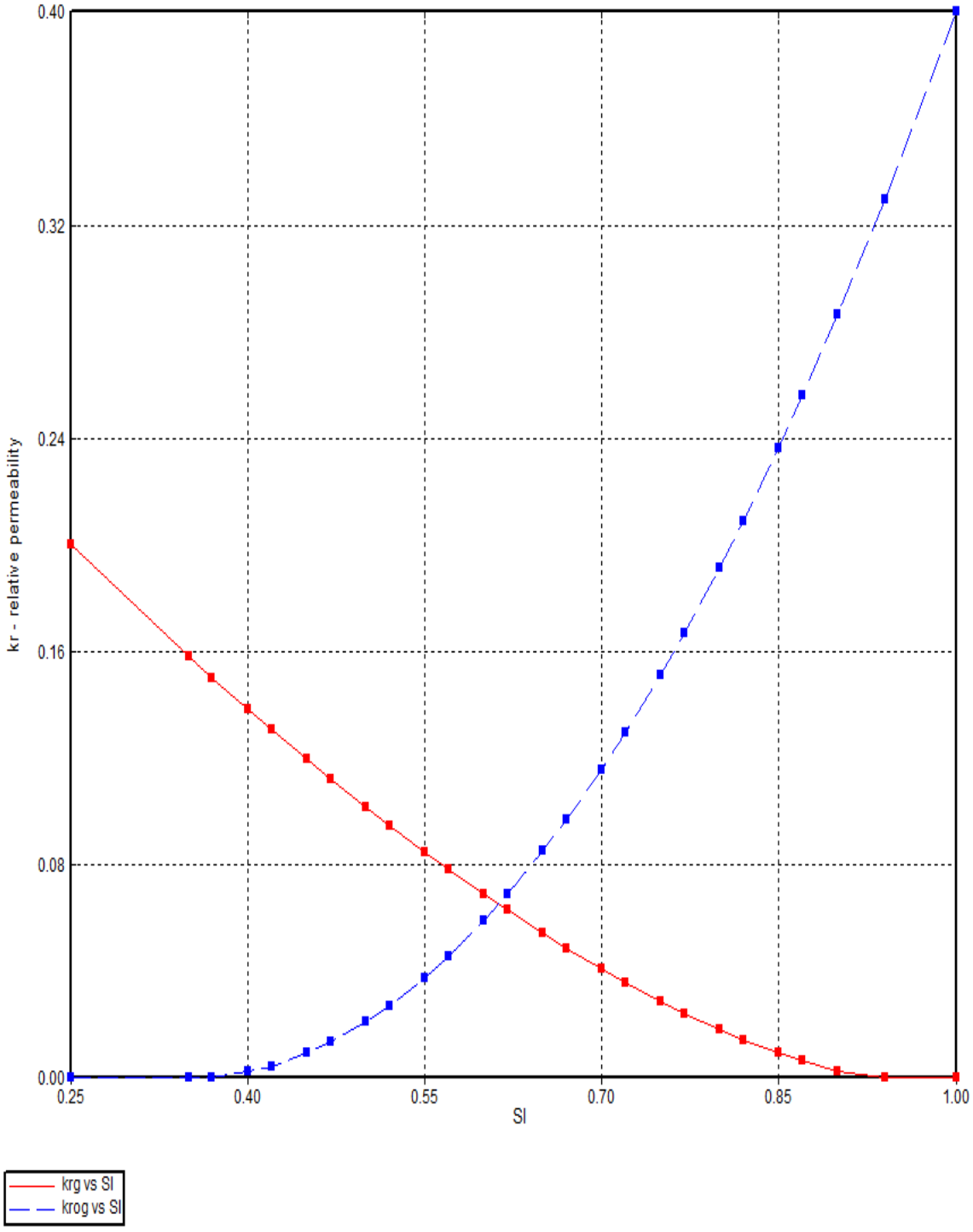

Figure **4-4**: Relative permeability of gas/liquid system.

S_G	K_{RG}	K_{ROG}
0.25	0.2	0
0.35	0.1581	0
0.37	0.1501	0.00038
0.4	0.1384	0.00237
0.42	0.1308	0.0046
0.45	0.1196	0.0095
0.47	0.1124	0.0136
0.5	0.1018	0.0213
0.52	0.0949	0.0273
0.55	0.0849	0.0378
0.57	0.0785	0.0458
0.6	0.0692	0.0592
0.62	0.0632	0.069
0.65	0.0545	0.0852
0.67	0.0489	0.0969
0.7	0.041	0.1159
0.72	0.036	0.1296
0.75	0.0289	0.1515
0.77	0.0244	0.167
0.8	0.0182	0.1917
0.82	0.0145	0.2091
0.85	0.0094	0.2366
0.87	0.0064	0.256
0.9	0.0028	0.2864
0.94	0	0.3295
1	0	0.4

Table **4-6**: Relative permeability values of gas/liquid system.

Stone's three phase relative permeability models were used to calculate three phase oil relative permeability k_{ro}.

4.2 Data File Generation

In order to study the performance of cyclic steam injection in naturally fractured reservoirs, the reservoir properties and design characteristics are varied between a range of values. Tables **4-7** and **4-8** show the ranges of reservoir properties and design characteristics respectively. A large number of random combinations of these parameters are generated using MATLAB. These combinations of reservoir properties and design characteristics are stored in an input file. The input file has 14 rows and around 250 columns of data. Each column represents a sample and rows represent either reservoir property or design characteristic. So each sample has 14 inputs whose value is randomly selected between the ranges. The input file is then used to create data sets containing a reservoir model corresponding to each sample. As described by [Bansal, 2009], a batch file was then created to run all the data sets in the simulator. The results of simulation of each data set were extracted by another code in MATLAB. The code extracted cumulative production of each cycle. The results were then stored in an output file. The output file thus had 4 rows and 250 columns of data. Again each column represents a sample and rows represent cumulative production of each cycle. The input and output data files were then screened to eliminate any incongruent data. The screened files were then used for training the artificial neural network. Finally, the procedure was repeated for all the five oils.

RESERVOIR PROPERTIES	MAXIMUM VALUE	MINIMUM VALUE	UNIT
Matrix Porosity (ϕ_m)	0.3	0.15	%
Matrix Permeability (k_m)	200	10	md
Fracture Porosity (ϕ_f)	0.05	0.01	%
Fracture Permeability (k_f)	2000	100	md
Fracture Spacing (S_f)	40	4	ft
Thickness (h)	200	20	ft
Initial Temperature (T_i)	240	120	^{0}F
Initial Oil Saturation (S_{oi})	0.75	0.4	-
Initial Pressure (P_i)	750	75	psia

Table **4-7**: Range of reservoir properties.

DESIGN CHARACTERISTICS	MAXIMUM VALUE	MINIMUM VALUE	UNIT
Drainage Area (A)	40	5	Acres
Steam Temperature (T_s)	600	450	^{0}F
Steam Quality (Q_s)	1	0.7	-
Steam Injection Rate (q_{inj})	5000	700	Barrels/day
Bottom Hole Pressure (P_{sf})	100	17	psia

Table **4-8**: Range of design characteristics.

Chapter 5

Results and Discussion

Initially, an expert system was developed for oil 1 using only five of the reservoir properties and three of design characteristics given in Tables **4-7** & **4-8**. Later additional reservoir properties like thickness of reservoir, initial temperature and initial oil saturation were added and expert systems were developed for five oils. Finally, the system was further complicated by including initial pressure in the reservoir properties and steam injection rate, bottom hole pressure in design characteristics. Hence in the final stage of this project there were 14 inputs and 4 outputs.

After generating the input and output data files for all the oils, an artificial expert system was developed for each oil. Training an artificial neural network is a heuristic procedure. Many rules of thumb are proposed in literature but each case is different. An attempt was made to replicate the architecture of ANN from previous works. They did not work for the system in this study. Hence the networks were trained using trial and error procedure. Different training algorithms were used and the number of neurons was increased. When that did not yield any good results, the procedure was repeated by including functional links. Then the number of hidden layers was increased. For all the networks the thumb rule of "funneling" the number of neurons as one went from input layer/zeroth layer to output layer improved the performance of the network. Around 200 samples were used for training the neural network, 25 samples were used for validation and 25 samples were used for testing the trained network. The error percentage of training and testing samples was evaluated based on Equation **5.1**:

$$error\ percentage\ \%\ (e) = \left[\frac{Q_i\ |_{SIM} - Q_i\ |_{ANN}}{Q_i\ |_{SIM}} \right] \times 100 \qquad (5.1)$$

The performance of the network was decided based on error percentage of the testing samples. Though the overall performance of the network was satisfactory, there were around two or three outliers during the testing of each network. The outliers are worst predictions of a network. They increased the mean error.

In order to improve the performance of the network further an error filter was used. In this approach a new artificial neural network was trained in which the outputs of the network were error percentages (e) instead of the cumulative production of each cycle. The purpose of this error filter was to provide prediction of error percentage of the original network. By knowing what error percentage the original network would generate, it was thought the results of the network could be improved. However after training the new network it was found that the errors worsened. A new testing sample was taken and a comparison was made between the simulator results and the prediction of original network. The new sample was then tested with the new network to predict the error. Based on this error, the prediction of original network was corrected and a new comparison was made with result of commercial simulator. It was found that implementation of error filter worsened the error and original network prediction was better. The possible reason why error filter did not work in this project is because the number of outputs in this project is only four. This means, presence of one or more outliers in the prediction of error filter would affect the cumulative production at the end of four cycles. On the other hand, if there were 20 outputs, presence of one or more outliers would not have affected the prediction as much as it did in this project.

This chapter provides a description of the best prediction, the worst prediction and the error frequency of five artificial neural networks. It also contains the sensitivity of the reservoir properties and design characteristics.

5.1 Results of ANN for Oil 1 (Network 1)

For training network 1, 187 samples were used for training, 23 were used for validation and 23 were used for testing. Scaled conjugate gradient (trainscg) training algorithm was implemented. Five hidden layers were used. The first layer has 61 neurons, second layer 47 neurons, third layer 23 neurons, fourth layer 11 neurons and fifth layer has 9 neurons. As discussed before the input layer or zeroth layer originally had 14 inputs. In addition to this 5 functional links containing maximum eigenvalue of 2 X 2 matrices containing various input properties were included in the input layer. The inclusion of eigenvalues improved the performance of the network. No functional links were included in the output layer as it did not improve the performance of the network. Tangent sigmoidal transfer function (tansig) was used in all the hidden layers. Linear transfer function (purelin) was used in the final layer. Figure **5-1** shows the reservoir properties and design characteristics of the best and worst testing sample.

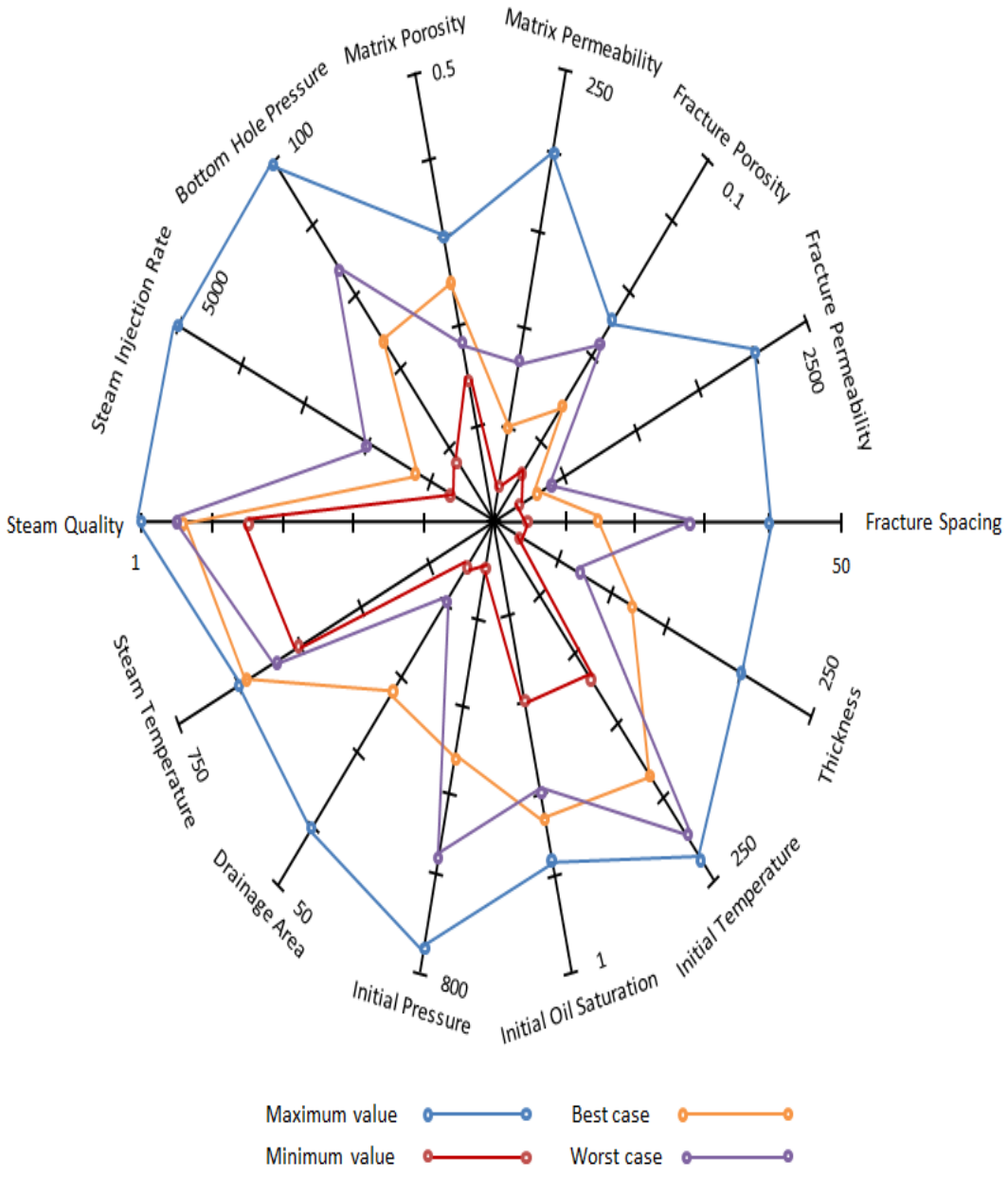

Figure **5-1**: Inputs for best and worst predictions of network 1.

5.1.1 Best Prediction of Network 1

Out of 23 testing samples, network 1 predicts very well for sample 5. The input for this sample is shown as best case in Figure **5-1**.Figure **5-2** shows a comparison of the cumulative production of each cycle as predicted by the commercial simulator and ANN. The error percentage (e) values for all the cycles for this sample are reported in Table **5-1**. This is the best prediction of the neural network for oil 1.

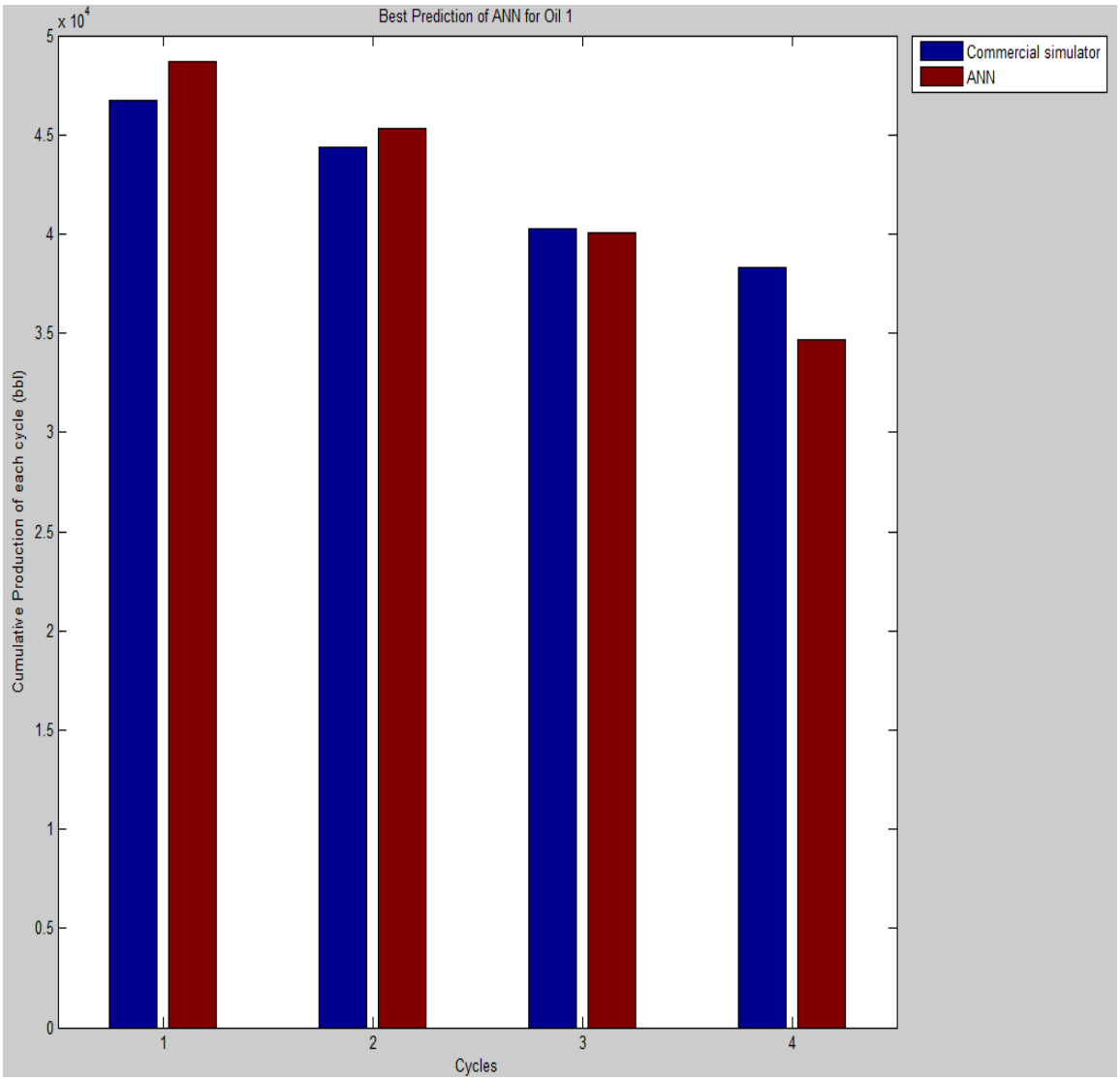

Figure **5-2**: Best prediction of network 1.

CYCLE	ERROR PERCENTAGE (%)
1	-4.14
2	-2.18
3	0.441
4	9.43

Table **5-1**: Error percentage values of best prediction of network 1.

5.1.2 Worst Prediction of Network 1

The prediction of network 1 for sample 6 is worst of all the 23 testing samples. The input for this sample is shown as worst case in Figure **5-1**. Figure **5-3** shows a comparison of the cumulative production of each cycle as predicted by the commercial simulator and ANN. The error percentage (e) values for all the cycles for this sample are reported in Table **5-2**.

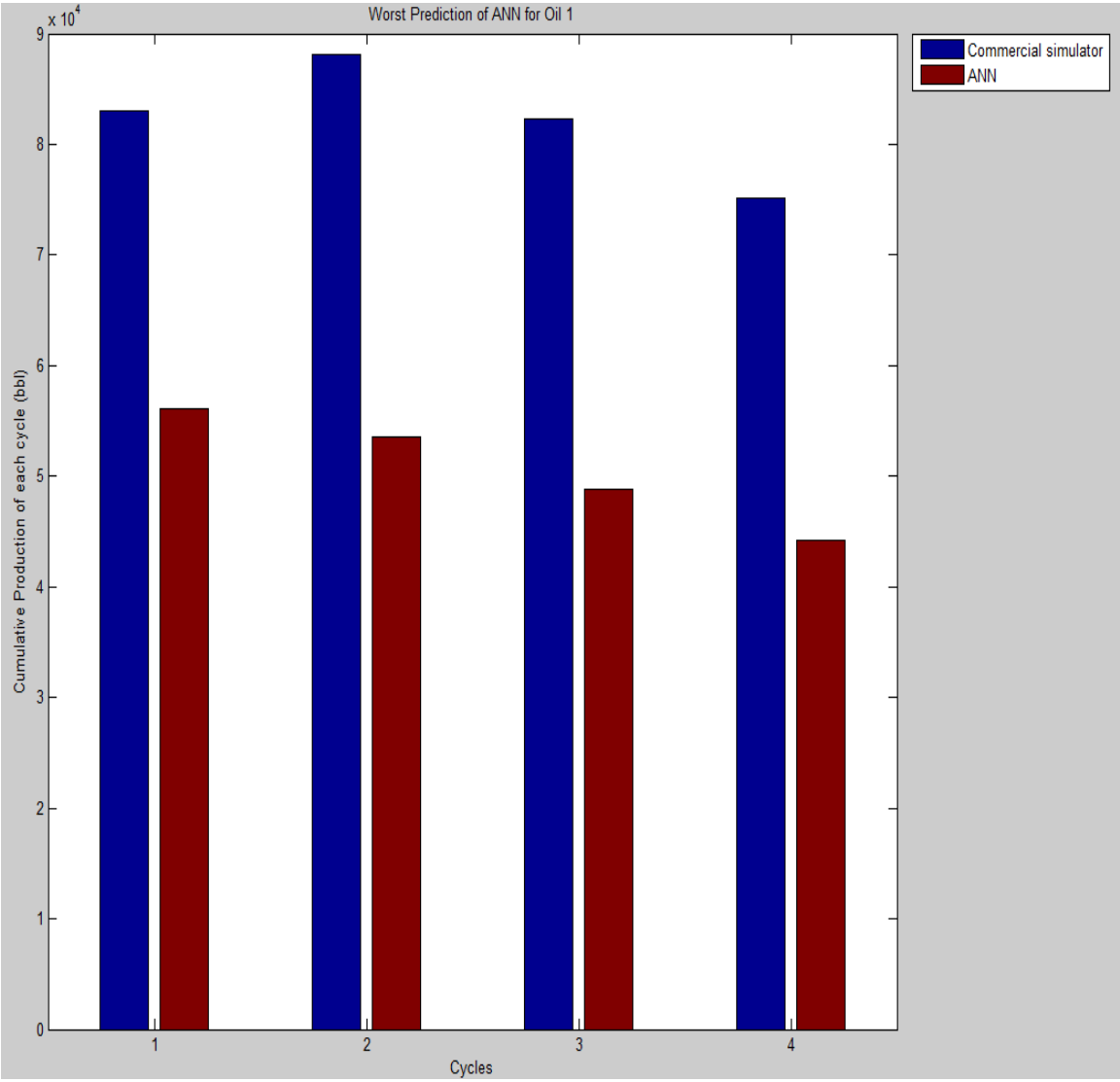

Figure **5-3**: Worst prediction of network 1.

CYCLE	ERROR PERCENTAGE (%)
1	32.33
2	39.29
3	40.69
4	41.25

Table **5-2**: Error percentage values of worst prediction of network 1.

5.1.3 Error Frequency of Network 1

The error percentages (e) of all the four cycles of 23 testing samples were recorded and a bar plot was made to study the frequency of error. In all, there were 92 points (23 samples X 4 cycles). Figure **5-4** is the bar plot reporting the error frequency of network 1. The mean error percentage of these 23 testing samples is 15.8%.

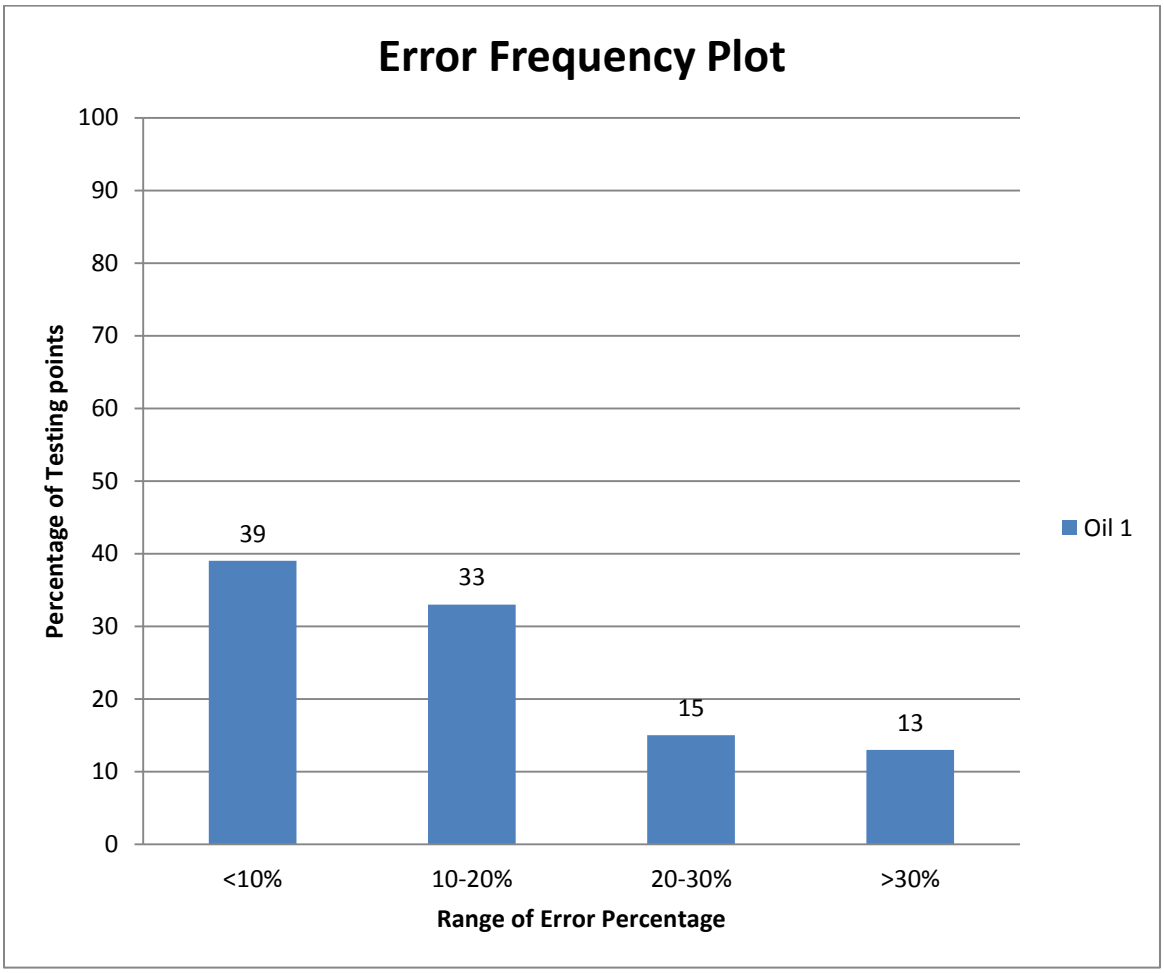

Figure **5-4**: Error frequency of network 1.

The cumulative production values at the end of each cycle for oil 1 are in the range of 10^3 – 10^4 barrels. As oil 1 is heavy, the production is lower compared to other oils. It can be observed that 39% of the points are below 10% error percentage and 72% of the points are below 20% error percentage. However 28% of the points are above the error percentage of 20. Though the percentage of outliers is high, it should be noted that the absolute difference between the result of commercial simulator and ANN prediction is small.

5.2 Results of ANN for Oil 2 (Network 2)

For training network 2, 212 samples were used for training, 26 were used for validation and 26 were used for testing. Scaled conjugate gradient (trainscg) training algorithm was implemented. Four hidden layers were used. The first layer has 79 neurons, second layer 41 neurons, third layer 17 neurons and fourth layer has 11 neurons. As discussed earlier the input layer or zeroth layer has 14 inputs. The inclusion of eigenvalues did not improve the performance of the network. No functional links were included in the output layer as it did not improve the performance of the network either. Tangent sigmoidal transfer function (tansig) was used in all the hidden layers. Linear transfer function (purelin) was used in the final layer. Figure **5-5** shows the reservoir properties and design characteristics of the best and worst testing sample.

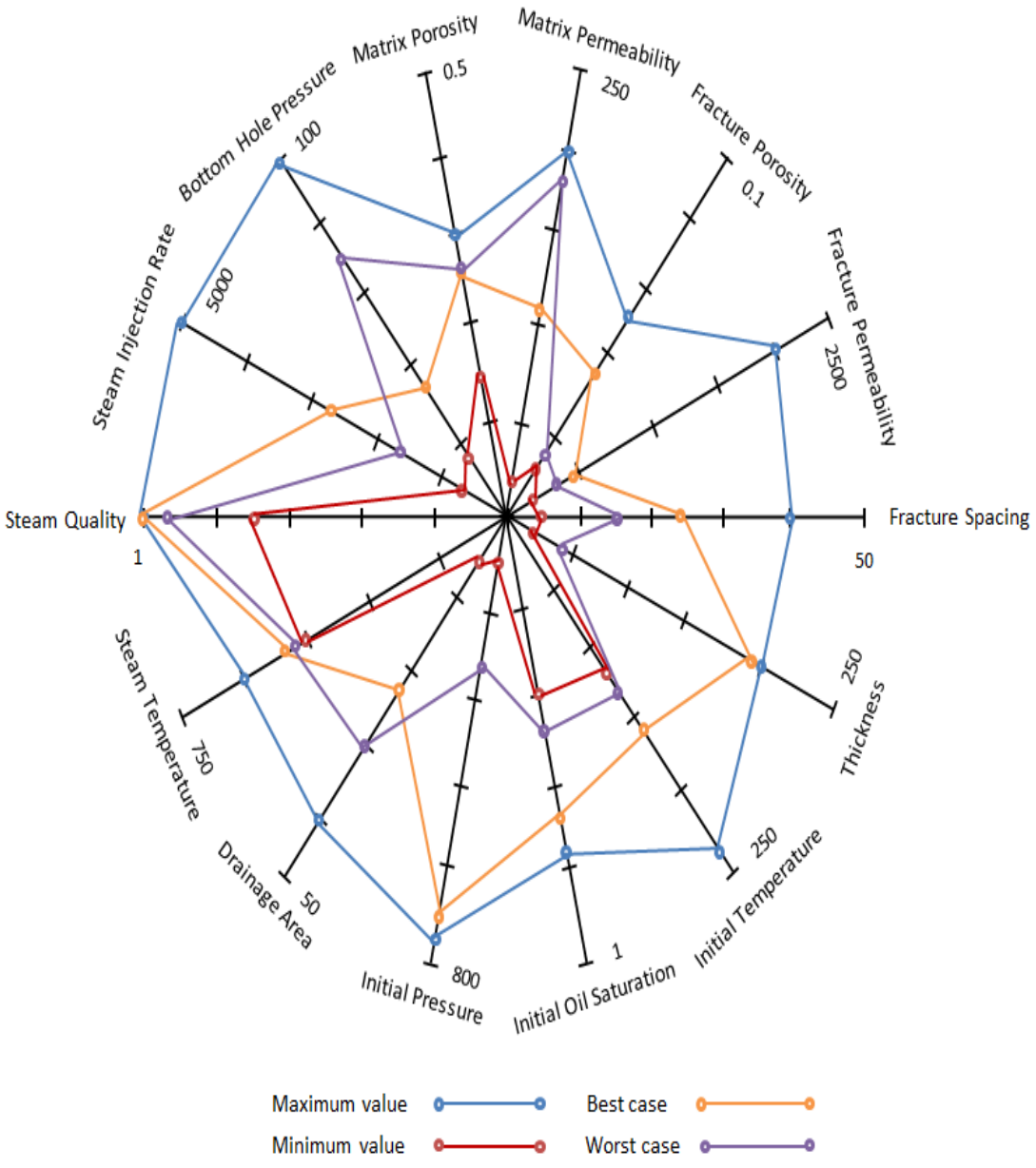

Figure **5-5**: Inputs for best and worst predictions of network 2.

5.2.1 Best Prediction of Network 2

Out of 26 testing samples, network 2 predicts very well for sample 17. The input for this sample is shown as best case in Figure **5-5**. Figure **5-6** shows a comparison of the cumulative production of each cycle as predicted by the commercial simulator and ANN. The error percentage (e) values for all the cycles for this sample are reported in Table **5-3**. This is the best prediction of the neural network for oil 2.

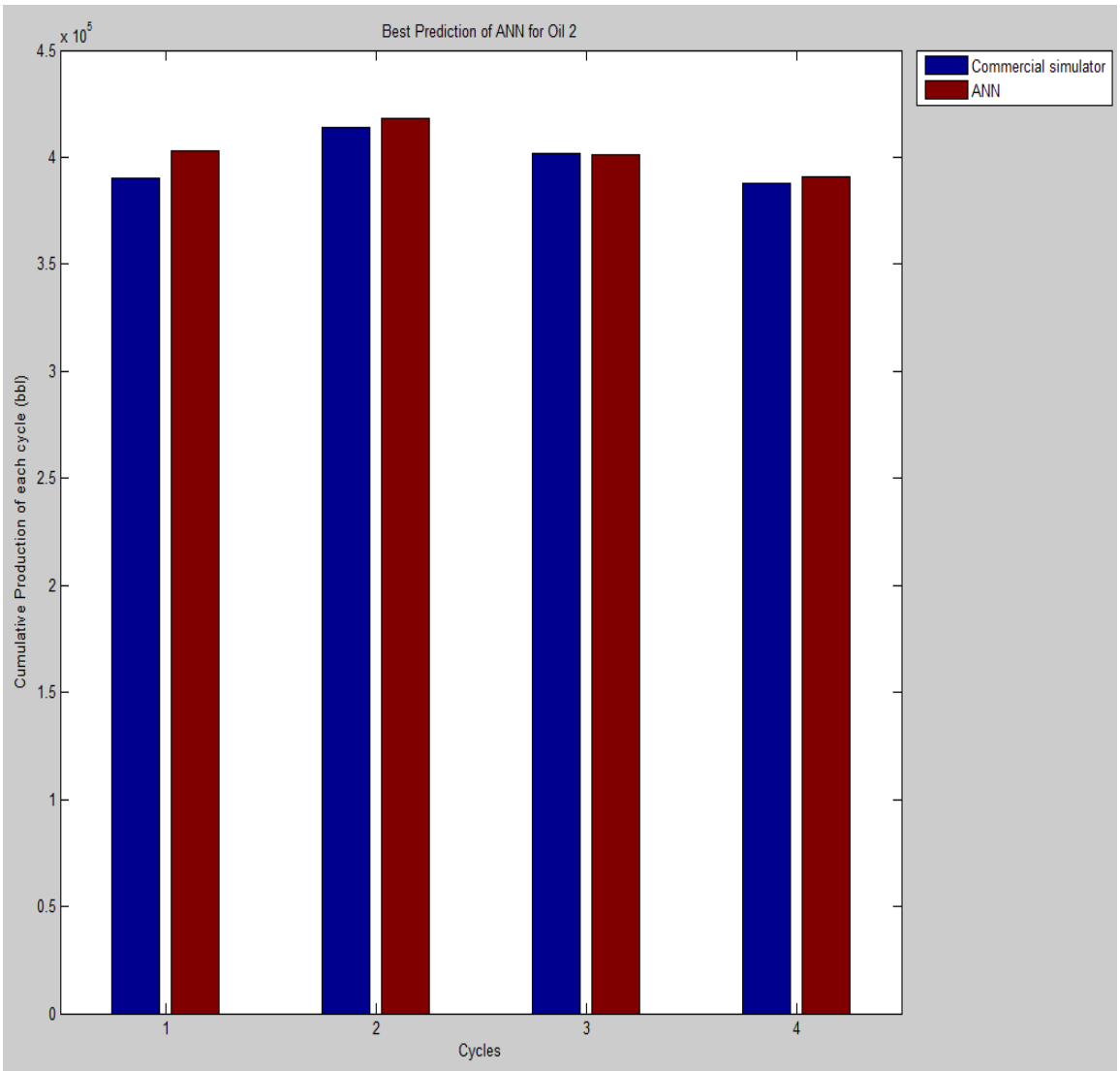

Figure **5-6**: Best prediction of network 2.

CYCLE	ERROR PERCENTAGE (%)
1	-3.36
2	-1.02
3	0.12
4	-0.79

Table **5-3**: Error percentage values of best prediction of network 2.

5.2.2 Worst Prediction of Network 2

The prediction of network 2 for sample 6 is worst of all the 26 testing samples. The input for this sample is shown as worst case in Figure **5-5**. Figure **5-7** shows a comparison of the cumulative production of each cycle as predicted by the commercial simulator and ANN. The error percentage (e) values for all the cycles for this sample are reported in Table **5-4**.

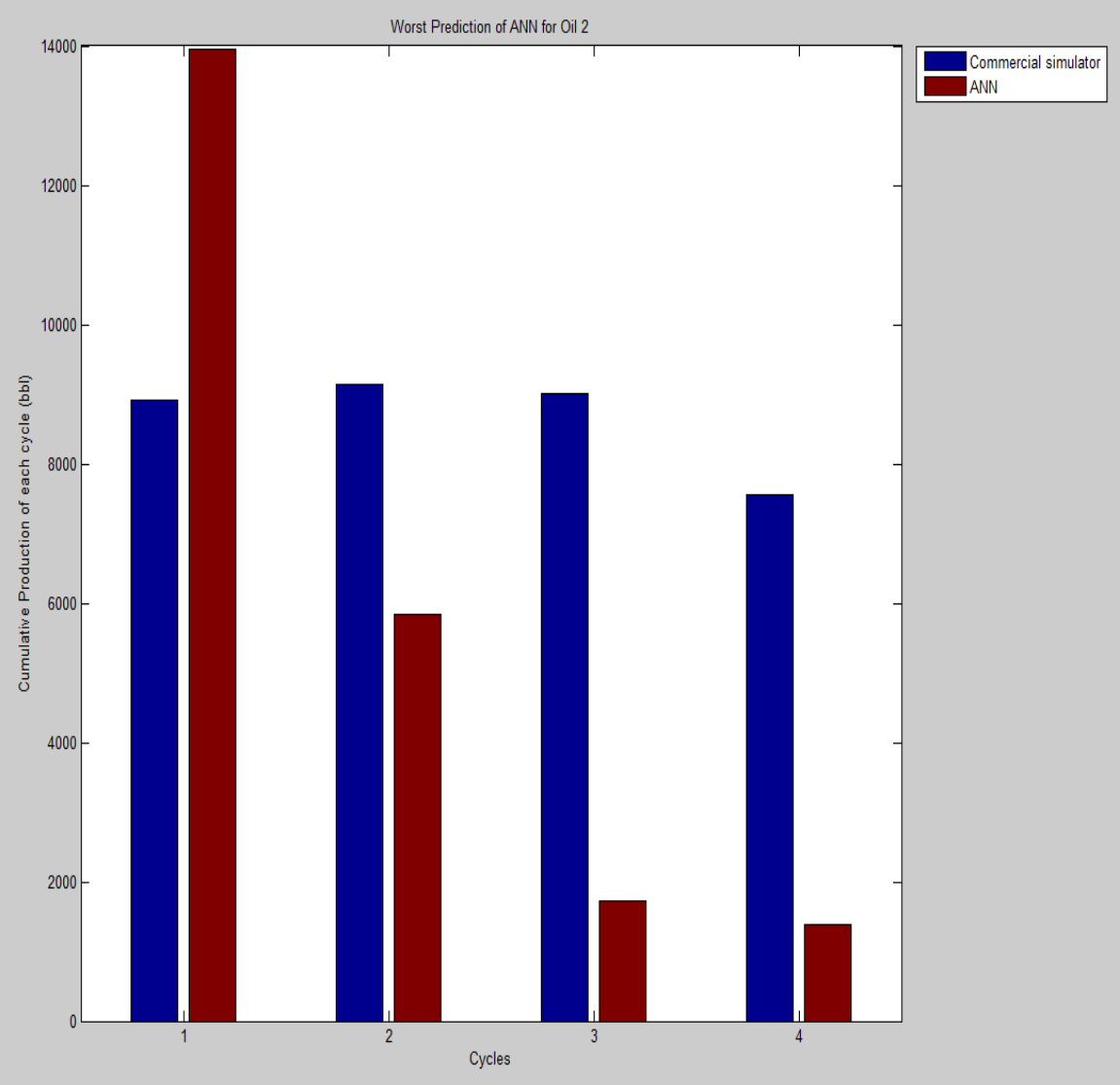

Figure **5-7**: Worst prediction of network 2.

CYCLE	ERROR PERCENTAGE (%)
1	-56.7
2	36.02
3	80.83
4	118.33

Table **5-4**: Error percentage values of worst prediction of network 2.

5.2.3 Error Frequency of Network 2

The error percentages (e) of all the four cycles of 26 testing samples were recorded and a bar plot was made to study the frequency of error. In all, there were 104 points (26 samples X 4 cycles). Figure **5-8** is the bar plot reporting the error frequency of network 2. The mean error percentage of these 26 testing samples is 20%.

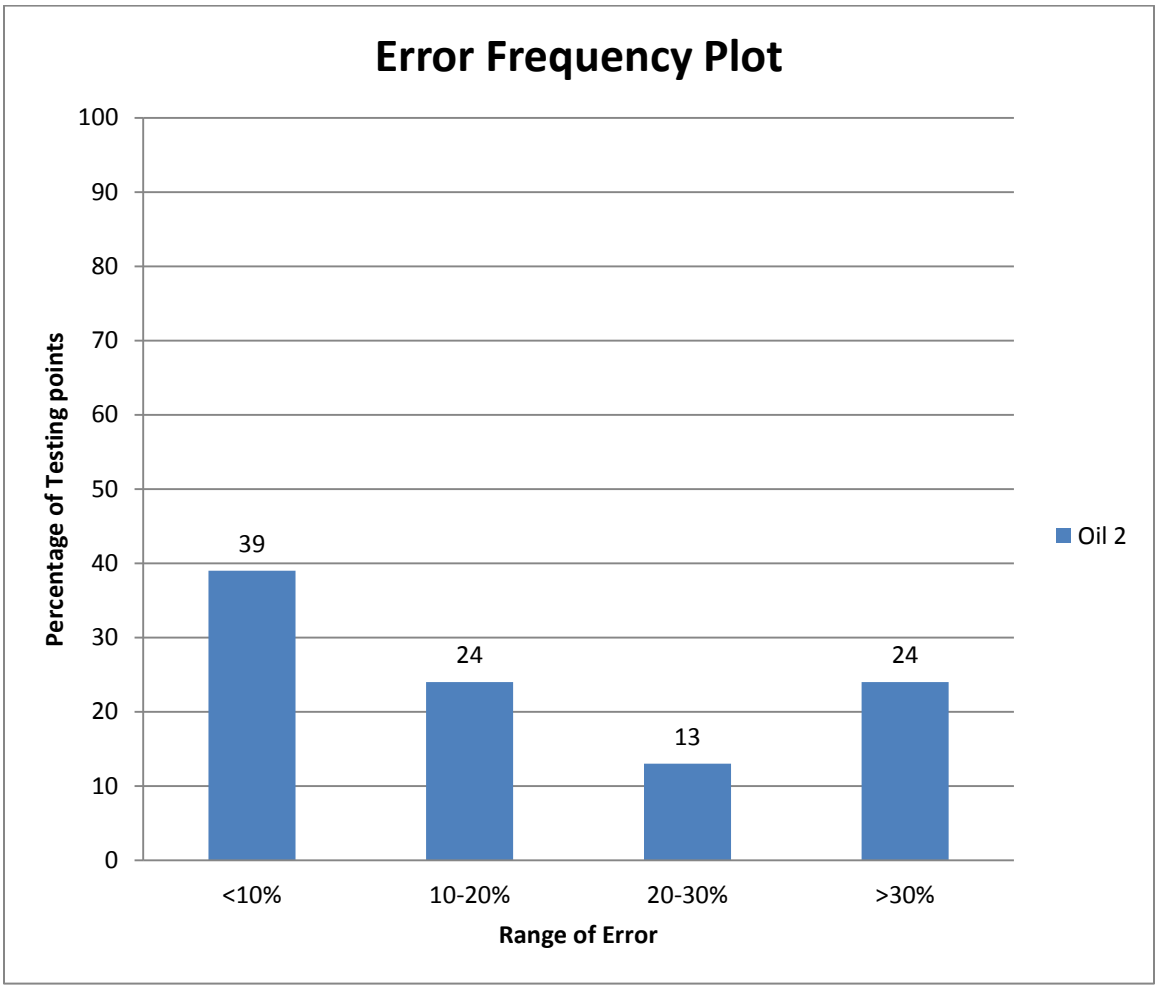

Figure **5-8**: Error frequency of network 2.

The percentage of outliers is large for network 2. Around 37% of the points are above error percentage of 20. Also since the cumulative productions are in the order of 10^4-10^5 barrels, the absolute difference between the result of commercial simulator and ANN prediction is high. However as 73% of testing points are below error percentage of 20 network 2 is the best trained ANN for oil 2.

5.3 Results of ANN for Oil 3 (Network 3)

For training network 3, 195 samples were used for training, 25 were used for validation and 25 were used for testing. Scaled conjugate gradient (trainscg) training algorithm was implemented. Five hidden layers were used. The first layer has 71 neurons, second layer 47 neurons, third layer 23 neurons, fourth layer 17 neurons and fifth layer has 11 neurons. As discussed earlier the input layer or zeroth layer originally had 14 inputs. In addition to this 5 functional links containing maximum eigenvalue of 2 X 2 matrices containing various input properties were included in the input layer. The inclusion of eigenvalues improved the performance of the network. No functional links were included in the output layer as it did not improve the performance of the network. Tangent sigmoidal transfer function (tansig) was used in all the hidden layers. Linear transfer function (purelin) was used in the final layer. Figure **5-9** shows the reservoir properties and design characteristics of the best and worst testing sample.

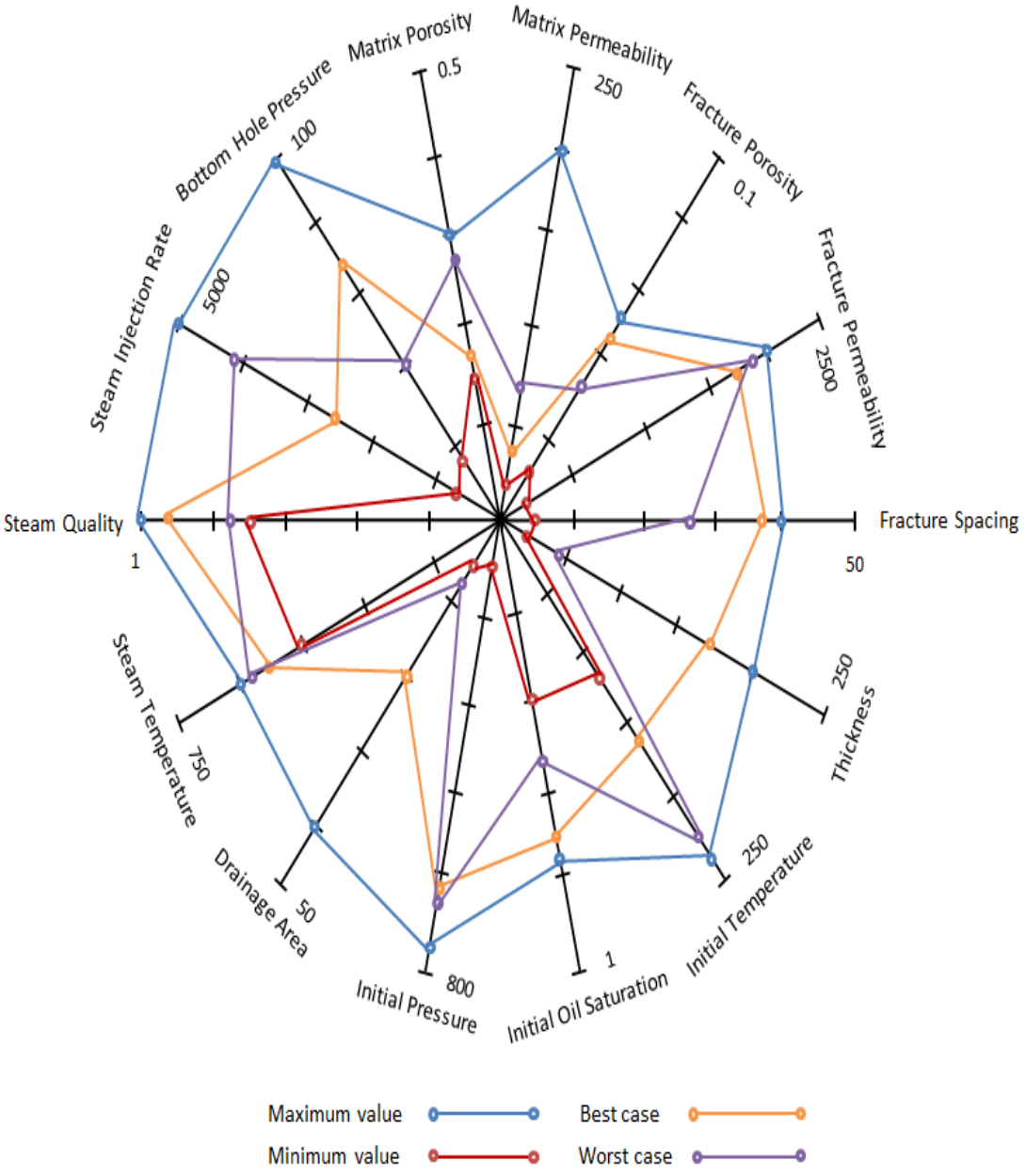

Figure **5-9**: Inputs for best and worst predictions of network 3.

5.3.1 Best Prediction of Network 3

Out of 25 testing samples, network 3 predicts very well for sample 10. The input for this sample is shown as best case in Figure **5-9**. Figure **5-10** shows a comparison of the cumulative production of each cycle as predicted by the commercial simulator and ANN. The error percentage (e) values for all the cycles for this sample are reported in Table **5-5**. This is the best prediction of the neural network for oil 3.

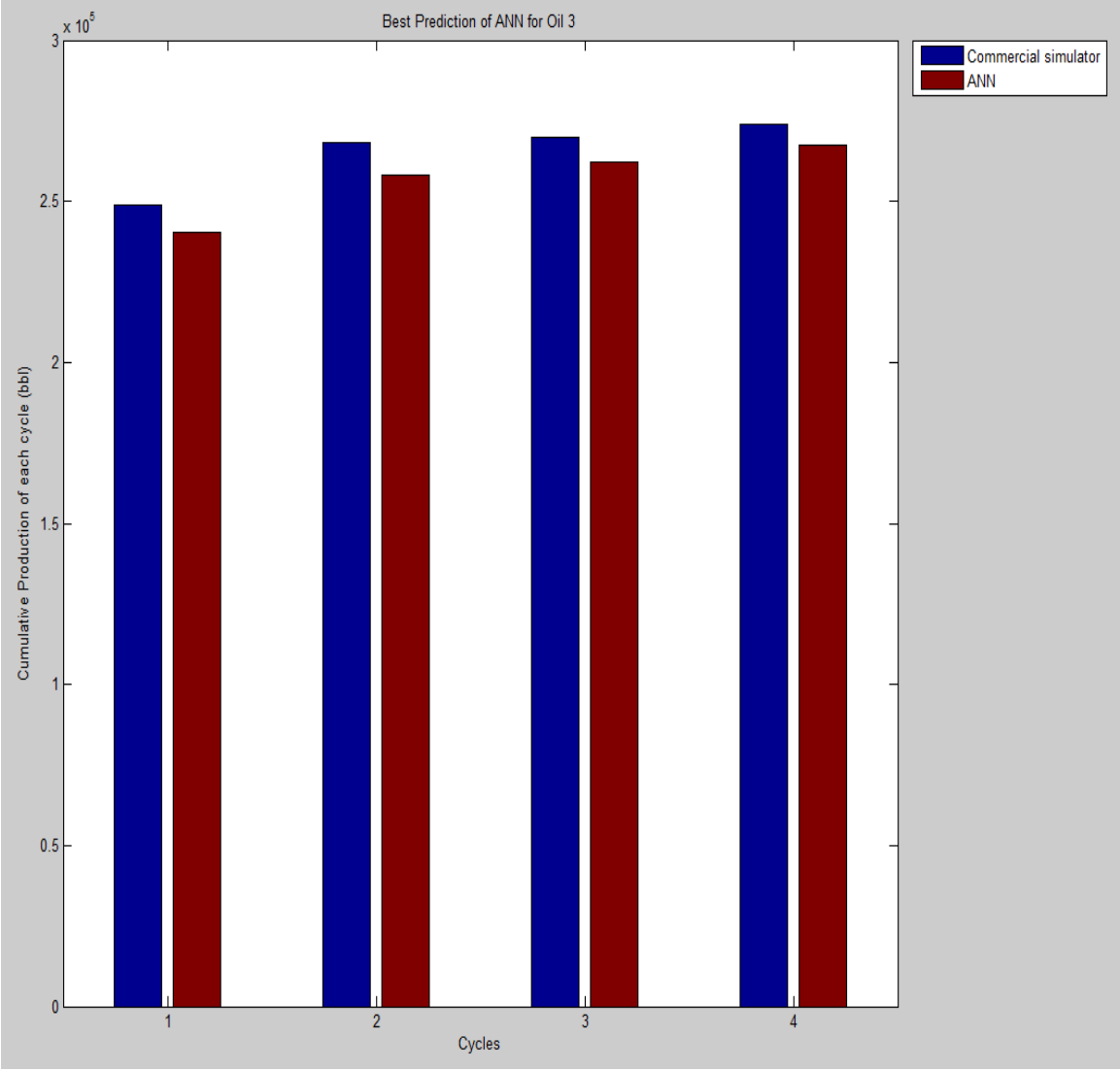

Figure **5-10**: Best prediction of network 3.

CYCLE	ERROR PERCENTAGE (%)
1	3.46
2	3.8
3	2.78
4	2.35

Table **5-5**: Error percentage values for best prediction of network 3.

5.3.2 Worst Prediction of Network 3

The prediction of network 3 for sample 23 is worst of all the 25 testing samples. The input for this sample is shown as worst case in Figure **5-9**. Figure **5-11** shows a comparison of the cumulative production of each cycle as predicted by the commercial simulator and ANN. The error percentage (e) values for all the cycles for this sample are reported in Table **5-6**.

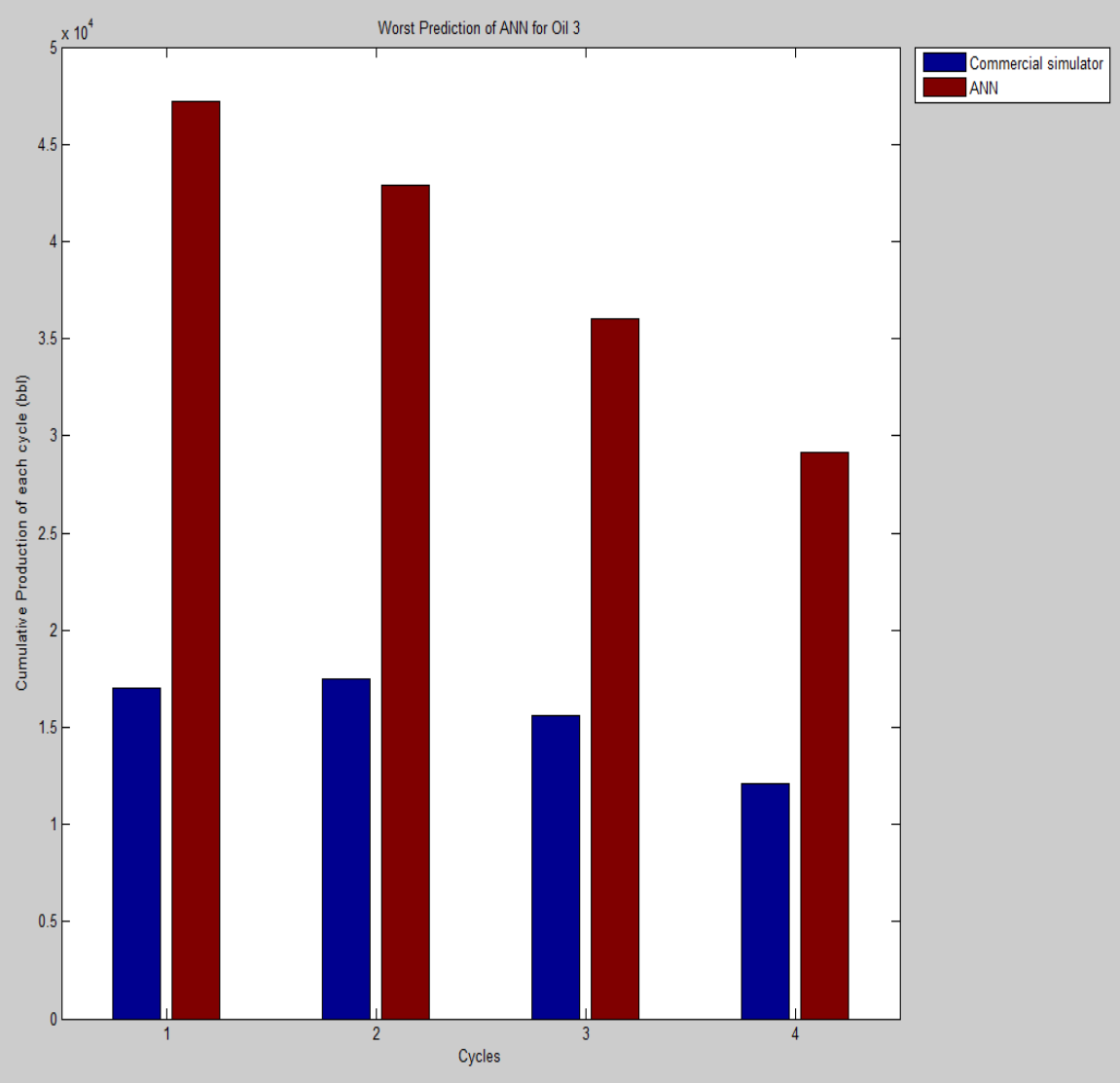

Figure **5-11**: Worst prediction of network 3.

CYCLE	ERROR PERCENTAGE (%)
1	-177.48
2	-145.12
3	-131.42
4	-141.09

Table **5-6**: Error percentage values of worst prediction of network 3.

5.3.3 Error Frequency of Network 3

The error percentages (e) of all the four cycles of 25 testing samples were recorded and a bar plot was made to study the frequency of error. In all, there were 100 points (25 samples X 4 cycles). Figure **5-12** is the bar plot reporting the error frequency of network 3. The mean error percentage of these 25 testing samples is 24.7%.

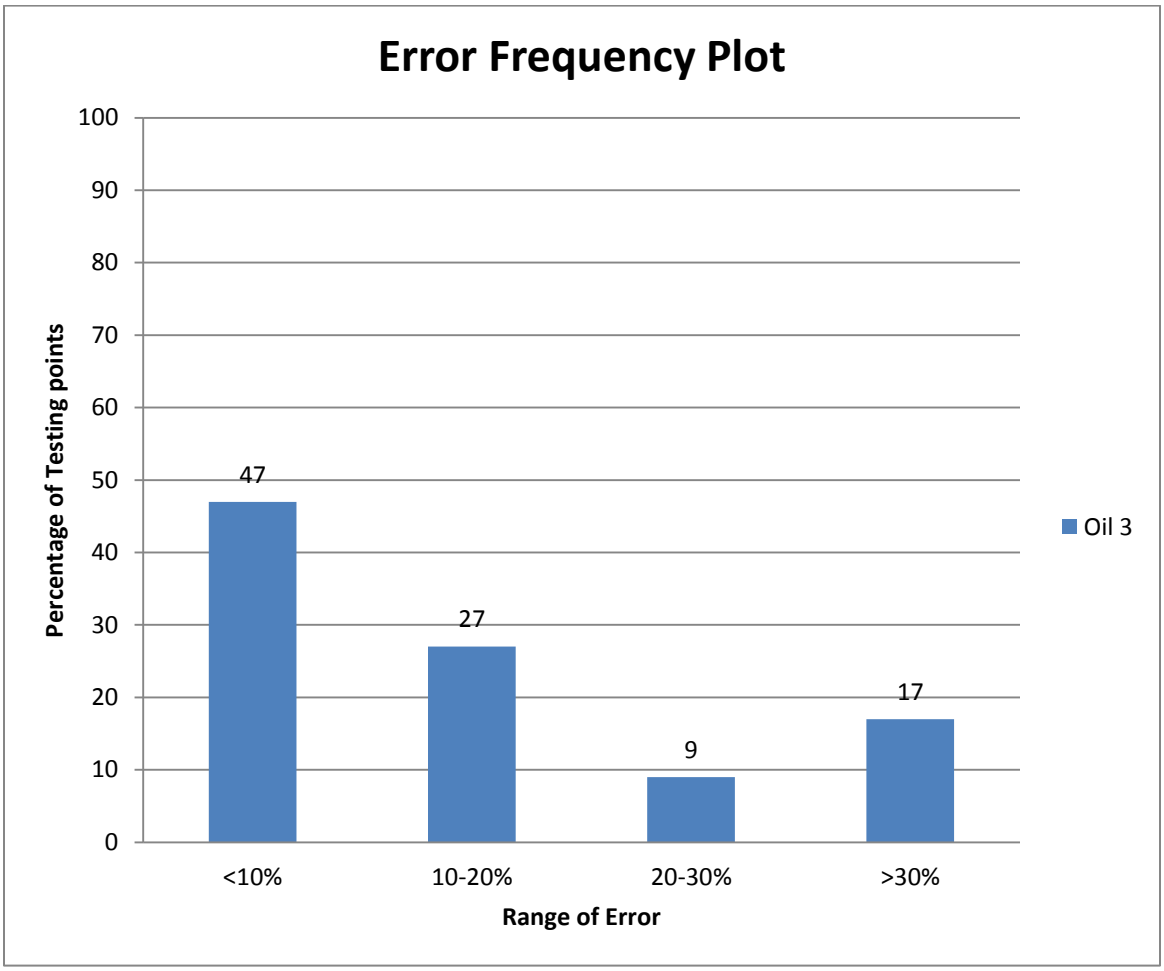

Figure **5-12**: Error frequency of network 3.

It can be observed that 74% of the testing points are below the error percentage of 20. More number of testing points are below 10% compared to oil 1 and 2.

5.4 Results of ANN for Oil 4 (Network 4)

For training network 4, 197 samples were used for training, 25 were used for validation and 25 were used for testing. Scaled conjugate gradient (trainscg) training algorithm was implemented. Four hidden layers were used. The first layer has 51 neurons, second layer 27 neurons, third layer 17 neurons and fourth layer has 13 neurons. As discussed earlier the input layer or zeroth layer originally had 14 inputs. In addition to this 5 functional links containing maximum eigenvalue of 2 X 2 matrices containing various input properties were included in the input layer. The inclusion of eigenvalues improved the performance of the network. No functional links were included in the output layer as it did not improve the performance of the network. Tangent sigmoidal transfer function (tansig) was used in all the hidden layers. Linear transfer function (purelin) was used in the final layer. Figure **5-13** shows the reservoir properties and design characteristics of the best and worst testing sample.

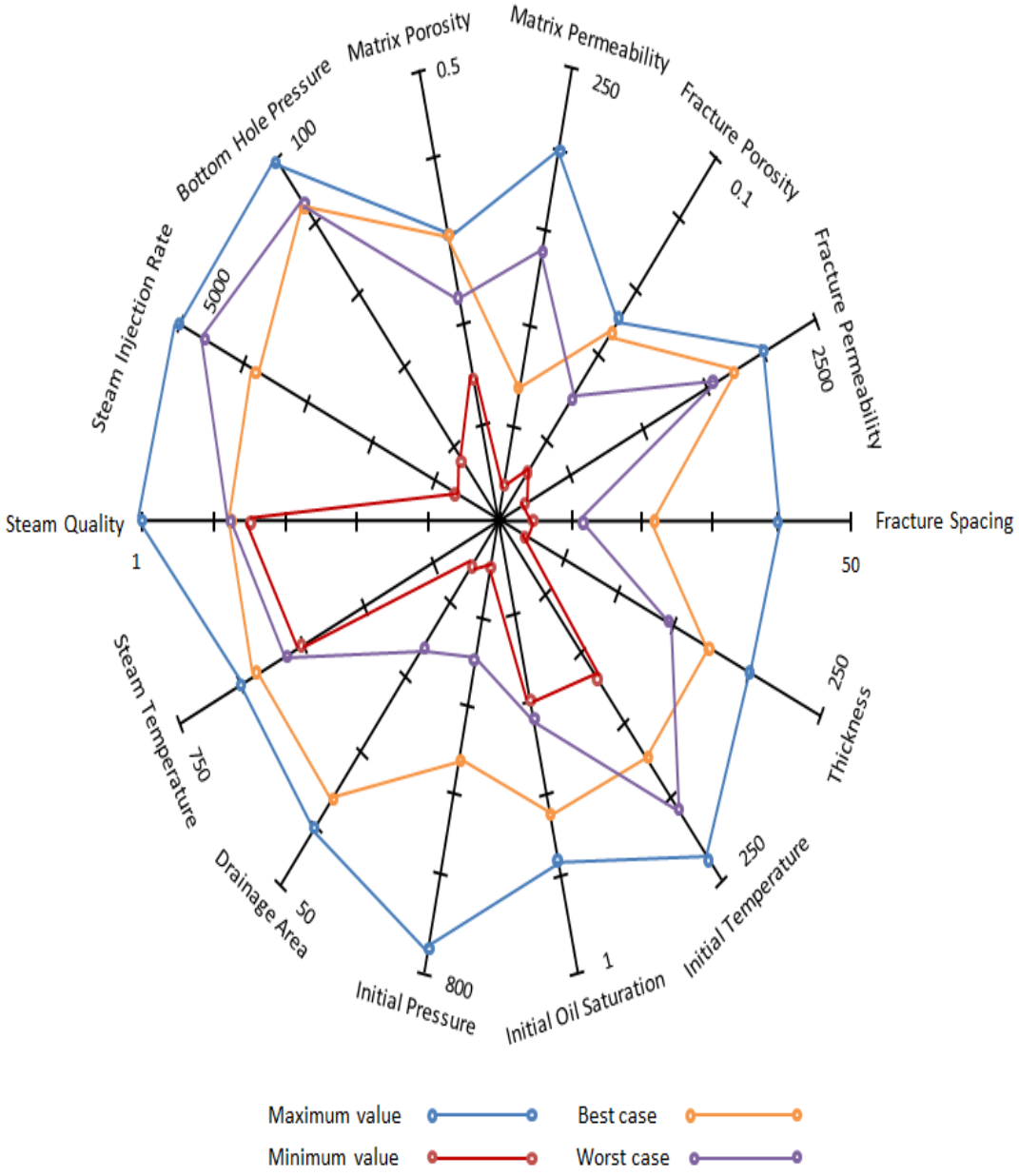

Figure **5-13**: Inputs for best and worst predictions of network 4.

5.4.1 Best Prediction of Network 4

Out of 25 testing samples, network 4 predicts very well for sample 16. The input for this sample is shown as best case in Figure **5-13**. Figure **5-14** shows a comparison of the cumulative production of each cycle as predicted by the commercial simulator and ANN. The error percentage (e) values for all the cycles for this sample are reported in Table **5-7**. This is the best prediction of the neural network for oil 4.

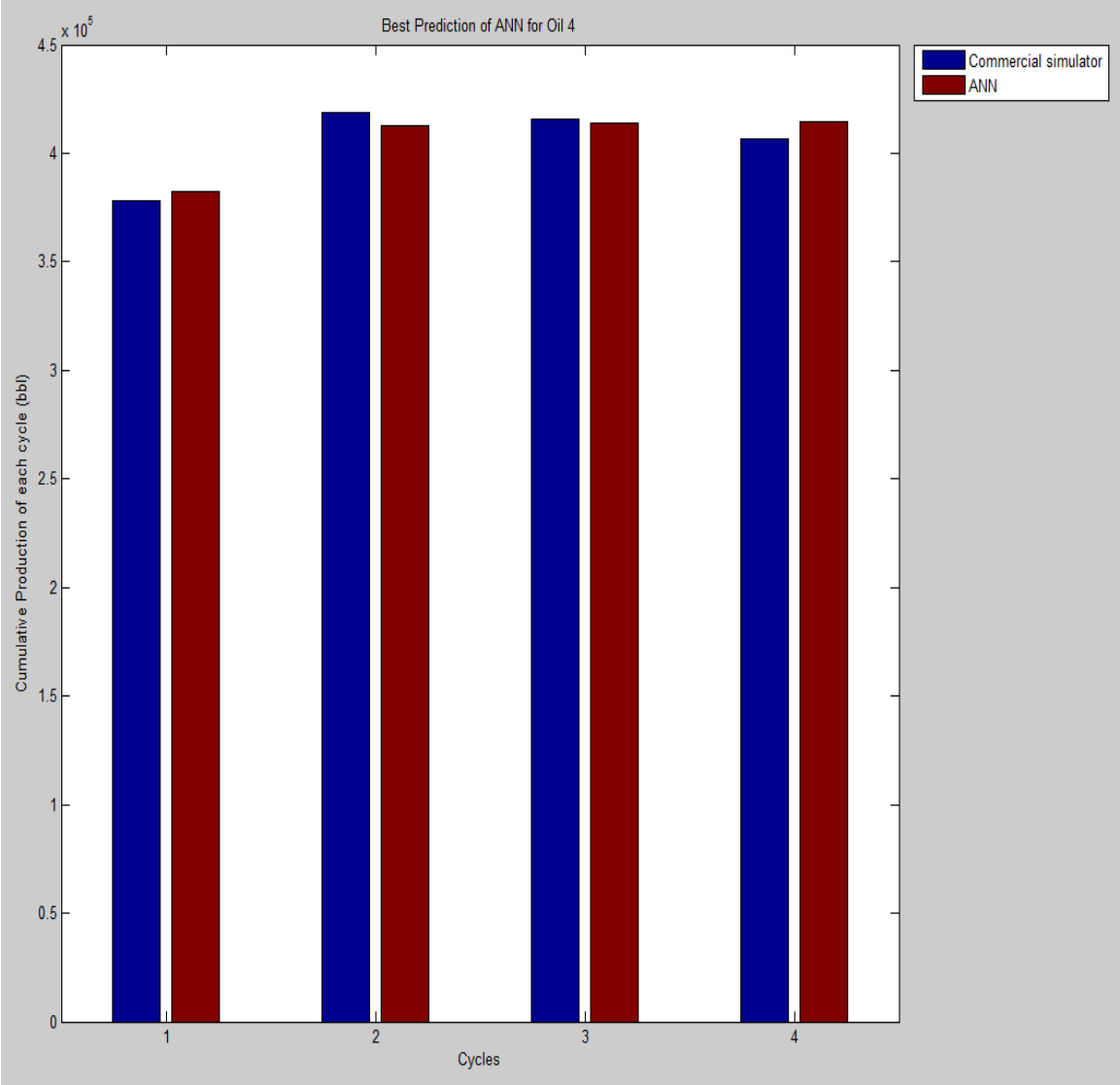

Figure **5-14**: Best prediction of network 4.

CYCLE	ERROR PERCENTAGE (%)
1	-1.04
2	1.51
3	0.38
4	-1.94

Table **5-7**: Error percentage values of best prediction of network 4.

5.4.2 Worst Prediction of Network 4

The prediction of network 4 for sample 8 is worst of all the 25 testing samples. The input for this sample is shown as worst case in Figure **5-13**. Figure **5-15** shows a comparison of the cumulative production of each cycle as predicted by the commercial simulator and ANN. The error percentage (e) values for all the cycles for this sample are reported in Table **5-8**.

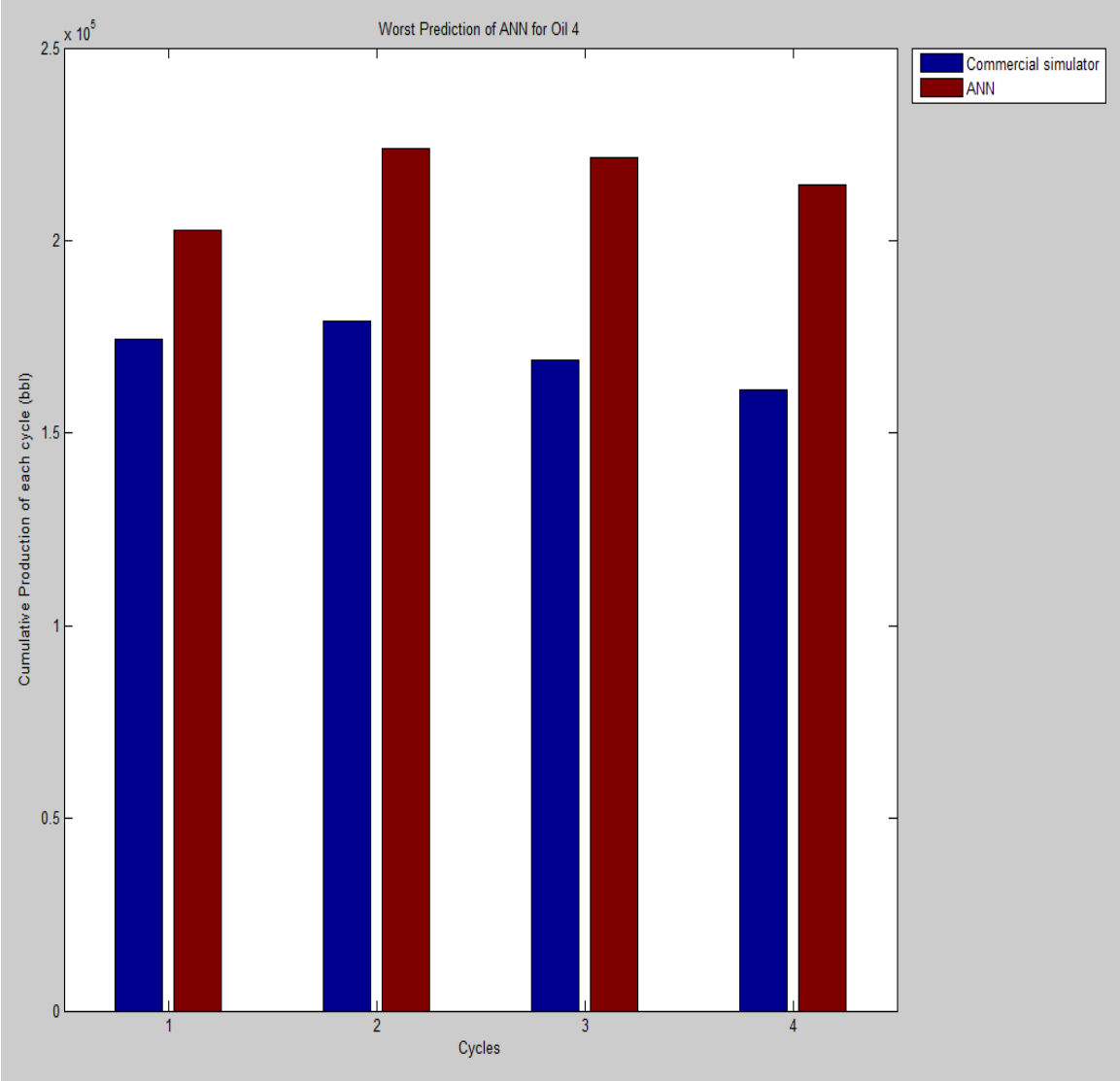

Figure **5-15**: Worst prediction of network 4.

CYCLE	ERROR PERCENTAGE (%)
1	-16.11
2	-24.93
3	-31.2
4	-33.07

Table **5-8**: Error percentage values of worst prediction of network 4.

5.4.3 Error Frequency of Network 4

The error percentages (e) of all the four cycles of 25 testing samples were recorded and a bar plot was made to study the frequency of error. In all, there were 100 points (25 samples X 4 cycles). Figure **5-16** is the bar plot reporting the error frequency of network 4. The mean error percentage of these 25 testing samples is 7.6%.

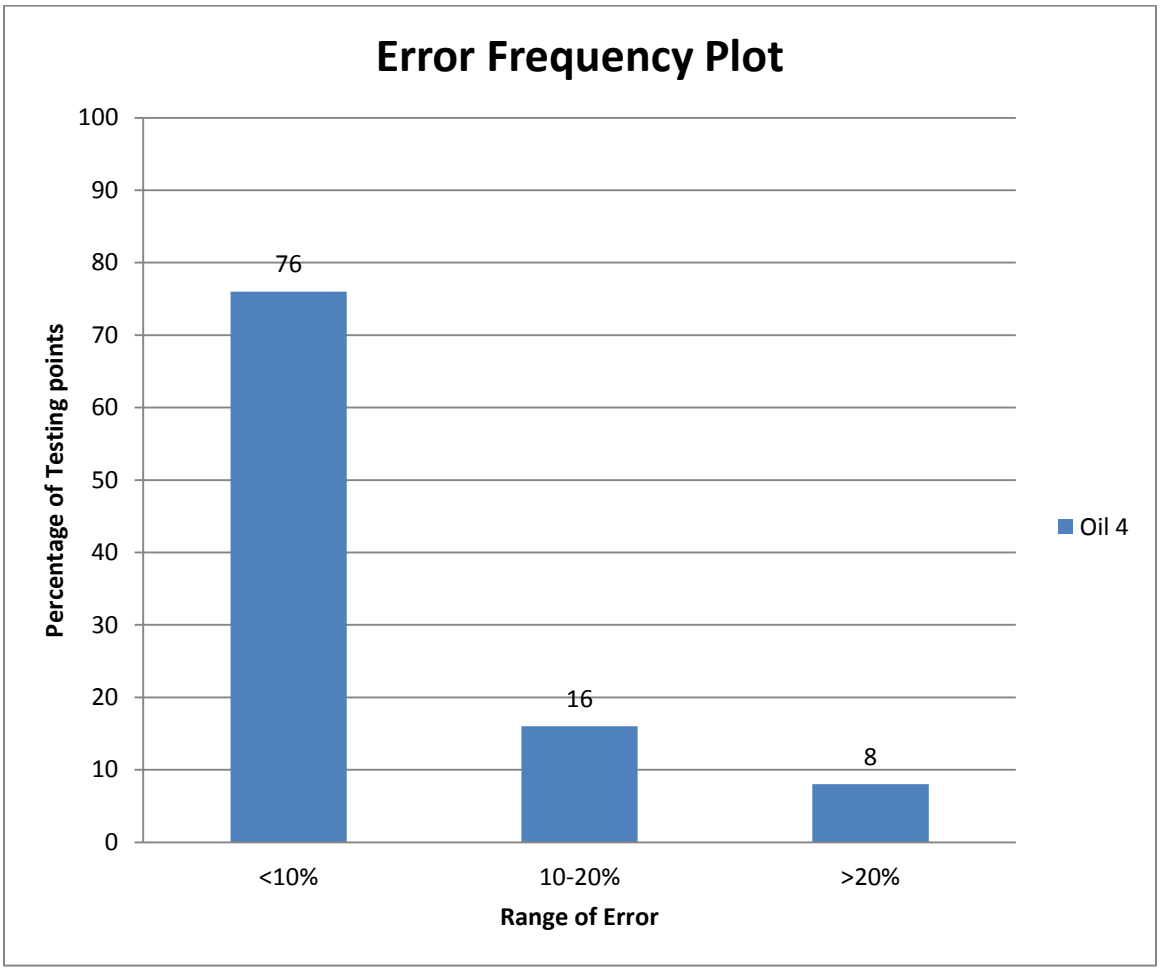

Figure **5-16**: Error frequency of network 4.

The cumulative production values for oil 4 are greater than 10^5 barrels. As the viscosity of oil is decreasing the cumulative production at the end of each cycle is increasing. Also it can be observed 92% of the testing points fall below error percentage of 20.

5.5 Results of ANN for Oil 5 (Network 5)

For training network 5, 210 samples were used for training, 26 were used for validation and 26 were used for testing. Scaled conjugate gradient (trainscg) training algorithm was implemented. Only one hidden layer was sufficient to satisfactorily train this network. The hidden layer had 53 neurons. As discussed before the input layer or zeroth layer originally had 14 inputs. In addition to this 5 functional links containing maximum eigenvalue of 2 X 2 matrices containing various input properties were included in the input layer. The inclusion of eigenvalues improved the performance of the network. No functional links were included in the output layer as it did not improve the performance of the network. Tangent sigmoidal transfer function (tansig) was used in the only hidden layer. Figure **5-17** shows the reservoir properties and design characteristics of the best and worst testing sample.

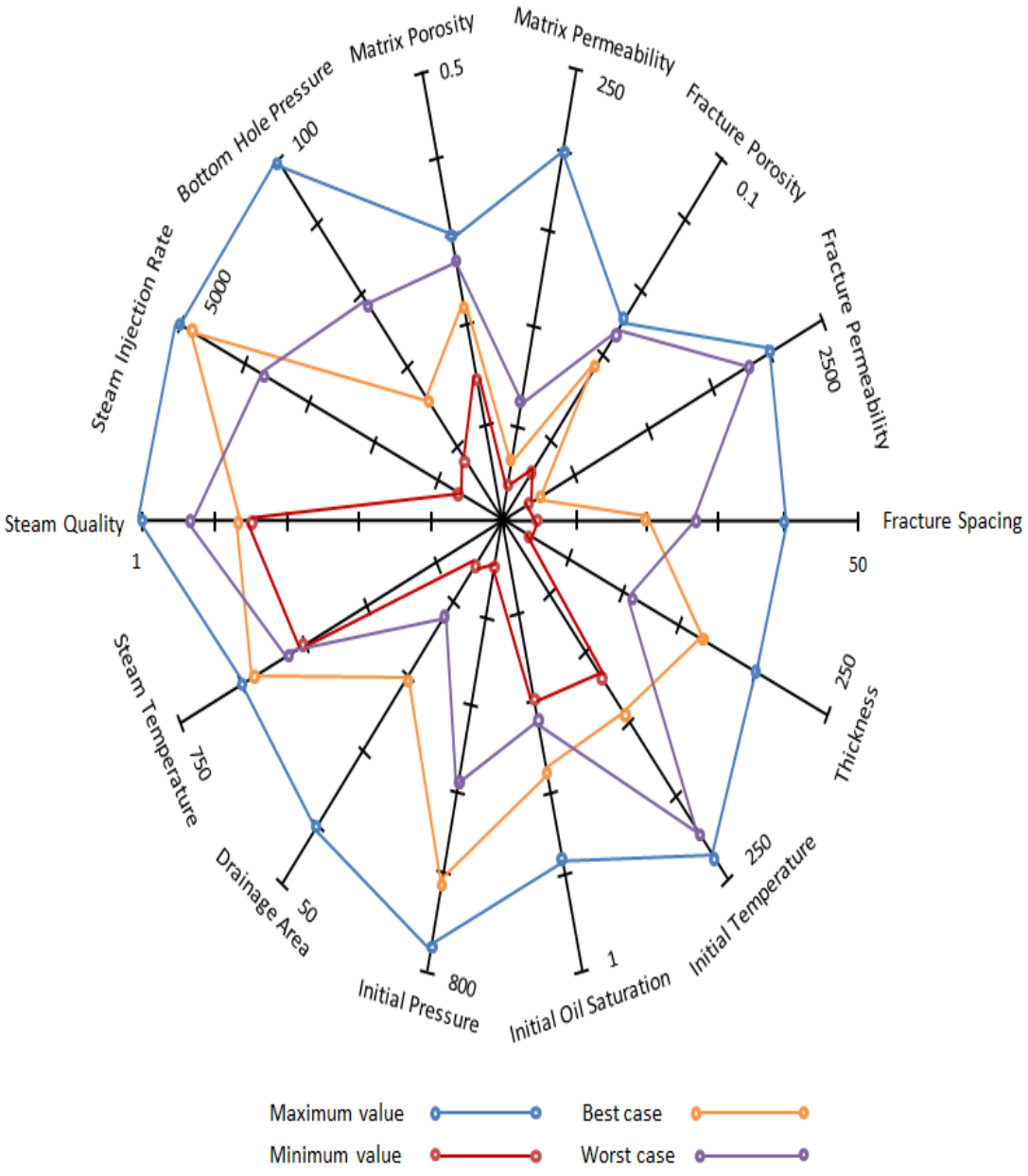

Figure **5-17**: Inputs for best and worst predictions of network 5.

5.5.1 Best Prediction of Network 5

Out of 26 testing samples, network 5 predicts very well for sample 2. The input for this sample is shown as best case in Figure **5-17**. Figure **5-18** shows a comparison of the cumulative production of each cycle as predicted by the commercial simulator and ANN. The error percentage (e) values for all the cycles for this sample are reported in Table **5-9**. This is the best prediction of the neural network for oil 5.

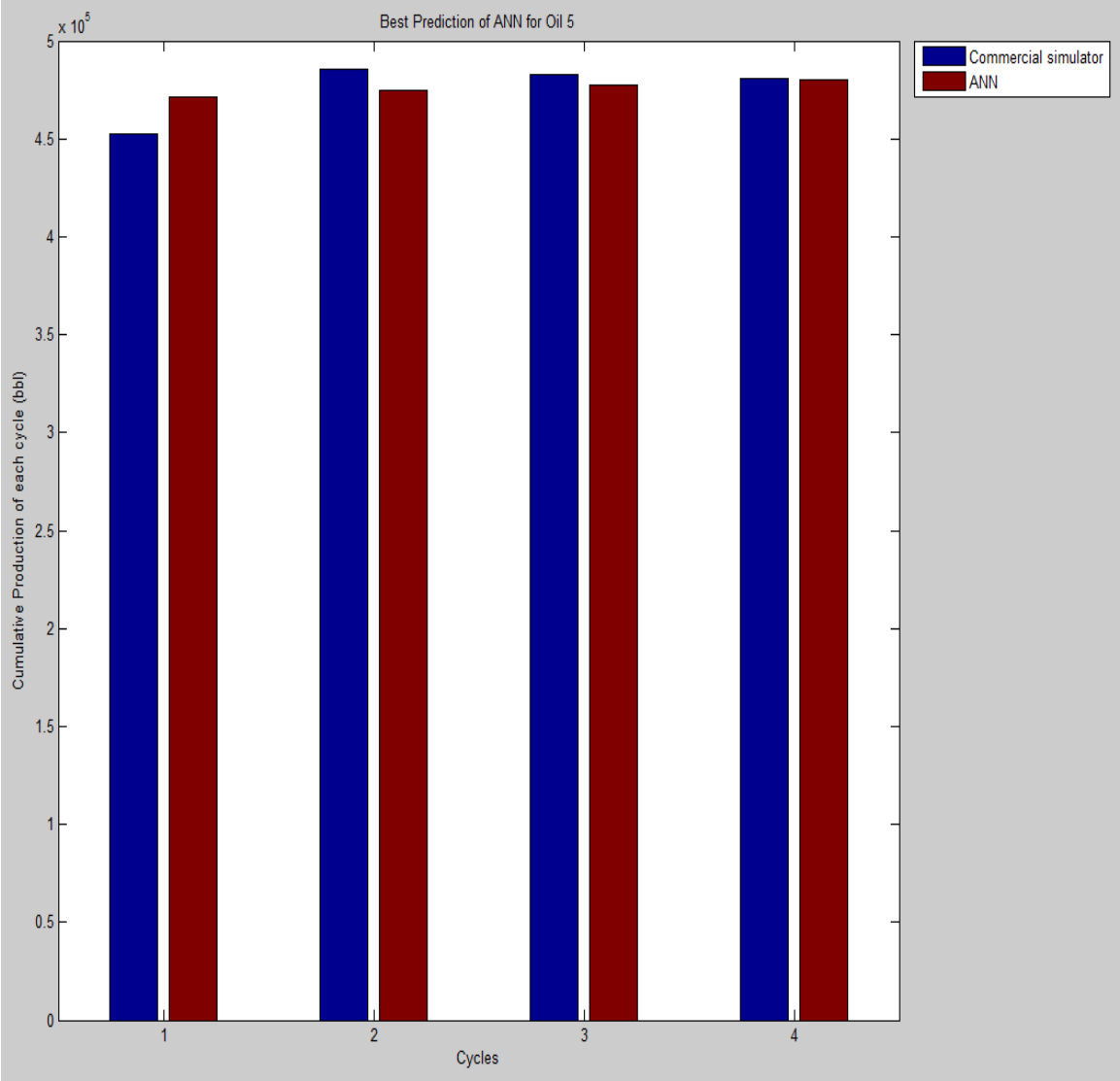

Figure **5-17**: Best prediction of network 5.

CYCLE	ERROR PERCENTAGE (%)
1	-4.11
2	2.22
3	1.11
4	0.21

Table **5-9**: Error percentage values of best prediction of network 5.

5.5.2 Worst Prediction of Network 5

The prediction of network 5 for sample 13 is worst of all the 26 testing samples. The input for this sample is shown as worst case in Figure **5-17**. Figure **5-19** shows a comparison of the cumulative production of each cycle as predicted by the commercial simulator and ANN. The error percentage (e) values for all the cycles for this sample are reported in Table **5-10**.

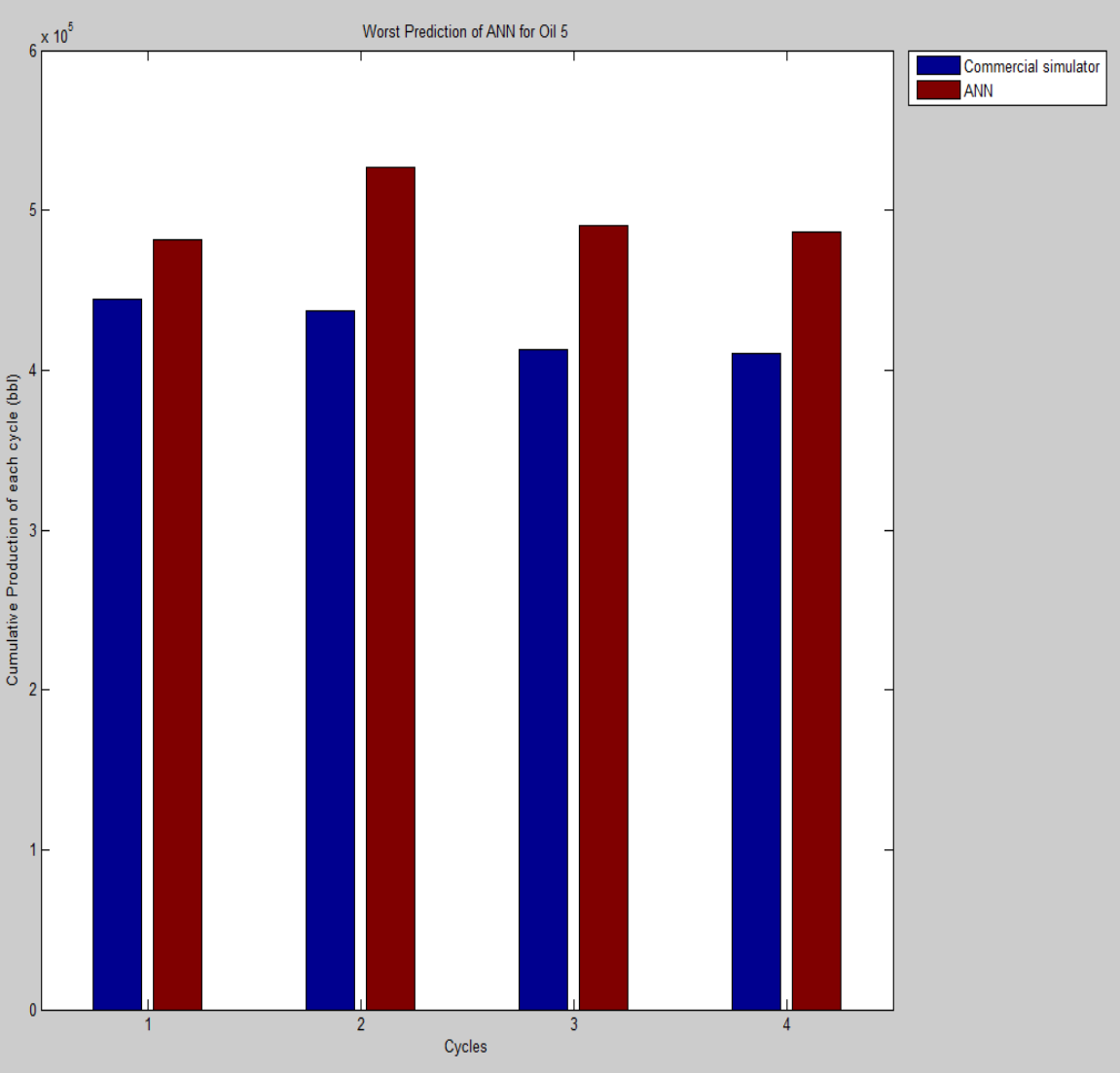

Figure **5-19**: Worst prediction of network 5.

CYCLE	ERROR PERCENTAGE (%)
1	-8.36
2	-20.47
3	-18.8
4	-18.54

Table **5-10**: Error percentage values of worst prediction of network 5.

5.5.3 Error Frequency of Network 5

The error percentages (e) of all the four cycles of 26 testing samples were recorded and a bar plot was made to study the frequency of error. In all, there were 104 points (26 samples X 4 cycles). Figure **5-20** is the bar plot reporting the error frequency of Network 5. The mean error percentage of these 26 testing samples is 6.75%.

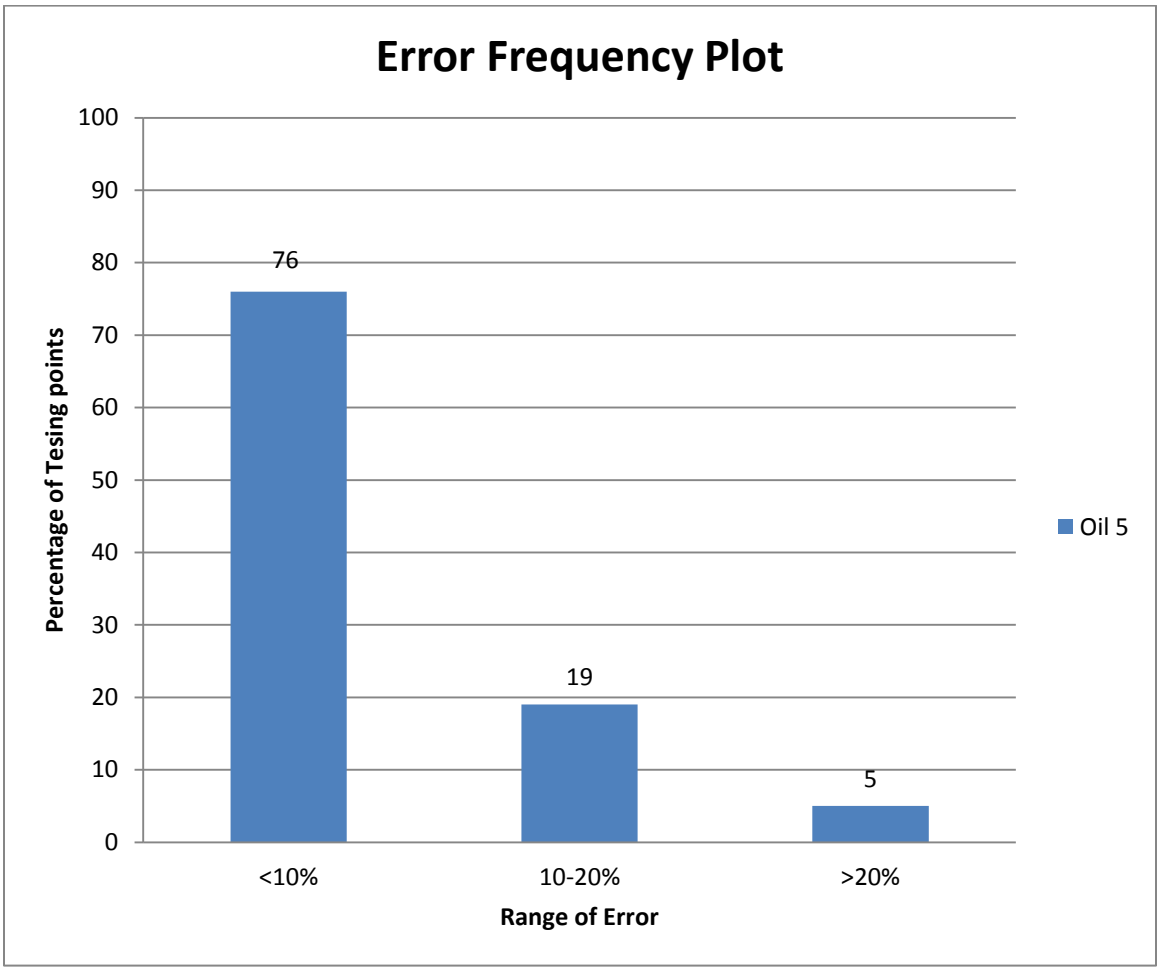

Figure **5-20**: Error frequency of Network 5.

The cumulative production at end of each cycle for oil 5 is also greater than 10^5 barrels. It can be observed that 95% of the testing points are below error percentage of 20. And there are no testing points with error percentage greater than 30%.

5.6 Sensitivity of Input Parameters

In order to study the effect of each input parameter on the output, sensitivity analysis was performed on all 14 input parameters. This was done by varying an input parameter to be studied between the minimum and maximum values given in Tables **4-7** and **4-8** and by keeping rest of the 13 parameters constant. The parameter was varied by dividing the range between minimum value and maximum value into ten equal points. Hence each input parameter was varied eleven times including the minimum and maximum value by keeping rest of the parameters constant. Table **5-11** shows how each input parameter was varied.

INPUT\RUN	1	2	3	4	5	6	7	8	9	10	11
Bhp (psi)	17	25.3	33.6	41.9	50.2	**58.5**	66.8	75.1	83.4	91.7	100
Drainage area (acres)	5	8.5	12	15.5	19	**22.5**	26	29.5	33	36.5	40
Fracture perm (md)	100	290	480	670	860	**1050**	1240	1430	1620	1810	2000
Fracture por	0.01	0.014	0.018	0.022	0.026	**0.03**	0.034	0.038	0.042	0.046	0.05
Fracture spacing (ft)	4	7.6	11.2	14.8	18.4	**22**	25.6	29.2	32.8	36.4	40
Initial oil saturation	0.4	0.435	0.47	0.505	0.54	**0.575**	0.61	0.645	0.68	0.715	0.75
Initial pressure (psi)	75	142.5	210	277.5	345	**412.5**	480	547.5	615	682.5	750
Initial temp (F)	120	132	144	156	168	**180**	192	204	216	228	240
Matrix perm (md)	10	29	48	67	86	**105**	124	143	162	181	200
Matrix por	0.15	0.165	0.18	0.195	0.21	**0.225**	0.24	0.255	0.27	0.285	0.3
Steam inj rate(bbl/d)	700	1130	1560	1990	2420	**2850**	3280	3710	4140	4570	5000
Steam quality	0.7	0.73	0.76	0.79	0.82	**0.85**	0.88	0.91	0.94	0.97	1
Steam temp (F)	450	465	480	495	510	**525**	540	555	570	585	600
Thickness (ft)	20	38	56	74	92	**110**	128	146	164	182	200

Table **5-11**: Values of input parameters when they are varied.

Run 1 is the minimum value of a parameter and run 11 is the maximum value. Run 6 is the base simulation file in entire sensitivity analysis. When sensitivity of matrix porosity was studied, it was varied from 0.15 to 0.3 as shown in Table **5-11**. However, rest of the parameters were kept at a constant with the values given in run 6 of Table **5-11**. For example, while studying the effect of matrix porosity on output, the input parameter values were assigned as shown in Table **5-12**.

INPUT\RUN	1	2	3	4	5	6	7	8	9	10	11
Bhp (psi)	58.5	58.5	58.5	58.5	58.5	**58.5**	58.5	58.5	58.5	58.5	58.5
Drainage area (acres)	22.5	22.5	22.5	22.5	22.5	**22.5**	22.5	22.5	22.5	22.5	22.5
Fracture perm (md)	1050	1050	1050	1050	1050	**1050**	1050	1050	1050	1050	1050
Fracture por	0.03	0.03	0.03	0.03	0.03	**0.03**	0.03	0.03	0.03	0.03	0.03
Fracture spacing (ft)	22	22	22	22	22	**22**	22	22	22	22	22
Initial oil saturation	0.575	0.575	0.575	0.575	0.575	**0.575**	0.575	0.575	0.575	0.575	0.575
Initial pressure (psi)	412.5	412.5	412.5	412.5	412.5	**412.5**	412.5	412.5	412.5	412.5	412.5
Initial temp (F)	180	180	180	180	180	**180**	180	180	180	180	180
Matrix perm (md)	105	105	105	105	105	**105**	105	105	105	105	105
Matrix por	0.15	0.165	0.18	0.195	0.21	**0.225**	0.24	0.255	0.27	0.285	0.3
Steam inj rate(bbl/d)	2850	2850	2850	2850	2850	**2850**	2850	2850	2850	2850	2850
Steam quality	0.85	0.85	0.85	0.85	0.85	**0.85**	0.85	0.85	0.85	0.85	0.85
Steam temp (F)	525	525	525	525	525	**525**	525	525	525	525	525
Thickness (ft)	110	110	110	110	110	**110**	110	110	110	110	110

Table **5-12**: Values of input parameters for studying sensitivity of matrix porosity.

Similarly when sensitivity of any other parameter say drainage area is studied, it is varied between 5-40 acres as shown in Table **5-11** and rest of parameters are kept constant with the base run (run 6) values. The values of input parameters while studying the sensitivity of drainage area are shown in Table **5-13**. While studying the effect of a particular parameter, same values were used irrespective of the oil i.e., Tables **5-12** &

5-13 were used to study Figure **5-20** is a schematic of run 6 also known as base run or base simulation file.

INPUT\RUN	1	2	3	4	5	6	7	8	9	10	11
Bhp (psi)	58.5	58.5	58.5	58.5	58.5	**58.5**	58.5	58.5	58.5	58.5	58.5
Drainage area (acres)	5	8.5	12	15.5	19	**22.5**	26	29.5	33	36.5	40
Fracture perm (md)	1050	1050	1050	1050	1050	**1050**	1050	1050	1050	1050	1050
Fracture por	0.03	0.03	0.03	0.03	0.03	**0.03**	0.03	0.03	0.03	0.03	0.03
Fracture spacing (ft)	22	22	22	22	22	**22**	22	22	22	22	22
Initial oil saturation	0.575	0.575	0.575	0.575	0.575	**0.575**	0.575	0.575	0.575	0.575	0.575
Initial pressure (psi)	412.5	412.5	412.5	412.5	412.5	**412.5**	412.5	412.5	412.5	412.5	412.5
Initial temp (F)	180	180	180	180	180	**180**	180	180	180	180	180
Matrix perm (md)	105	105	105	105	105	**105**	105	105	105	105	105
Matrix por	0.225	0.225	0.225	0.225	0.225	**0.225**	0.225	0.225	0.225	0.225	0.225
Steam inj rate(bbl/d)	2850	2850	2850	2850	2850	**2850**	2850	2850	2850	2850	2850
Steam quality	0.85	0.85	0.85	0.85	0.85	**0.85**	0.85	0.85	0.85	0.85	0.85
Steam temp (F)	525	525	525	525	525	**525**	525	525	525	525	525
Thickness (ft)	110	110	110	110	110	**110**	110	110	110	110	110

Table **5-13**: Values of input parameters for studying sensitivity of drainage area.

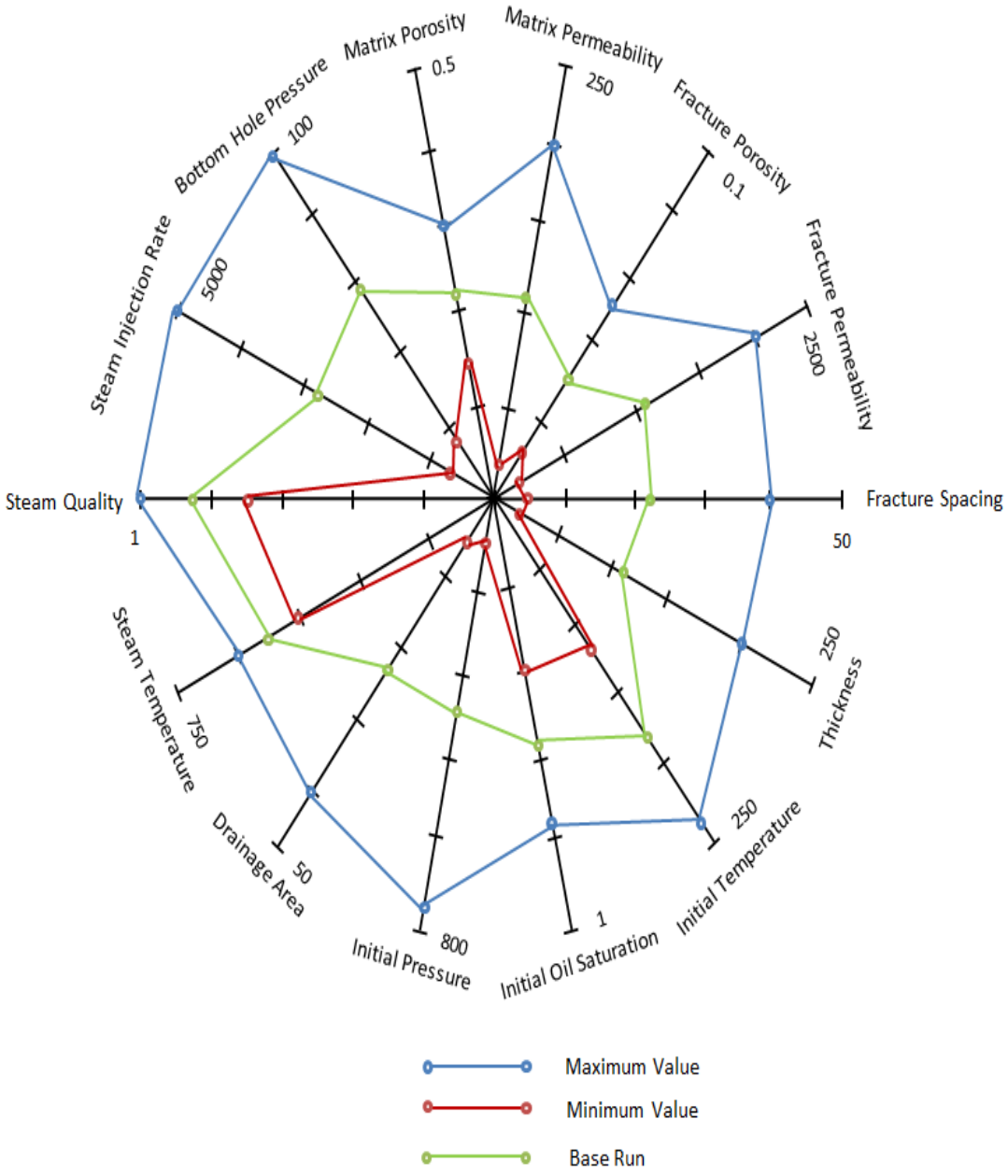

Figure **5-21**: Schematic of base run (run 6).

5.6.1 Sensitivity of Bottom Hole Pressure

Figures **5-22**, **5-23**, **5-24**, **5-25** & **5-26** show the sensitivity of bottom hole pressure on cumulative production for oils 1, 2, 3, 4 & 5 respectively. In all these figures, run 6 is the base simulation file.

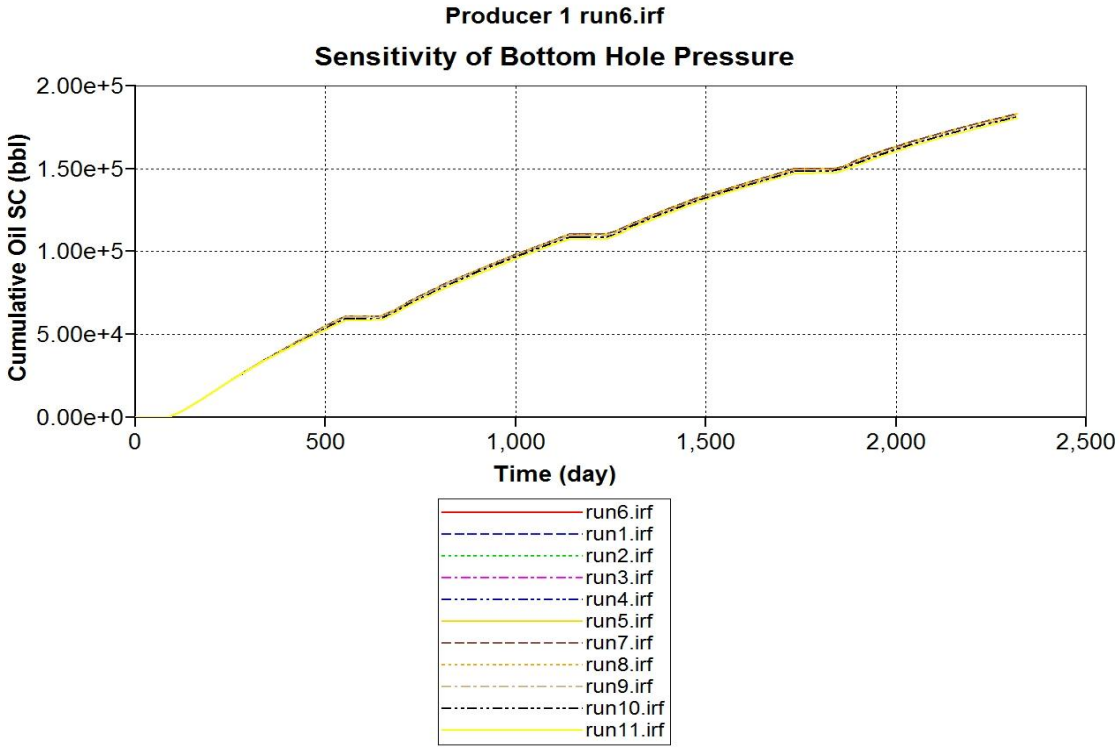

Figure **5-22**: Sensitivity of bottom hole pressure on cumulative production of oil 1.

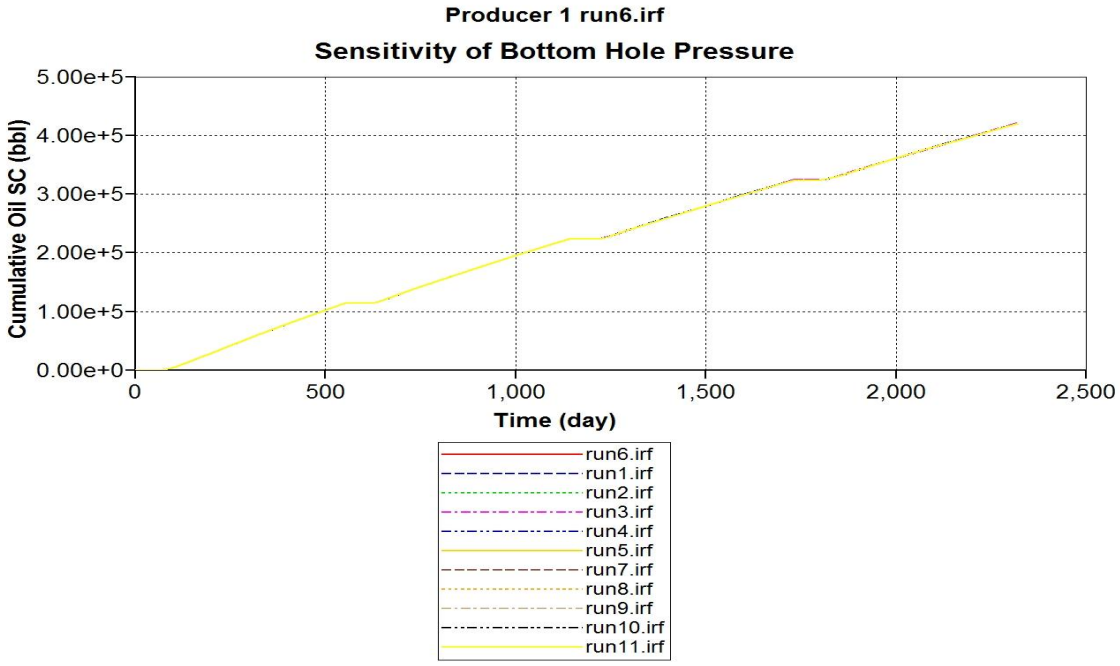

Figure **5-23**: Sensitivity of bottom hole pressure on cumulative production of oil 2.

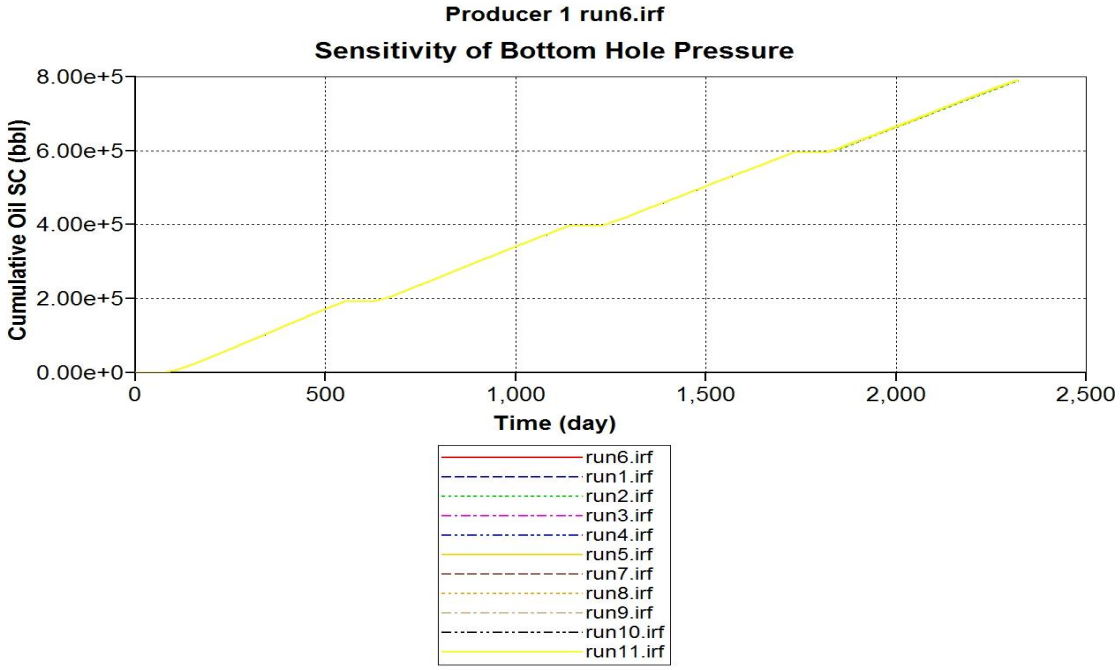

Figure **5-24**: Sensitivity of bottom hole pressure on cumulative production of oil 3.

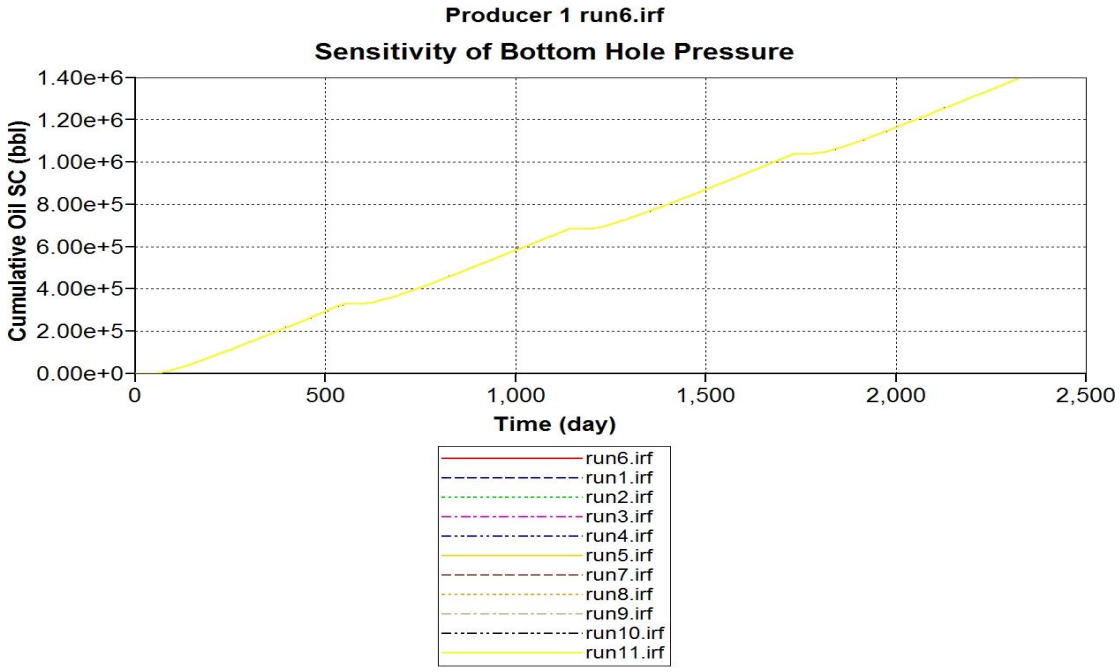

Figure **5-25**: Sensitivity of bottom hole pressure on cumulative production of oil 4.

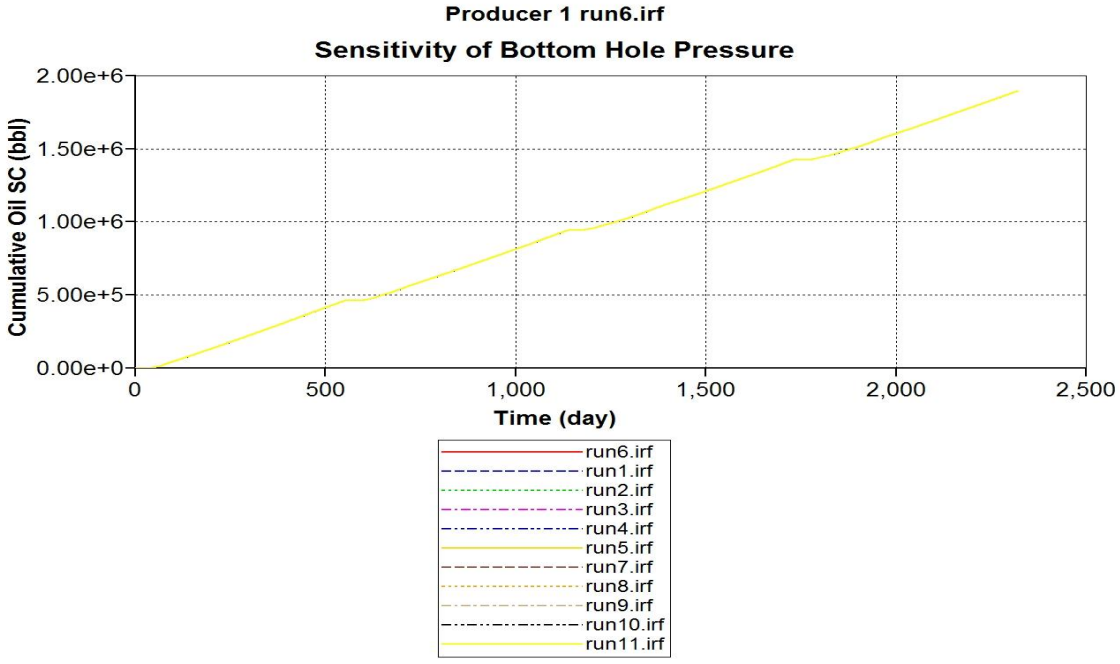

Figure **5-26**: Sensitivity of bottom hole pressure on cumulative production of oil 5.

It can be observed from the plots above that the effect of bottom hole pressure on cumulative production of reservoirs containing various oils is insignificant. Irrespective of the oil present in the reservoir variation in bottom hole pressure has insignificant account on the cumulative production. The possible reason for this is: the bottom hole pressure was varied only between 17 to 100 psia. This margin is too small to observe any significant difference in cumulative production.

5.6.2 Sensitivity of Drainage Area

Figures **5-27**, **5-28**, **5-29**, **5-30** & **5-31** show the sensitivity of drainage area on cumulative production for oils 1, 2, 3, 4 & 5 respectively. In all these figures, run 6 is the base simulation file.

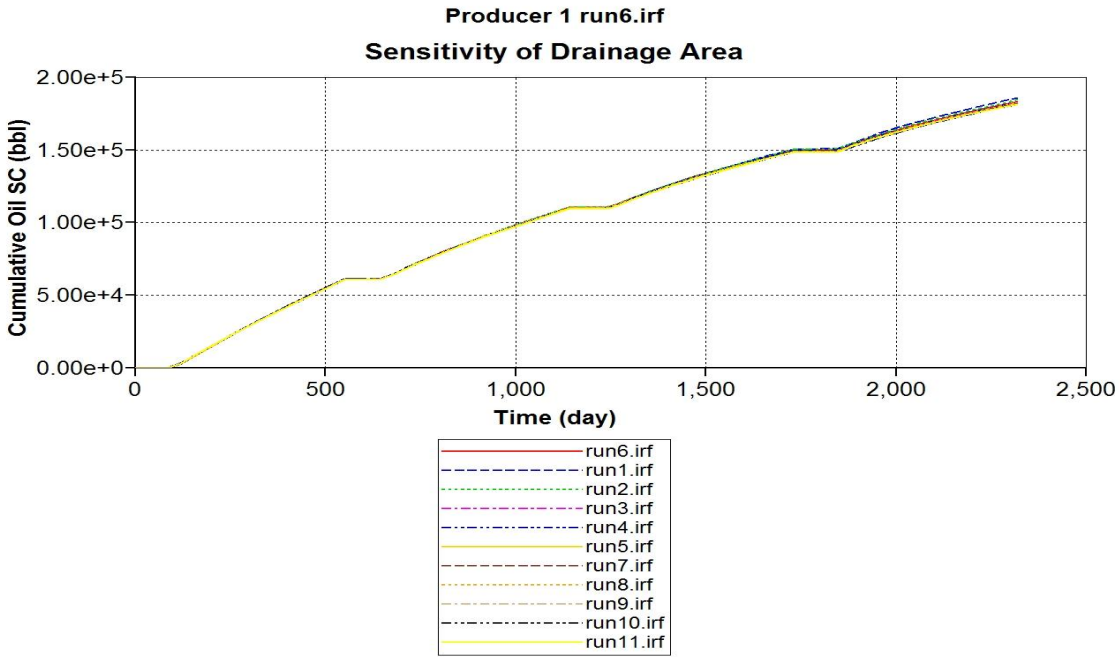

Figure **5-27**: Sensitivity of drainage area on cumulative production of oil 1.

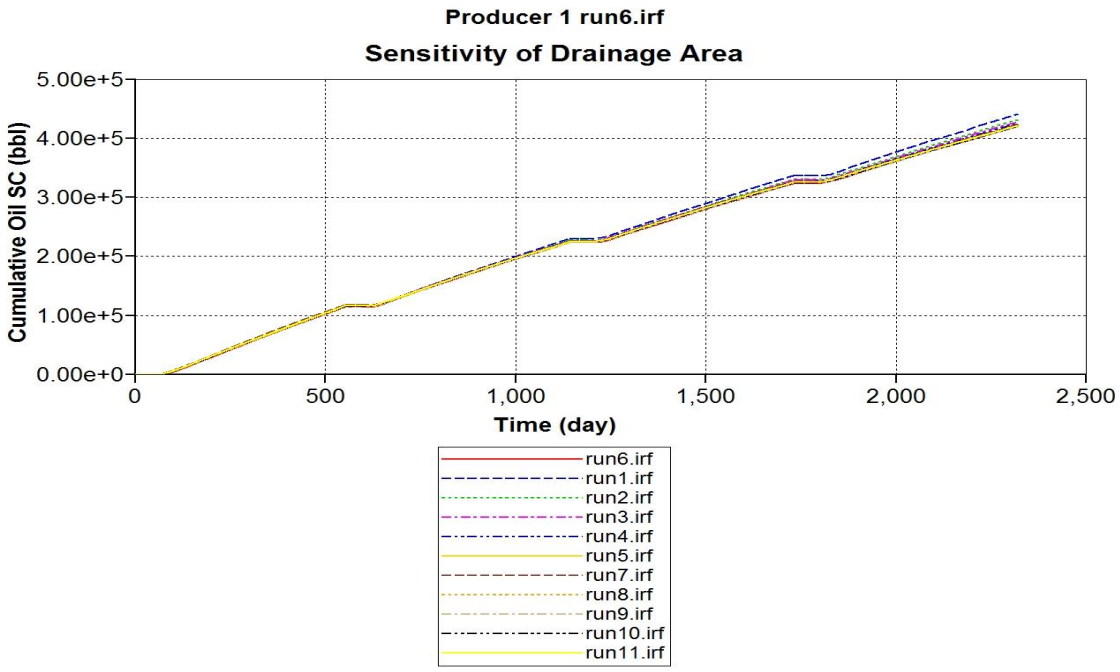

Figure **5-28**: Sensitivity of drainage area on cumulative production of oil 2.

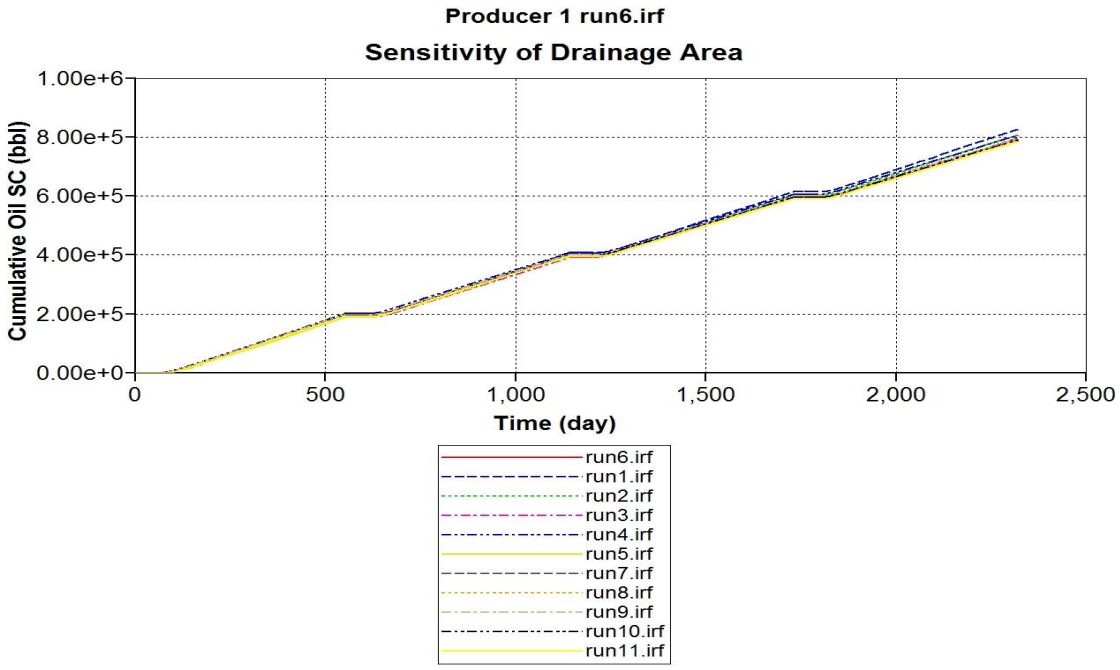

Figure **5-29**: Sensitivity of drainage area on cumulative production of oil 3.

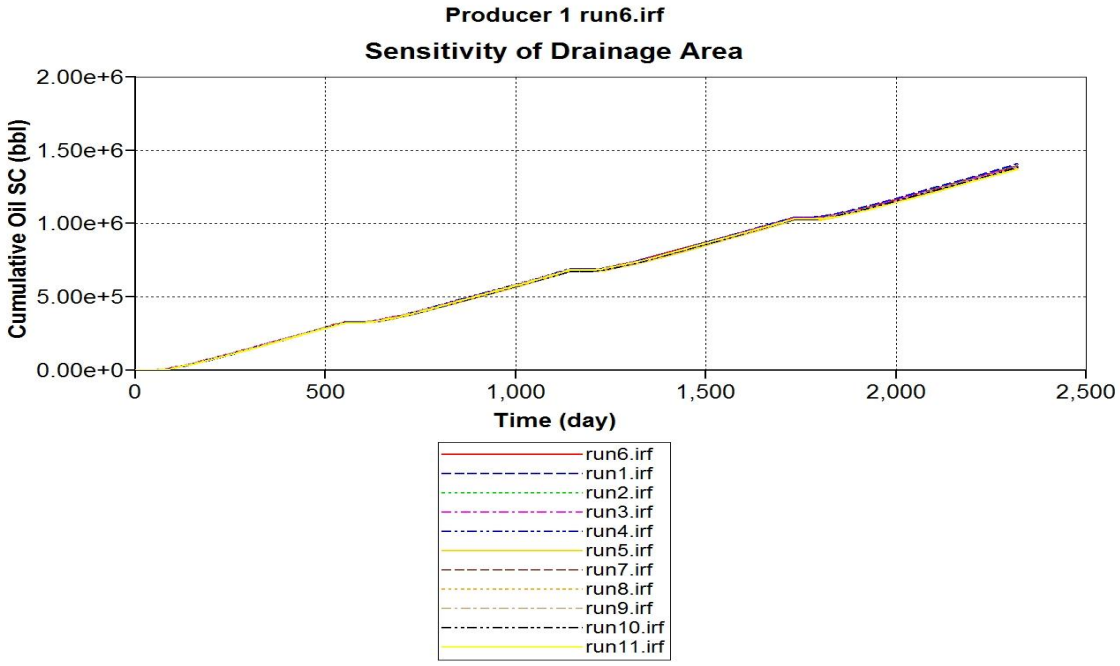

Figure **5-30**: Sensitivity of drainage area on cumulative production of oil 4.

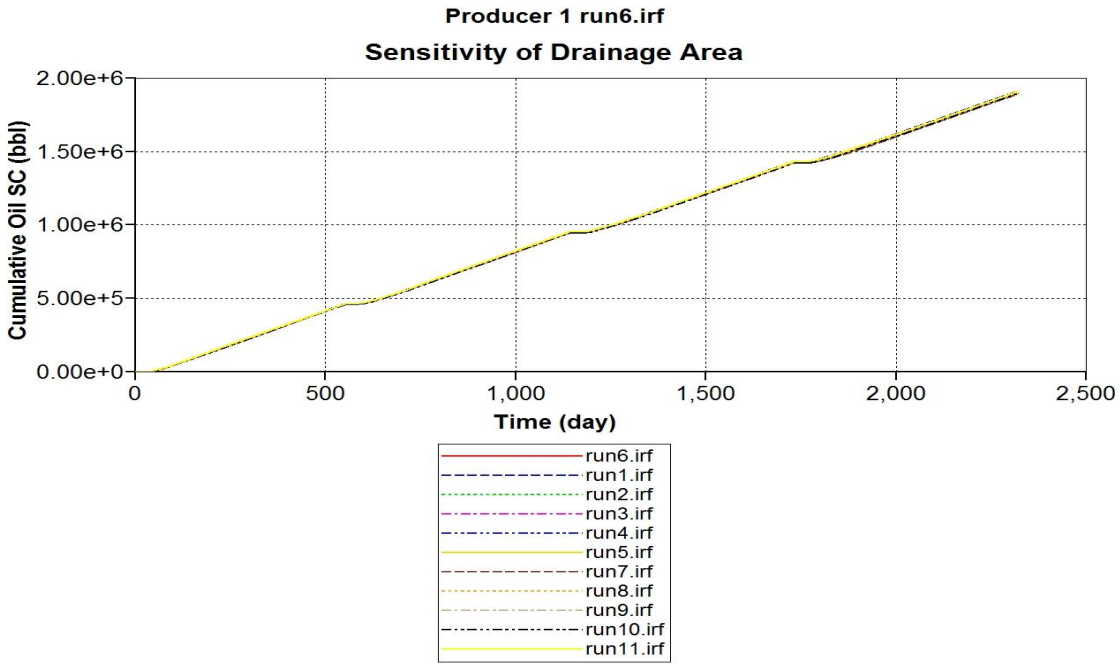

Figure **5-31**: Sensitivity of drainage area on cumulative production of oil 5.

It can be observed from plots above that drainage area has little effect on cumulative production of all the oils. For particular oil the variation in drainage area from 5 to 40 acres brings only small change in cumulative production. This could be because in this project the injection, soaking and production cycles have been kept constant. Hence even though the drainage area is increased, only certain portion of the reservoir is affected by injected steam.

5.6.3 Sensitivity of Fracture Permeability

Figures **5-32**, **5-33**, **5-34**, **5-35** & **5-36** show the sensitivity of fracture permeability on cumulative production for oils 1, 2, 3, 4 & 5 respectively. In all these figures, run 6 is the base simulation file.

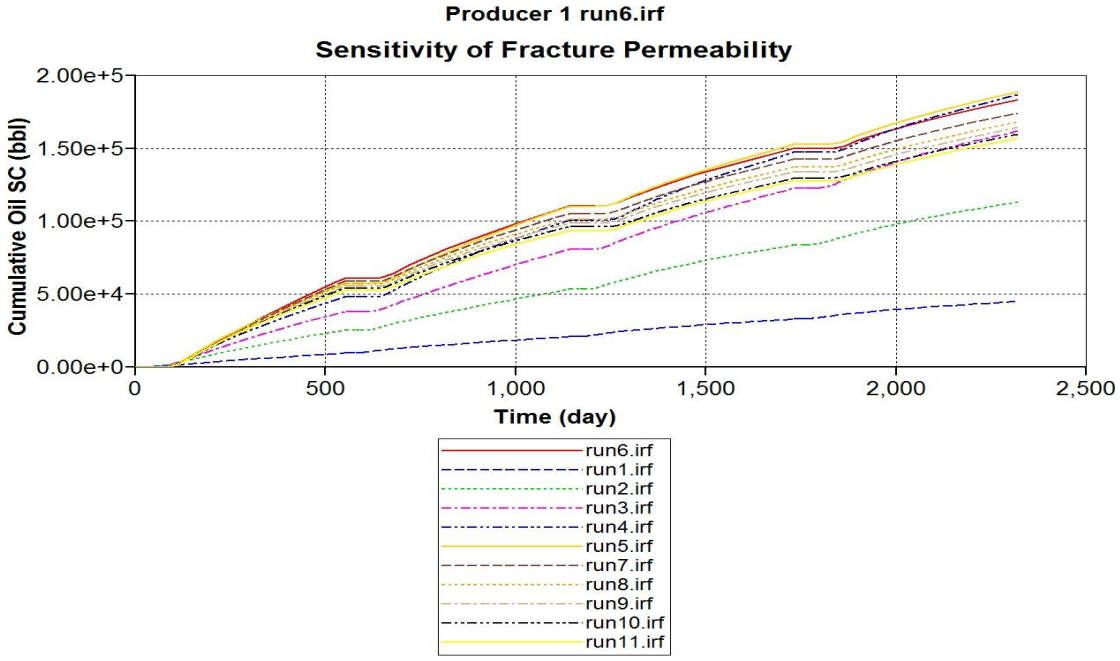

Figure **5-32**: Sensitivity of fracture permeability on cumulative production of oil 1.

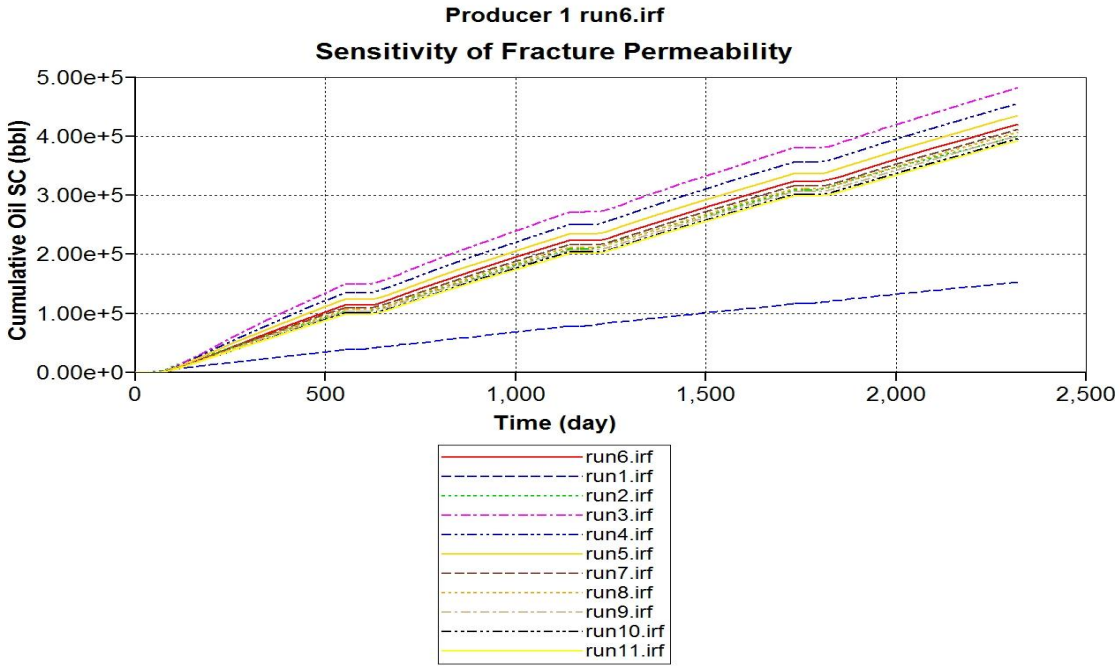

Figure **5-33**: Sensitivity of fracture permeability on cumulative production of oil 2.

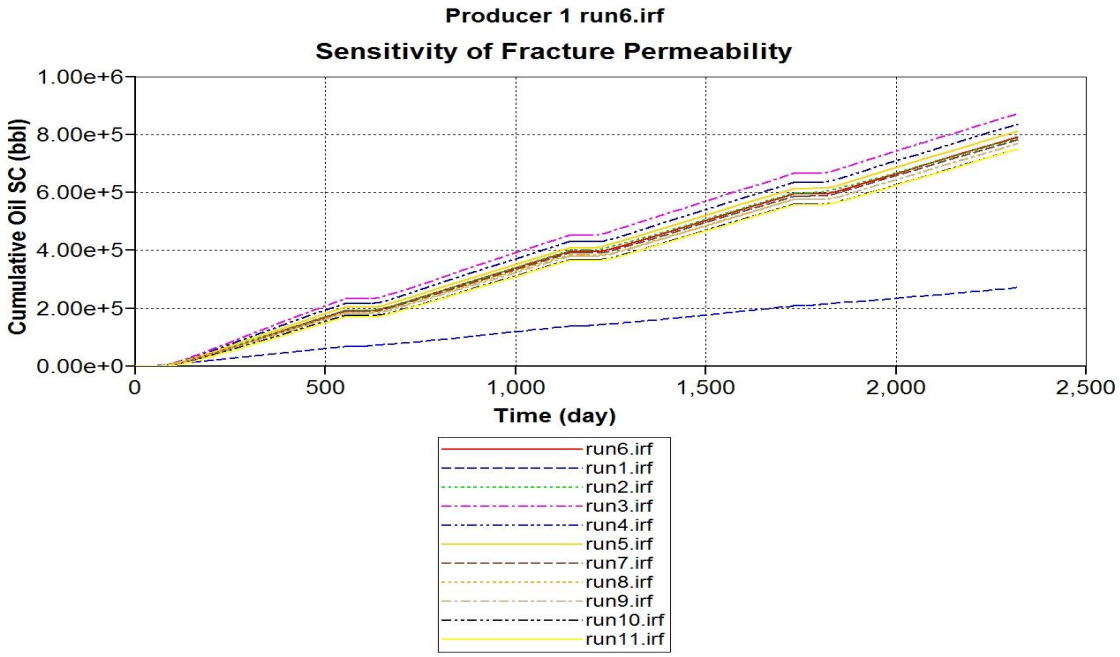

Figure **5-34**: Sensitivity of fracture permeability on cumulative production of oil 3.

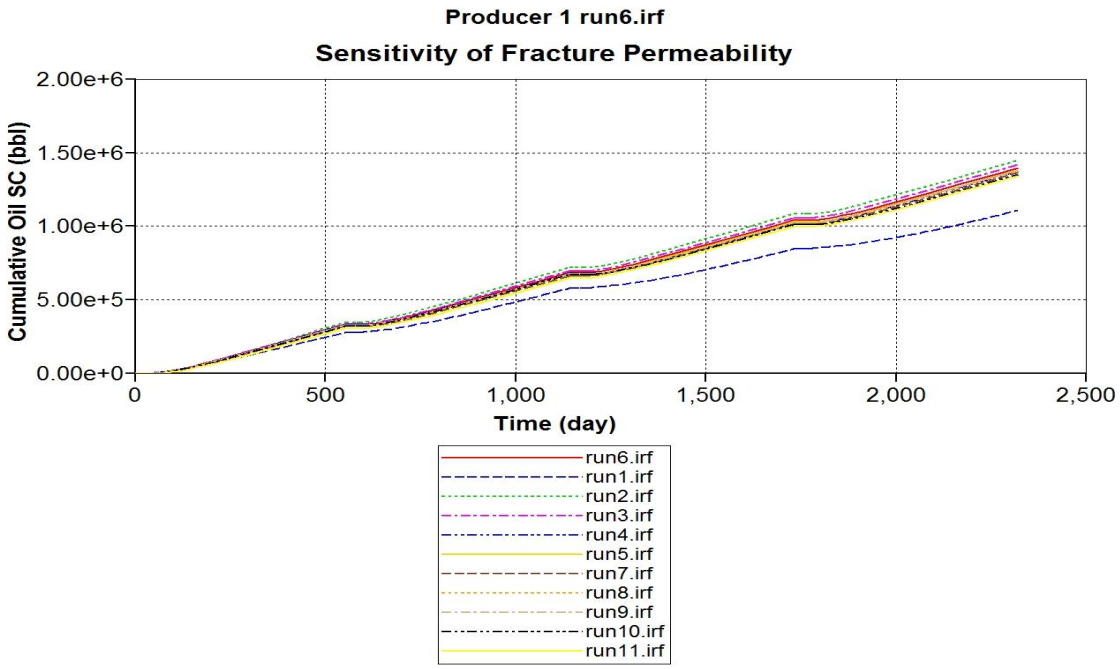

Figure **5-35**: Sensitivity of fracture permeability on cumulative production of oil 4.

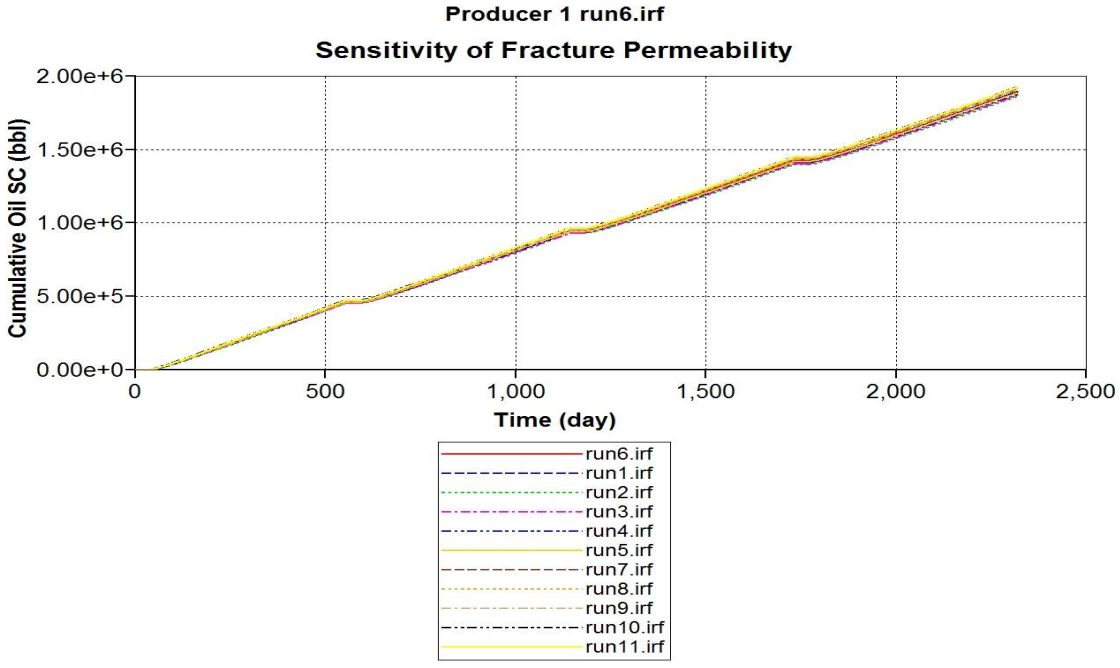

Figure **5-36**: Sensitivity of fracture permeability on cumulative production of oil 5.

It can be observed from the plots above that fracture permeability has significant effect on cumulative production. This is particularly true for oils 1, 2. 3 & 4.

5.6.4 Sensitivity of Fracture Porosity

Figures **5-37**, **5-38**, **5-39**, **5-40** & **5-41** show the sensitivity of fracture porosity on cumulative production for oils 1, 2, 3, 4 & 5 respectively. In all these figures, run 6 is the base simulation file.

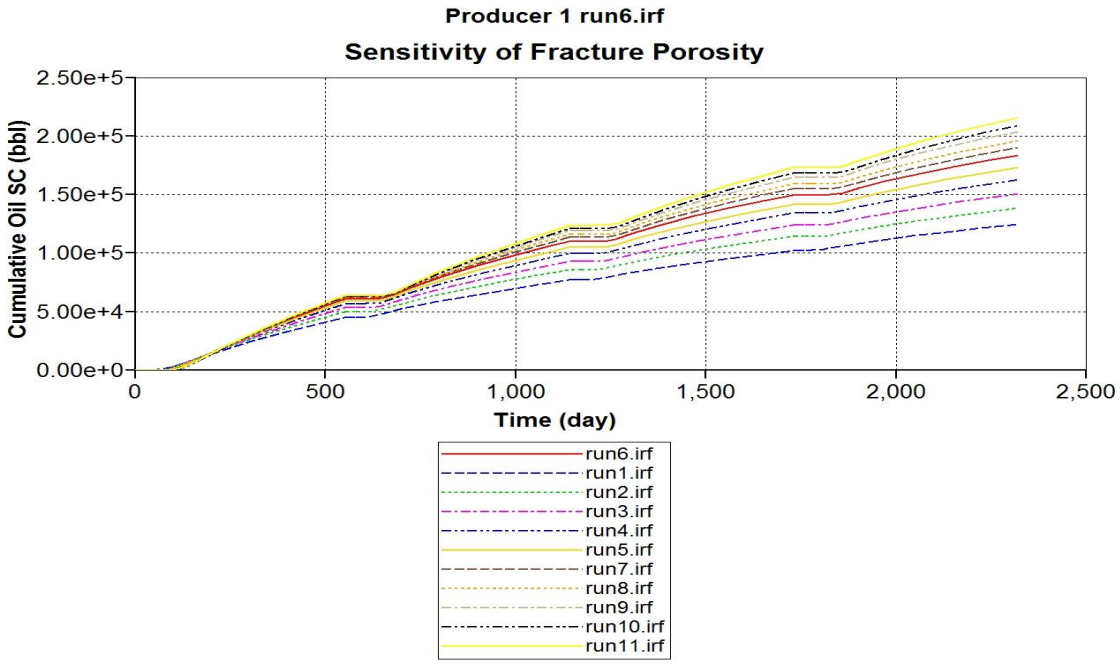

Figure **5-37**: Sensitivity of fracture porosity on cumulative production of oil 1.

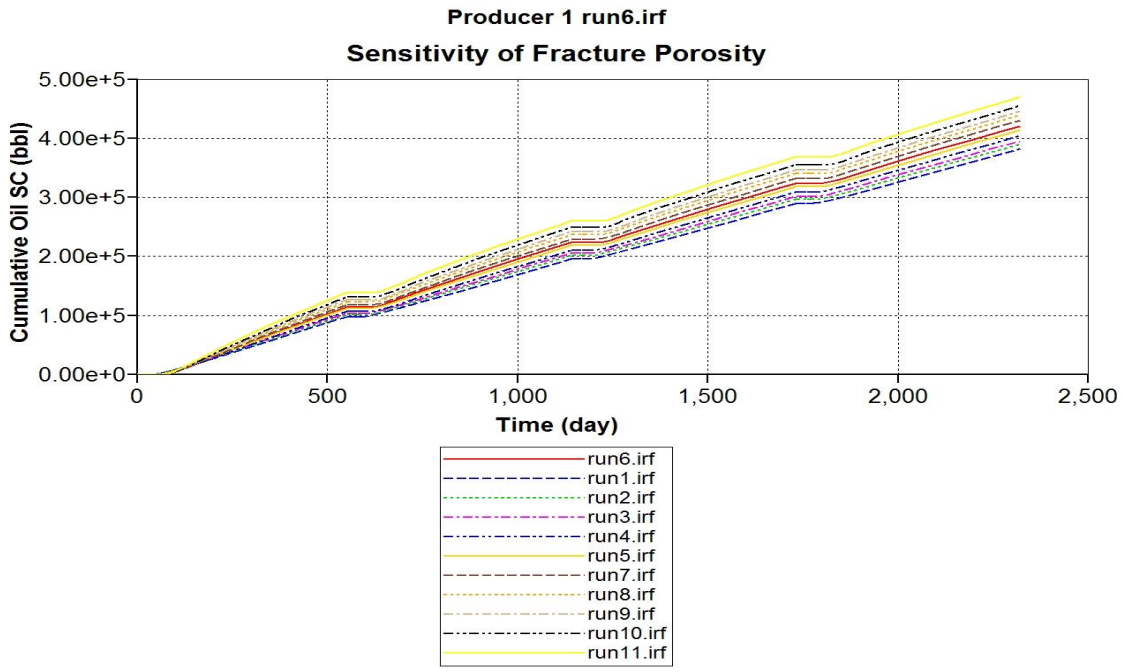

Figure **5-38**: Sensitivity of fracture porosity on cumulative production of oil 2.

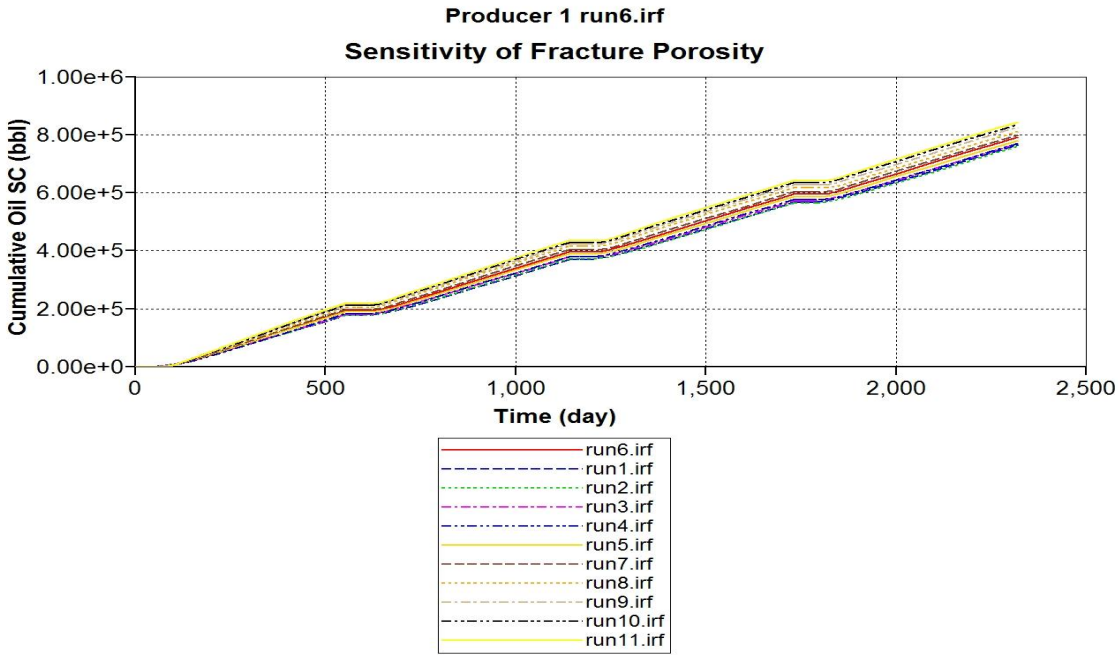

Figure **5-39**: Sensitivity of fracture porosity on cumulative production of oil 3.

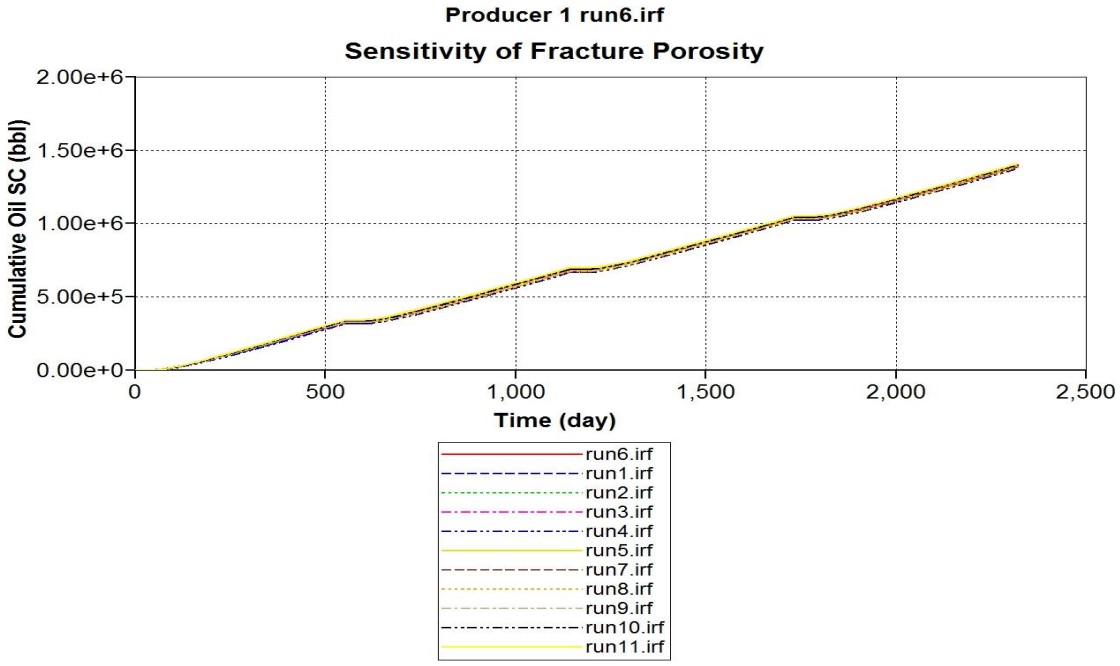

Figure **5-40**: Sensitivity of fracture porosity on cumulative production of oil 4.

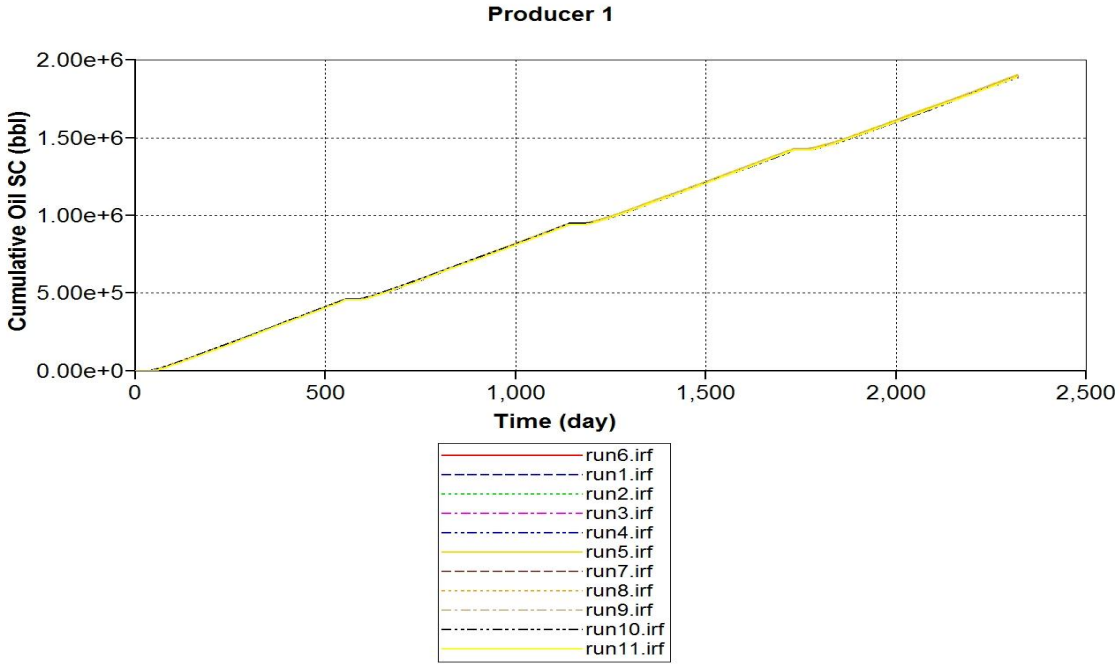

Figure **5-41**: Sensitivity of fracture porosity on cumulative production of oil 5.

It can be observed from the plots above that fracture porosity has significant effect on cumulative production. This effect cannot be clearly seen in Figures **5-40** & **5-41** because the scale is in the order of one million barrels and the difference between various runs is in the order of 10^5 barrels.

5.6.5 Sensitivity of Fracture Spacing

Figures **5-42**, **5-43**, **5-44**, **5-45** & **5-46** show the sensitivity of fracture spacing on cumulative production for oils 1, 2, 3, 4 & 5 respectively. In all these figures, run 6 is the base simulation file.

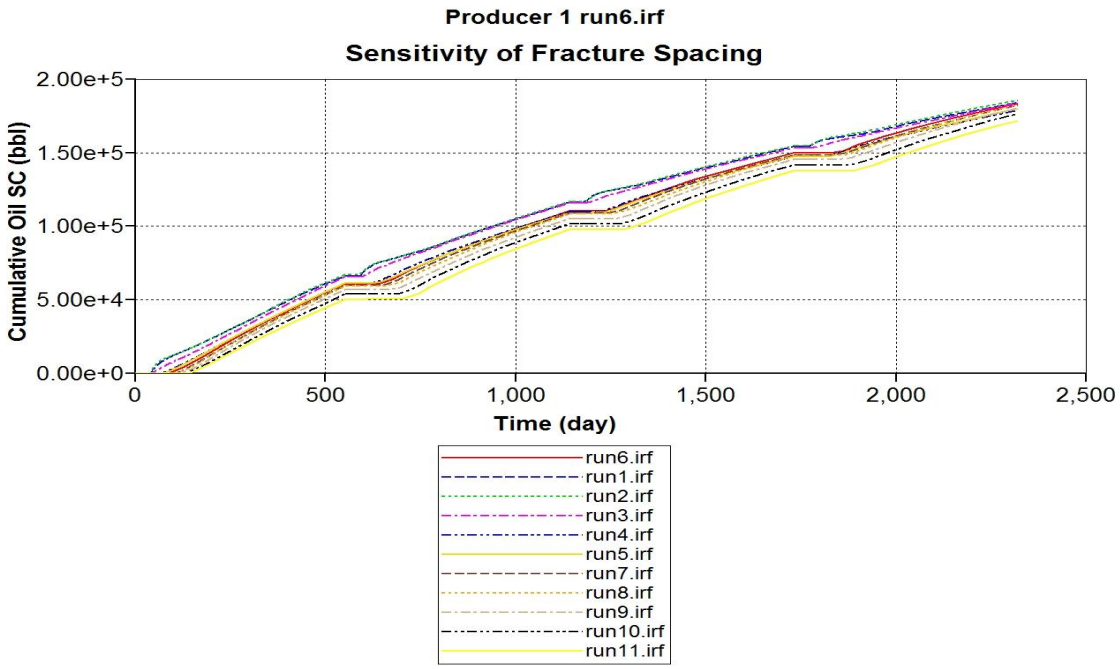

Figure **5-42**: Sensitivity of fracture spacing on cumulative production of oil 1.

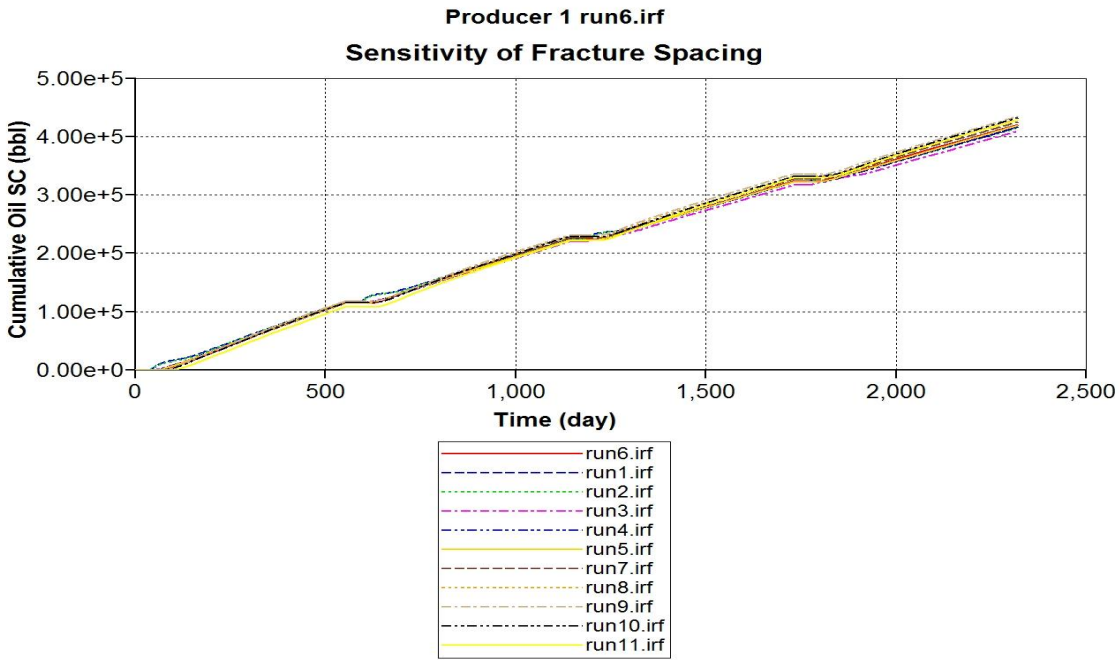

Figure **5-43**: Sensitivity of fracture spacing on cumulative production of oil 2.

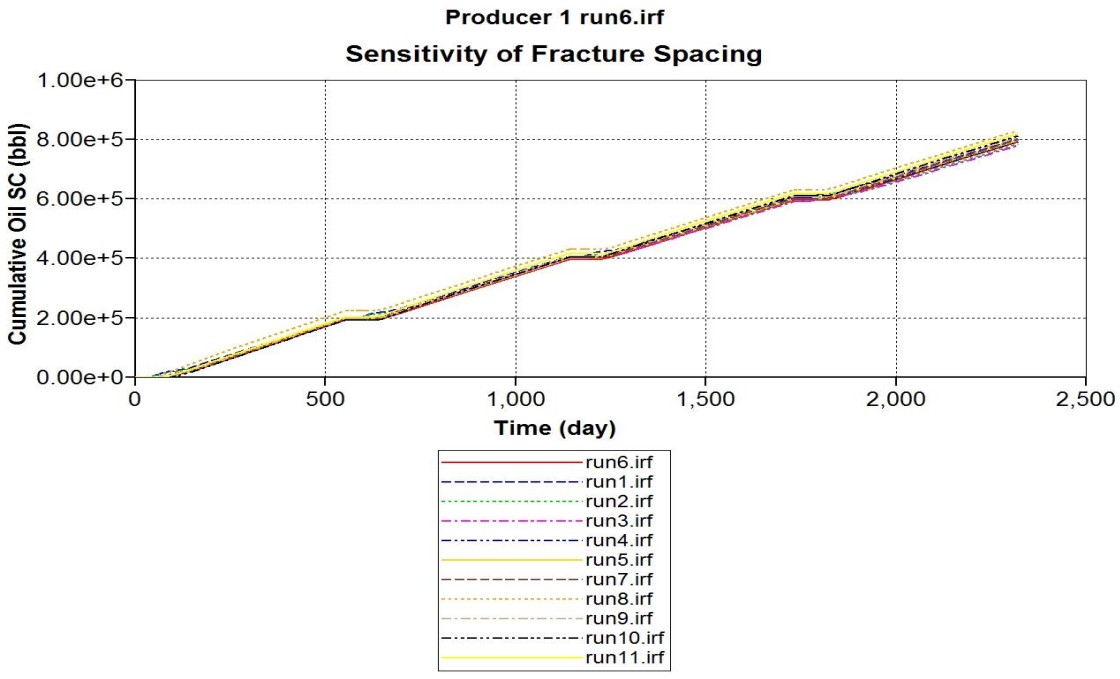

Figure **5-44**: Sensitivity of fracture spacing on cumulative production of oil 3.

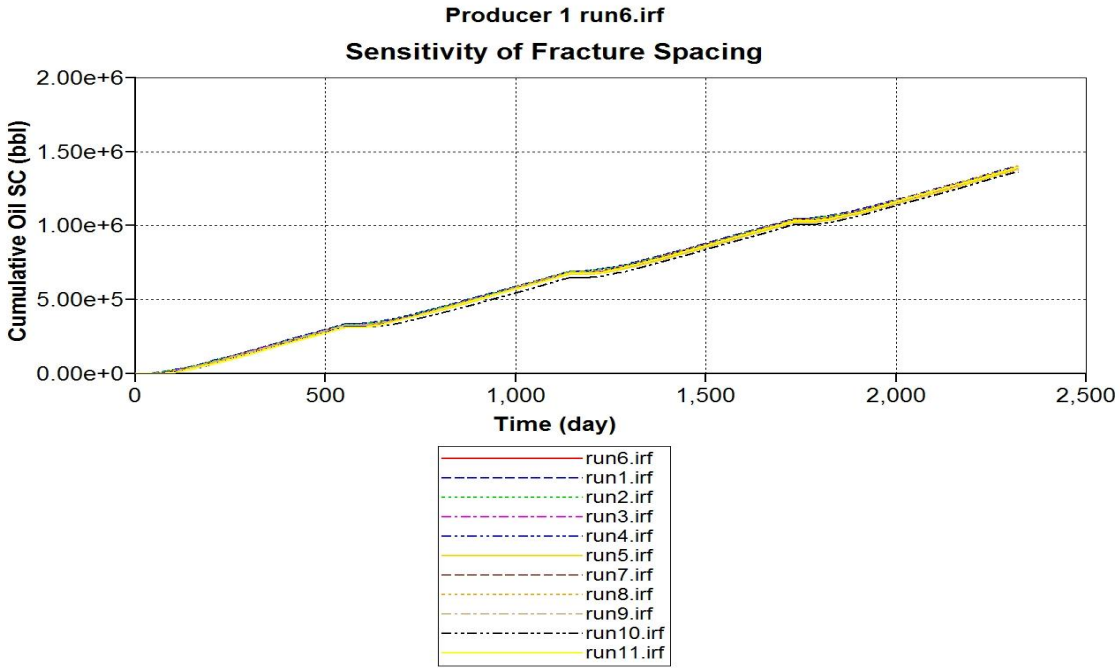

Figure **5-45**: Sensitivity of fracture spacing on cumulative production of oil 4.

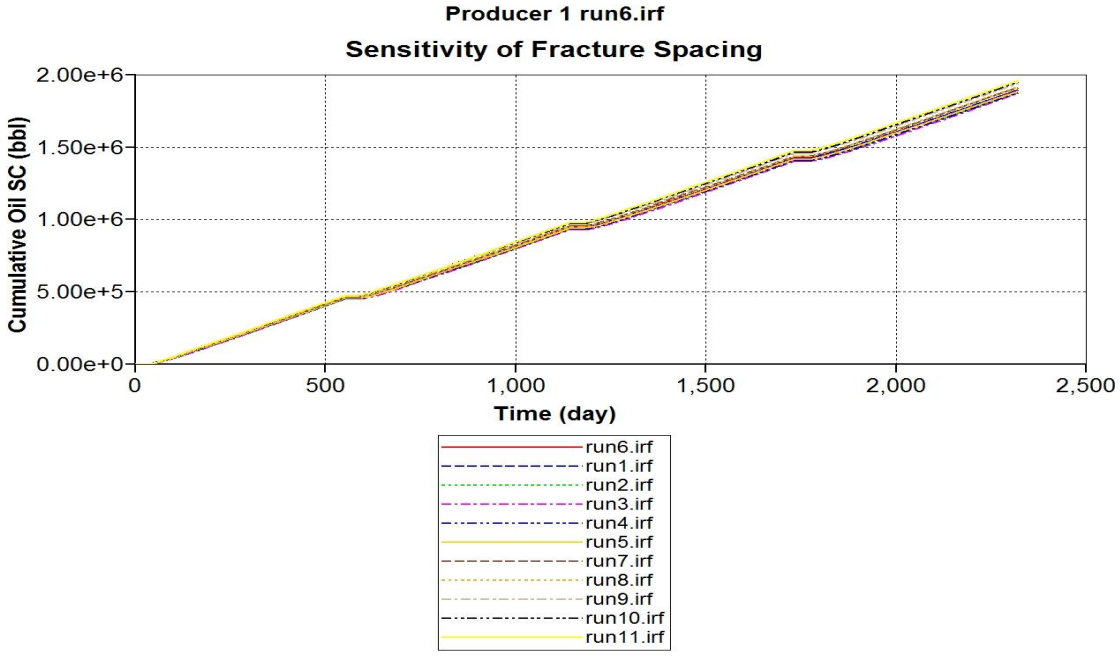

Figure **5-46**: Sensitivity of fracture spacing on cumulative production of oil 5.

It can be observed from plots above that fracture spacing does not have a very significant effect on cumulative production of any of the oils.

5.6.6 Sensitivity of Initial Oil Saturation (IOS)

Figures **5-47**, **5-48**, **5-49**, **5-50** & **5-51** show the sensitivity of initial oil saturation on cumulative production for oils 1, 2, 3, 4 & 5 respectively. In all these figures, run 6 is the base simulation file.

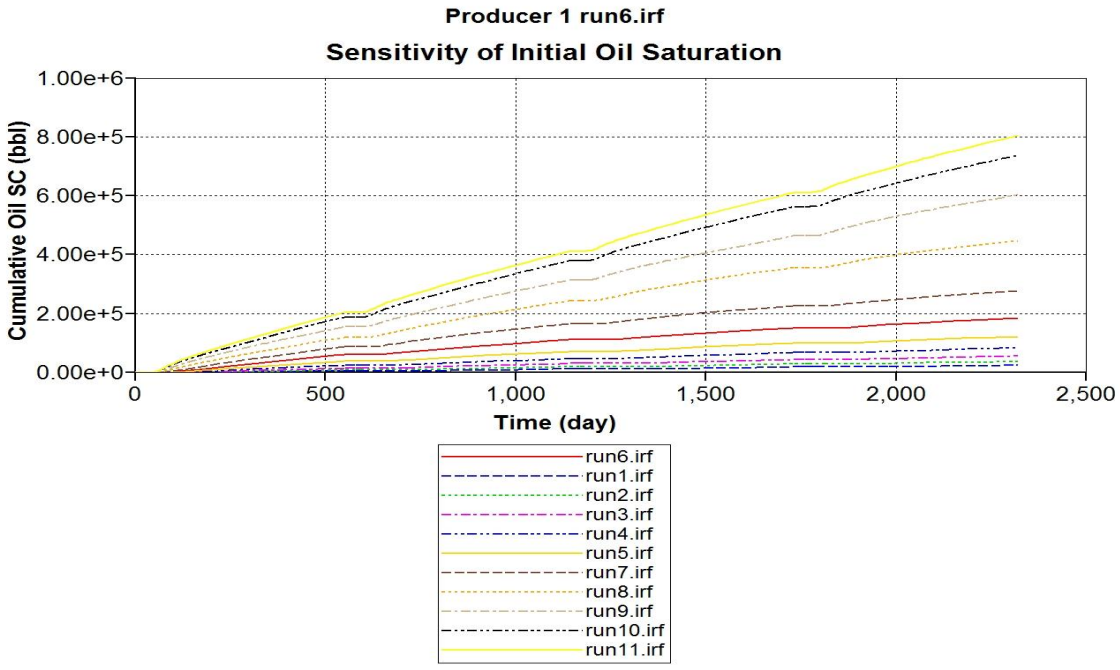

Figure **5-47**: Sensitivity of IOS on cumulative production of oil 1.

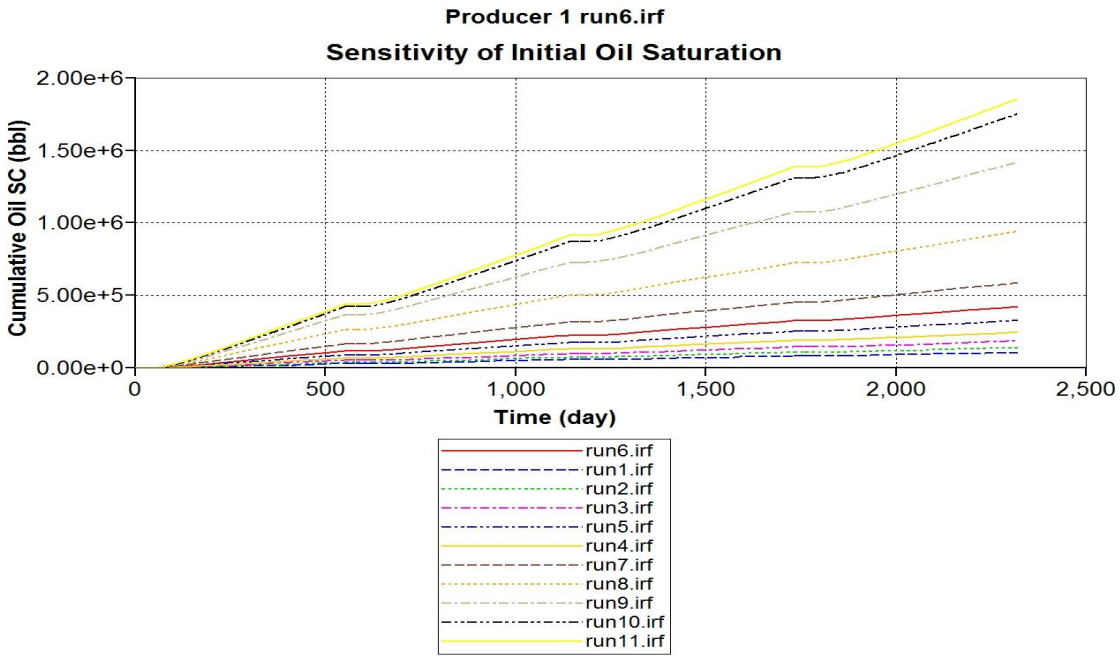

Figure **5-48**: Sensitivity of IOS on cumulative production of oil 2.

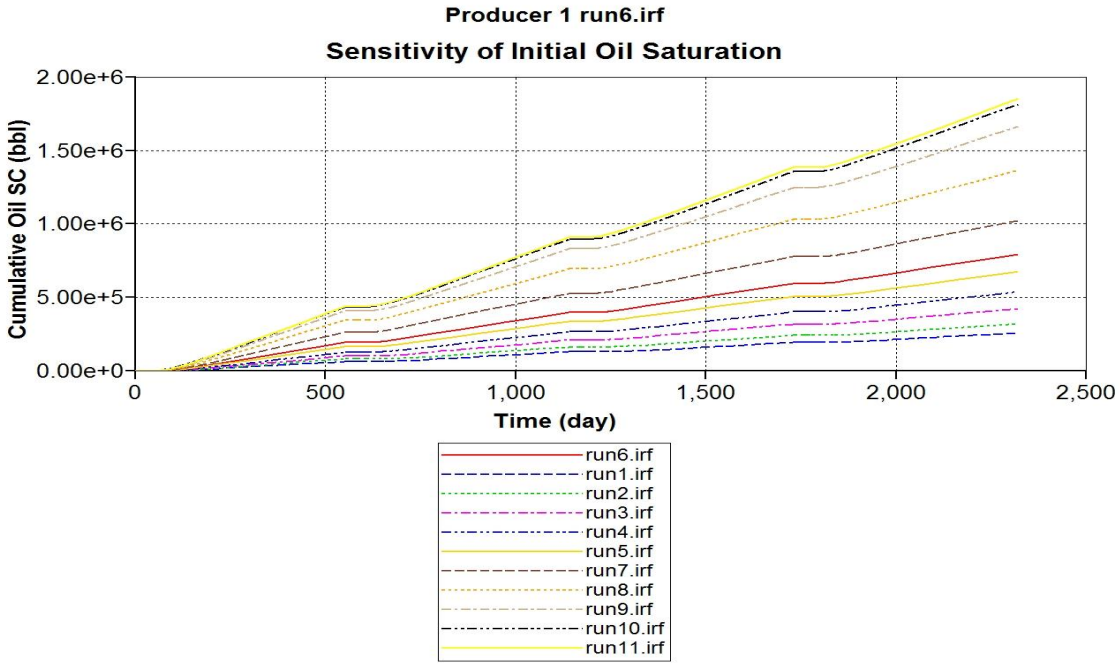

Figure **5-49**: Sensitivity of IOS on cumulative production of oil 3.

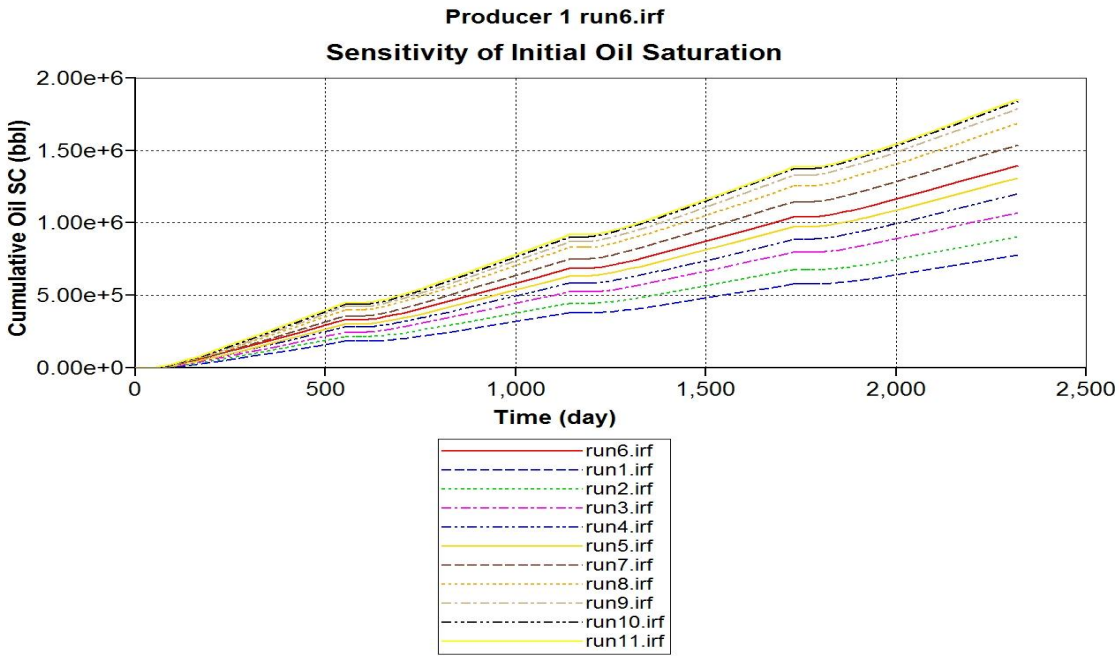

Figure **5-50**: Sensitivity of IOS on cumulative production of oil 4.

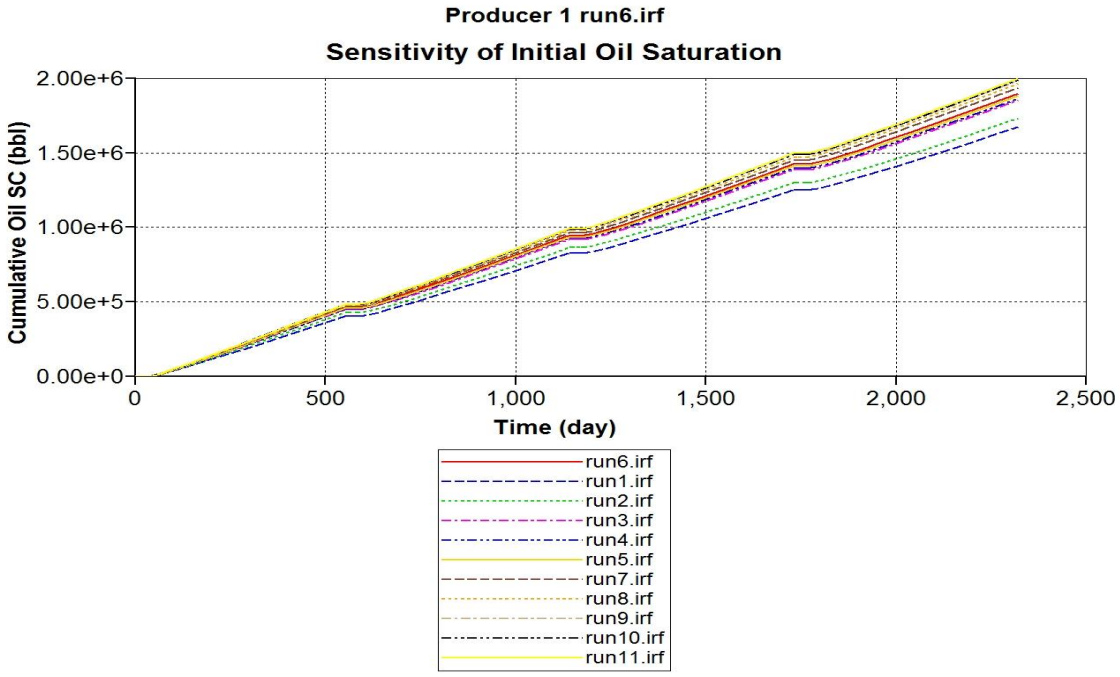

Figure **5-51**: Sensitivity of IOS on cumulative production of oil 5.

It can be observed from plots above that initial oil saturation has a very significant effect on cumulative production of all the oils. As a reservoir has more initial oil saturation more oil is produced from the reservoir. As we move from oil 1 to oil 4 it can be observed that more oil is produced from the reservoir as the oil saturation increases. However, as we move to oil 5 the increase in production at the end of all cycles is not as significant as oil 4. The possible reason for this could be that in this project the production period is constant at 550 days/cycle. If the production period was varied reservoir containing oil 5 would have produced more for longer periods.

5.6.7 Sensitivity of Initial Pressure

Figures **5-52**, **5-53**, **5-54**, **5-55** & **5-56** show the sensitivity of initial pressure on cumulative production for oils 1, 2, 3, 4 & 5 respectively. In all these figures, run 6 is the base simulation file.

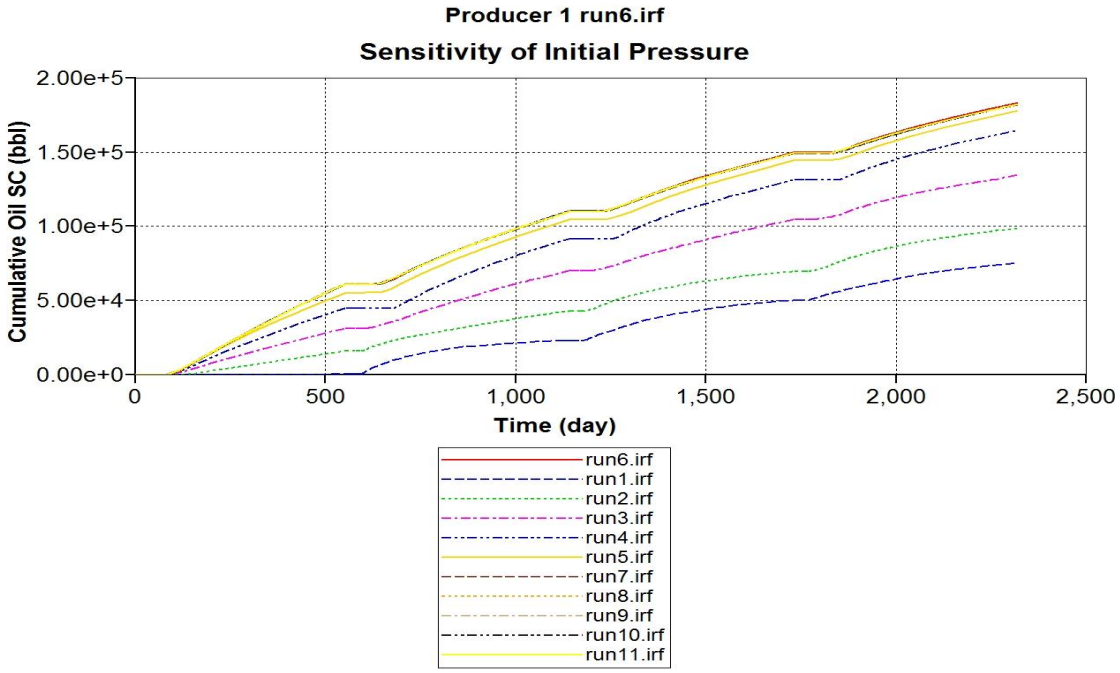

Figure **5-52**: Sensitivity of initial pressure on cumulative production of oil 1.

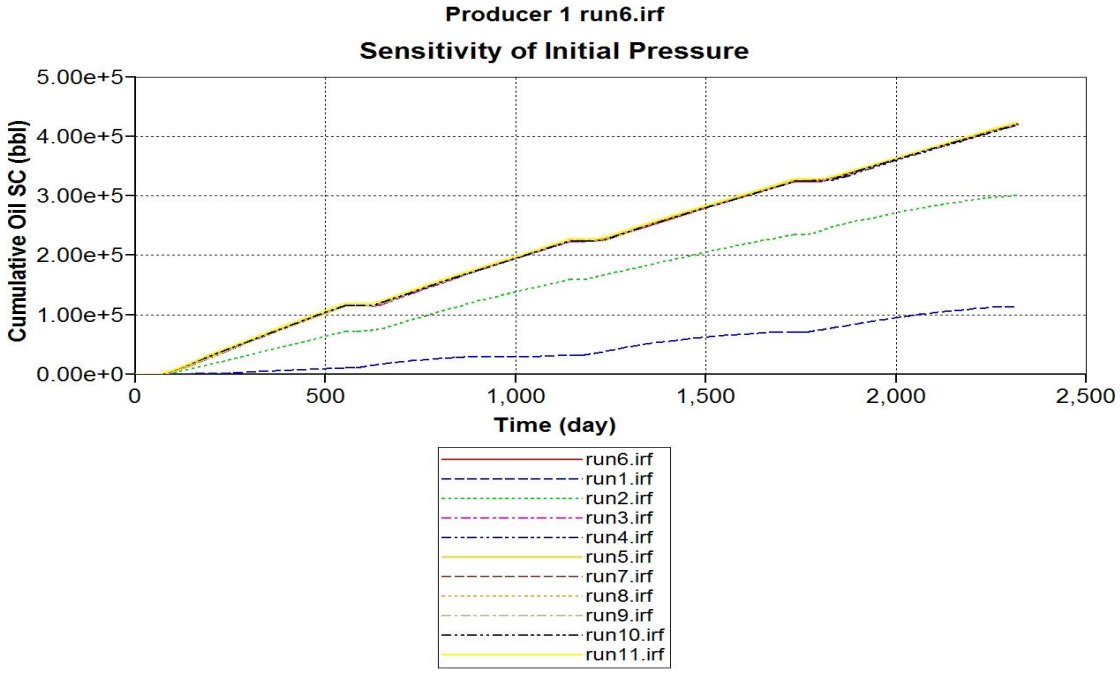

Figure **5-53**: Sensitivity of initial pressure on cumulative production of oil 2.

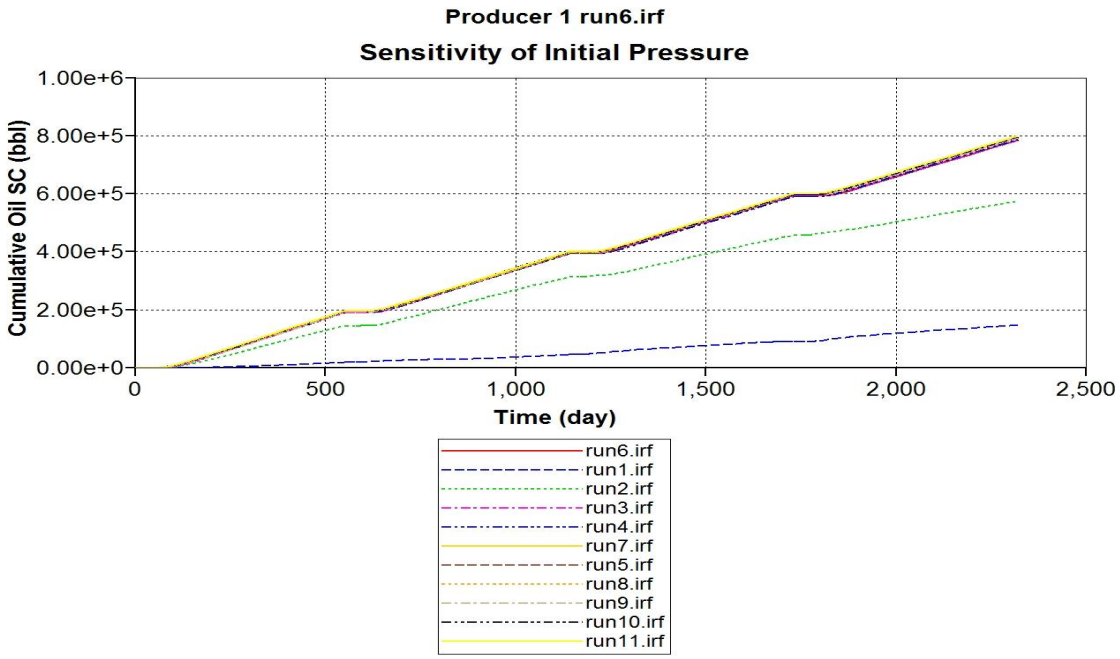

Figure **5-54**: Sensitivity of initial pressure on cumulative production of oil 3.

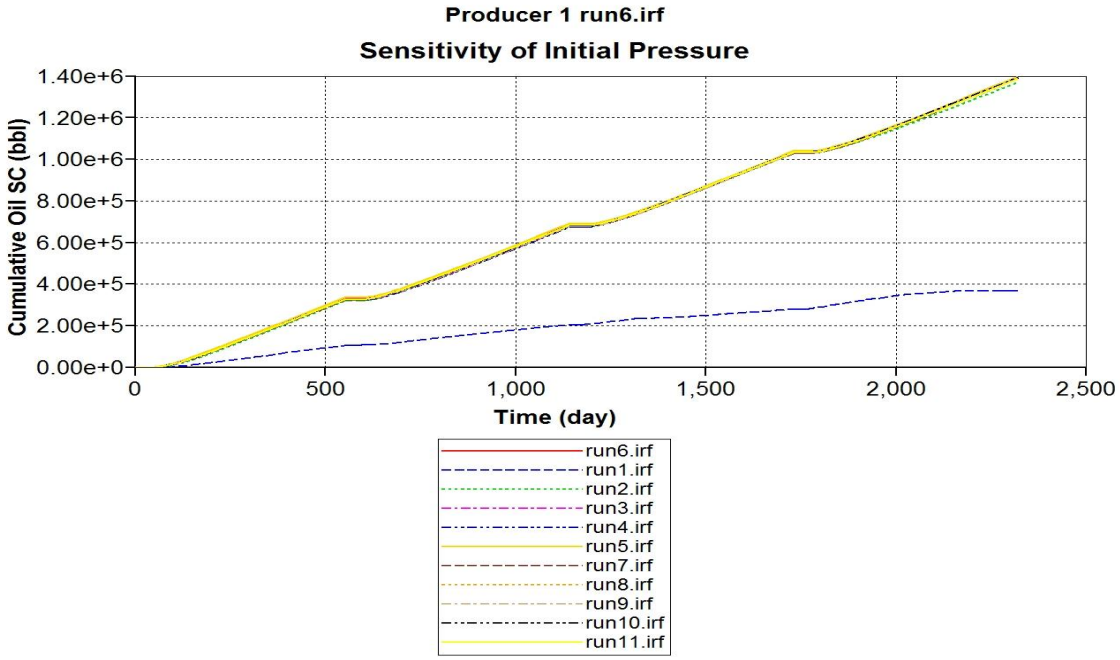

Figure **5-55**: Sensitivity of initial pressure on cumulative production of oil 4.

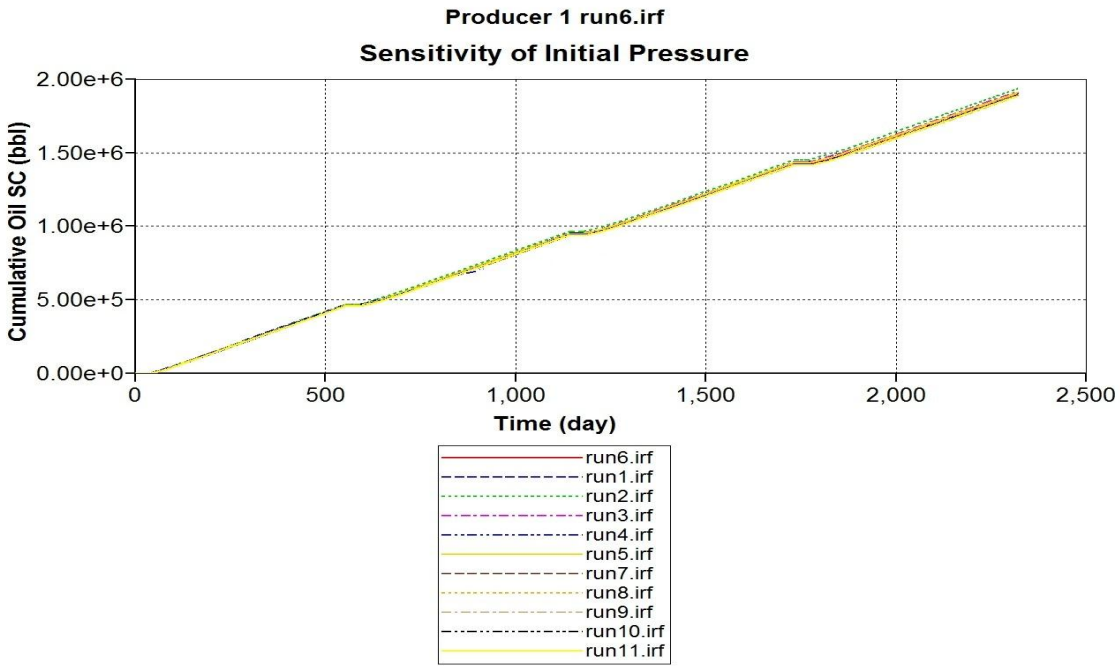

Figure **5-56**: Sensitivity of initial pressure on cumulative production of oil 5.

It can be observed from plots above that initial pressure has more effect on oil 1 than any other oils. For other oils the increase in initial pressure did not have much effect on cumulative production.

5.6.8 Sensitivity of Initial Temperature

Figures **5-57**, **5-58**, **5-59**, **5-60** & **5-61** show the sensitivity of initial temperature on cumulative production for oils 1, 2, 3, 4 & 5 respectively. In all these figures, run 6 is the base simulation file.

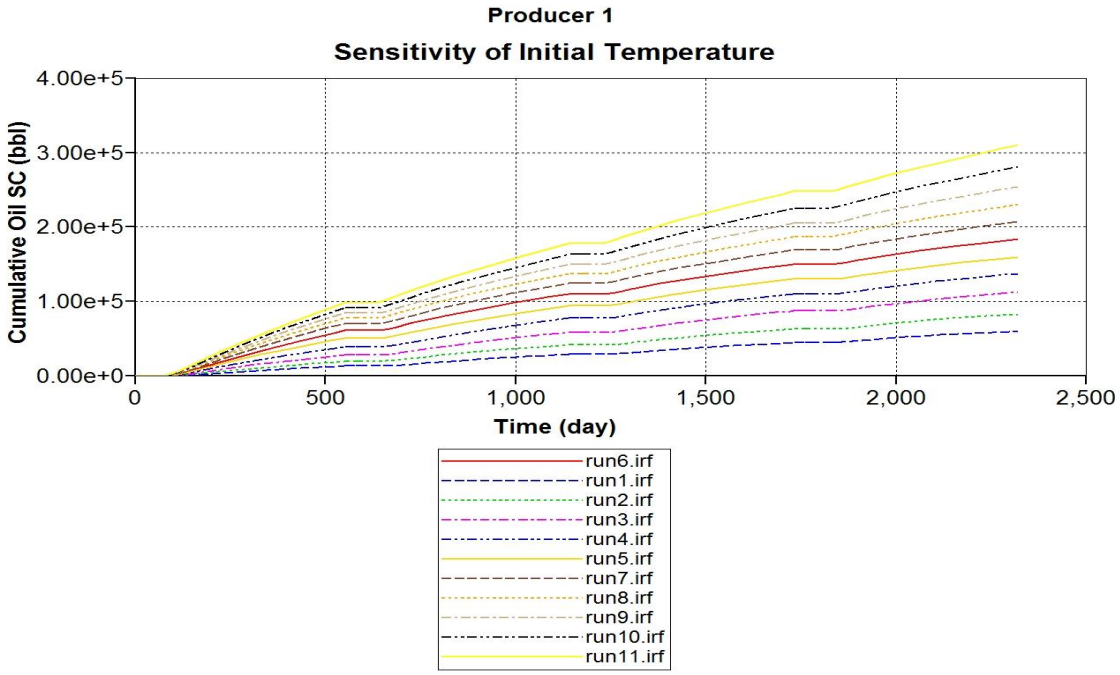

Figure **5-57**: Sensitivity of initial temperature on cumulative production of oil 1.

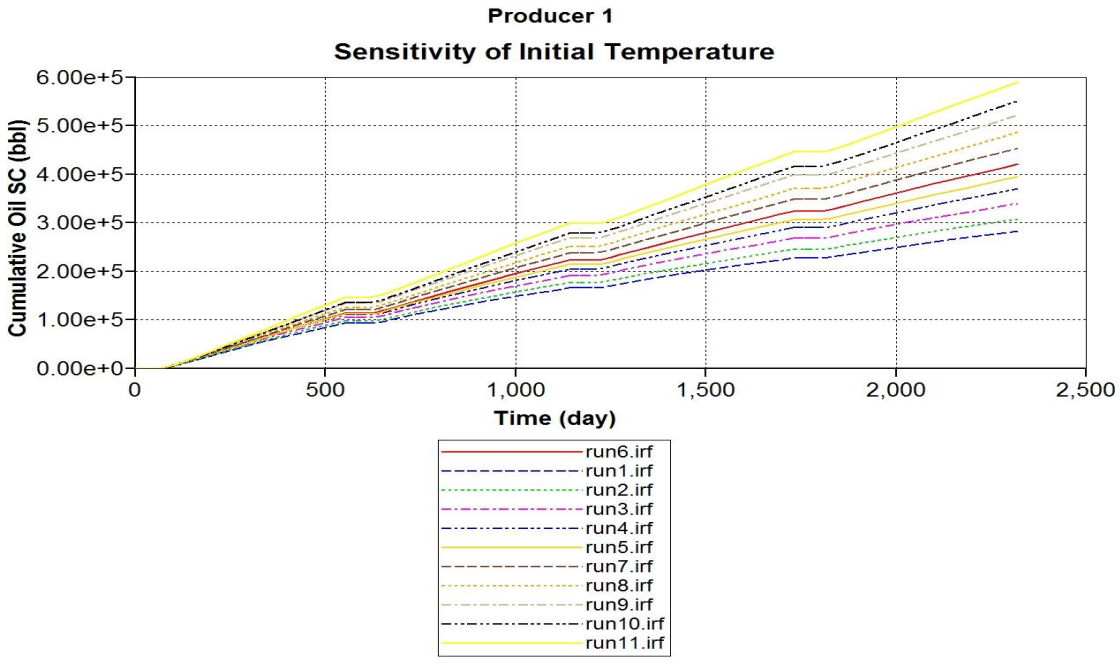

Figure **5-58**: Sensitivity of initial temperature on cumulative production of oil 2.

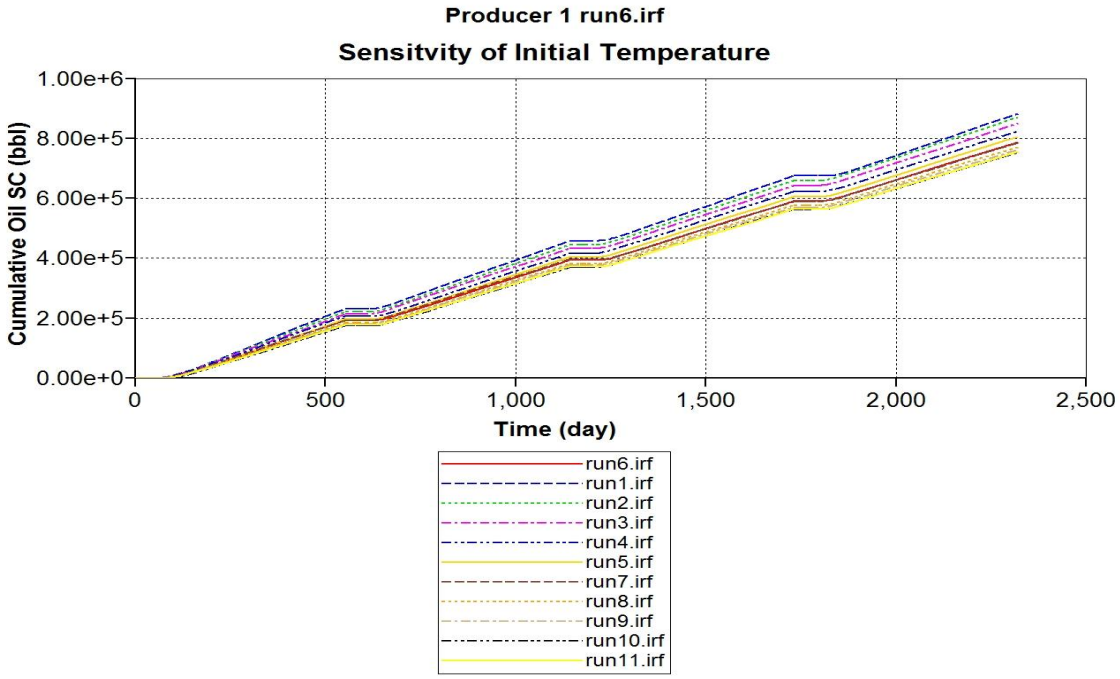

Figure **5-59**: Sensitivity of initial temperature on cumulative production of oil 3.

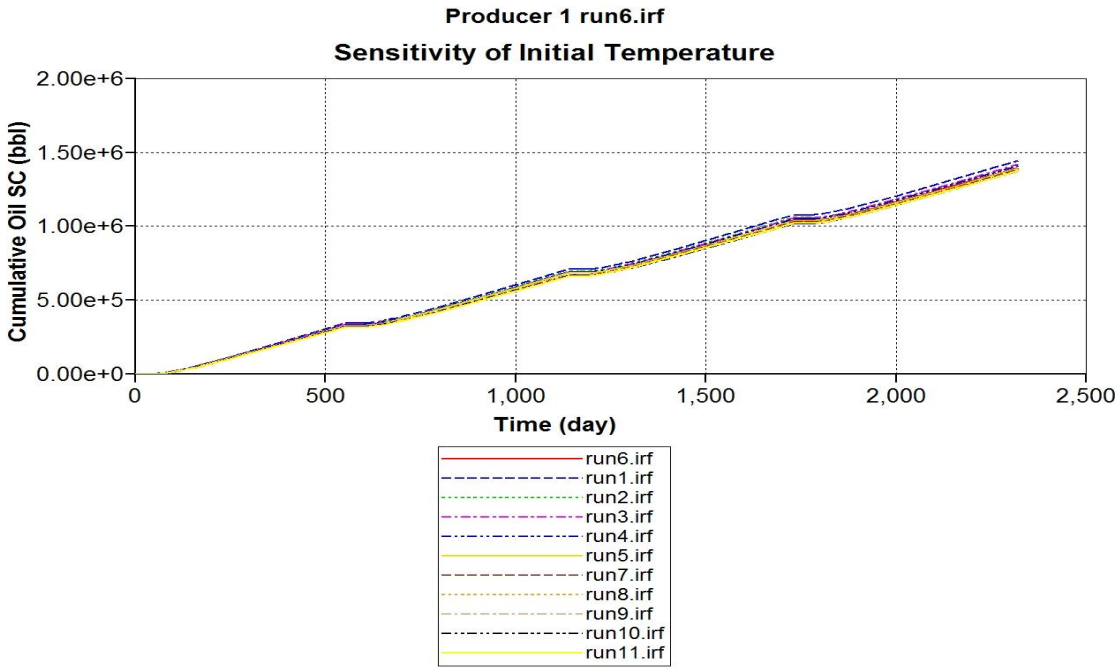

Figure **5-60**: Sensitivity of initial temperature on cumulative production of oil 4.

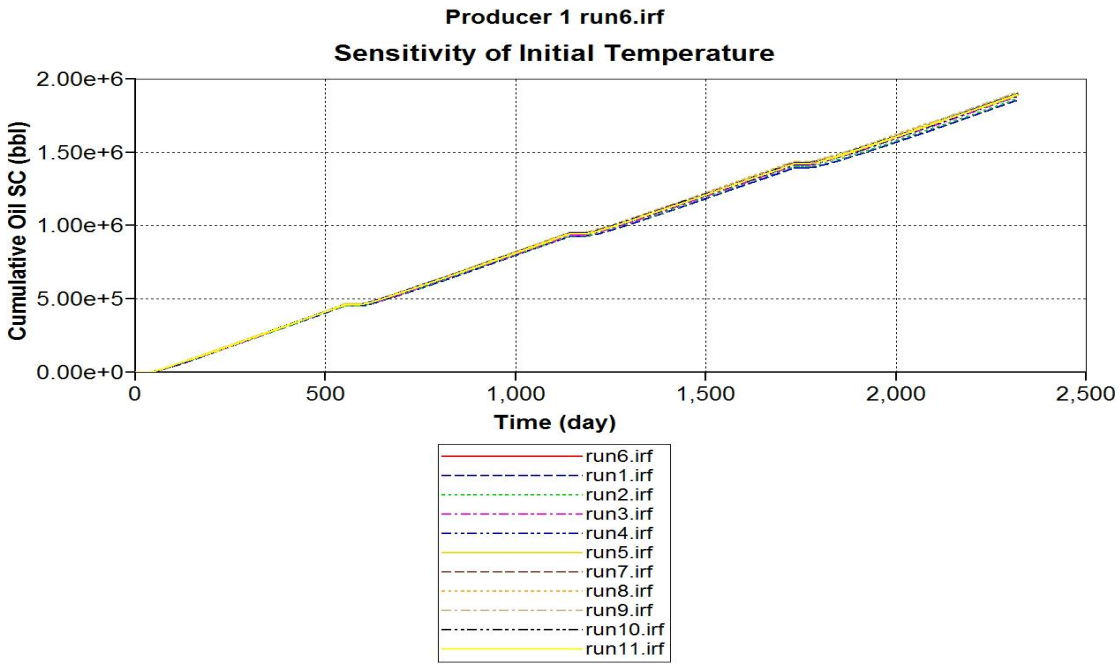

Figure **5-61**: Sensitivity of initial temperature on cumulative production of oil 5.

It can be observed from plots above that initial temperature of reservoir has significant effect on cumulative production of heavier oils. Even though the viscosity of oil 1 is high at room temperature, its effect on production is determined by its viscosity at reservoir temperature. Oil 1 has a viscosity of 5800 cp at 75 F, but at a reservoir temperature of 240 F, its viscosity is only 17 cp. For oil 5 the drop in viscosity of oil at higher temperatures is not as significant as other oils. Hence the effect of initial temperature is not very pronounced.

5.6.9 Sensitivity of Matrix Permeability

Figures **5-62**, **5-63**, **5-64**, **5-65** & **5-66** show the sensitivity of matrix permeability on cumulative production for oils 1, 2, 3, 4 & 5 respectively. In all these figures, run 6 is the base simulation file.

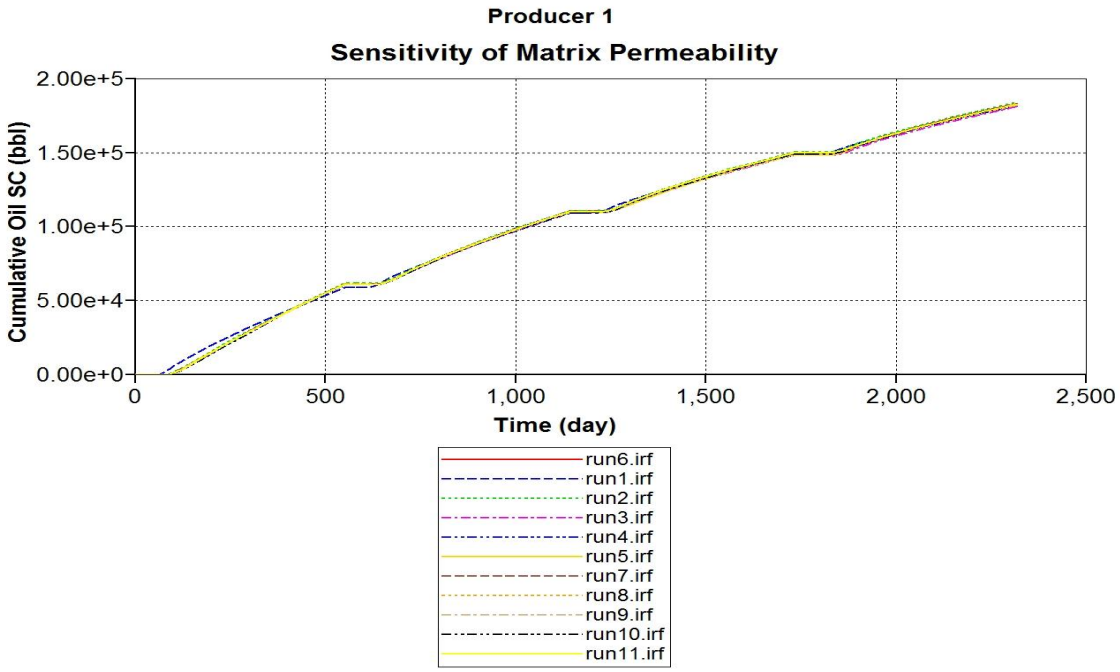

Figure **5-62**: Sensitivity of matrix permeability on cumulative production of oil 1.

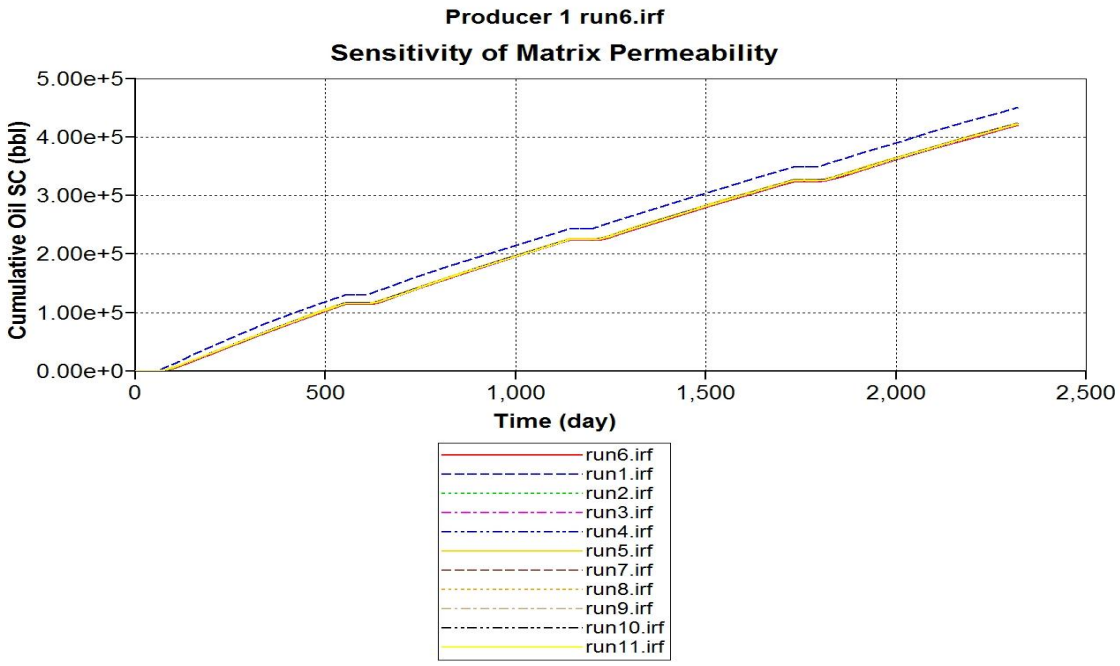

Figure **5-63**: Sensitivity of matrix permeability on cumulative production of oil 2.

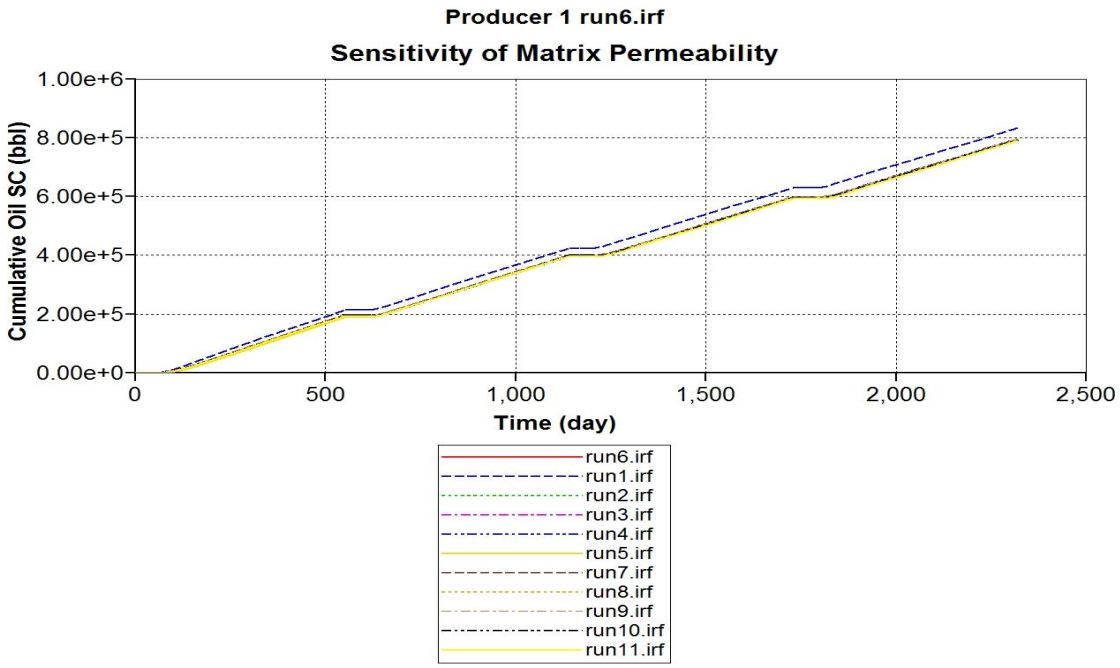

Figure **5-64**: Sensitivity of matrix permeability on cumulative production of oil 3.

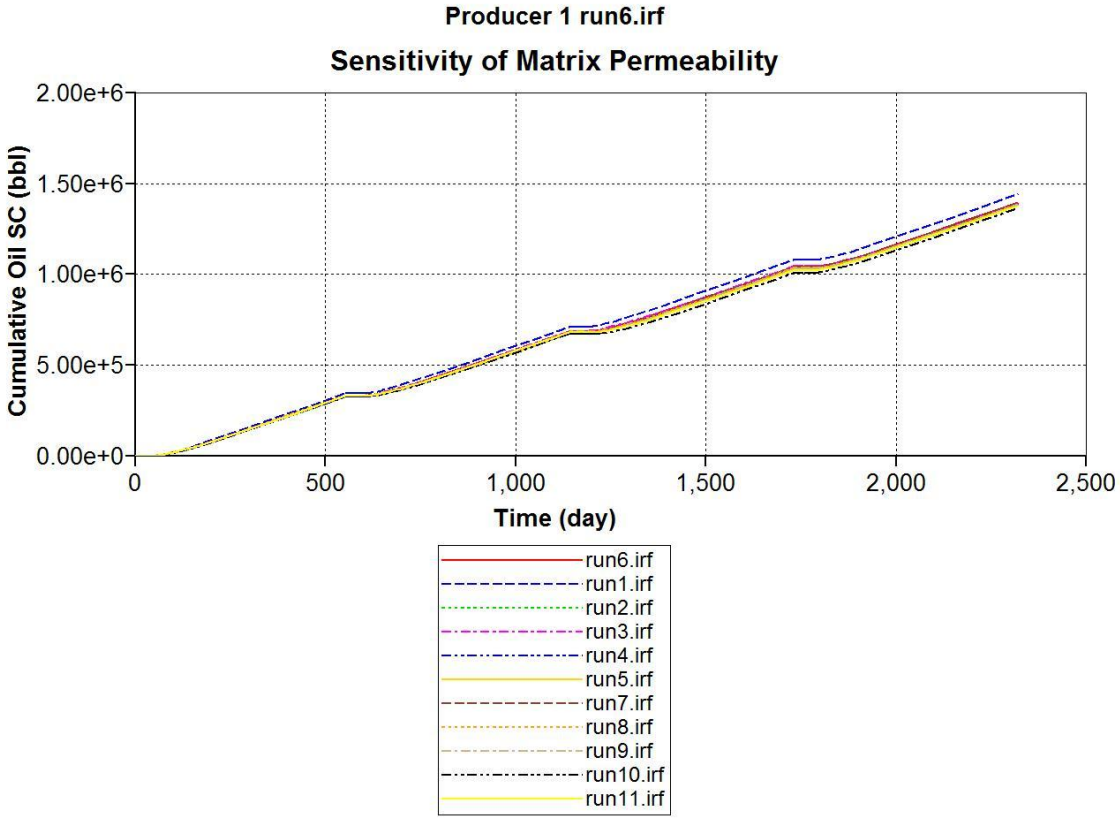

Figure **5-65**: Sensitivity of matrix permeability on cumulative production of oil 4.

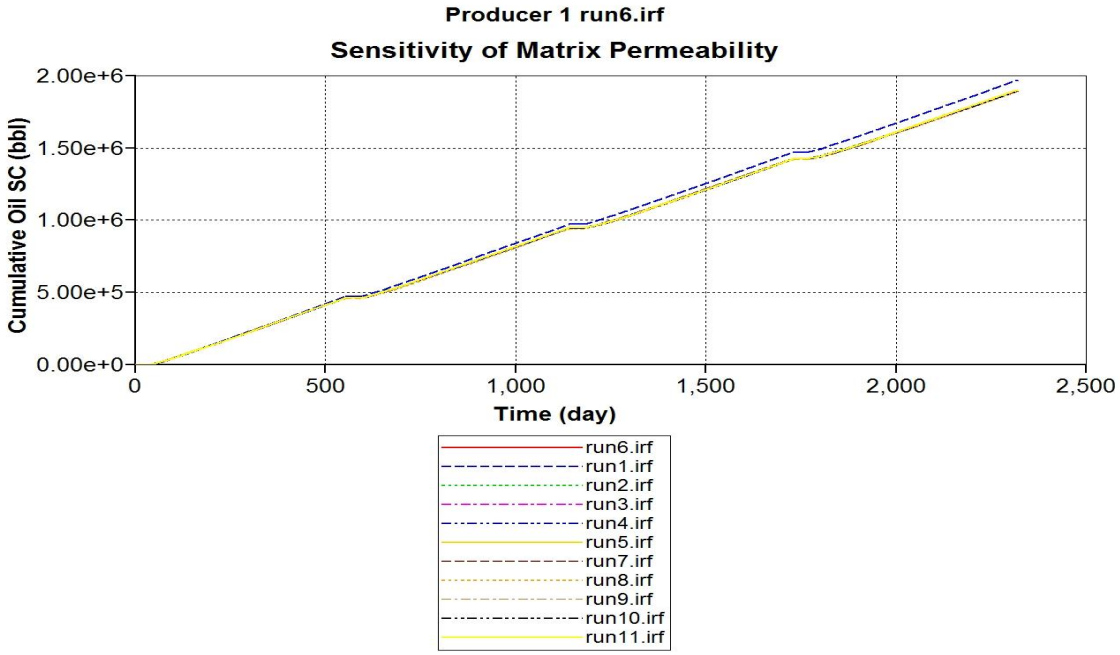

Figure **5-66**: Sensitivity of matrix permeability on cumulative production of oil 5.

It can be observed from above plots that the effect of matrix permeability on cumulative production is insignificant. This is true irrespective of the oil in the reservoir.

5.6.10 Sensitivity of Matrix Porosity

Figures **5-67**, **5-68**, **5-69**, **5-70** & **5-71** show the sensitivity of matrix porosity on cumulative production for oils 1, 2, 3, 4 & 5 respectively. In all these figures, run 6 is the base simulation file.

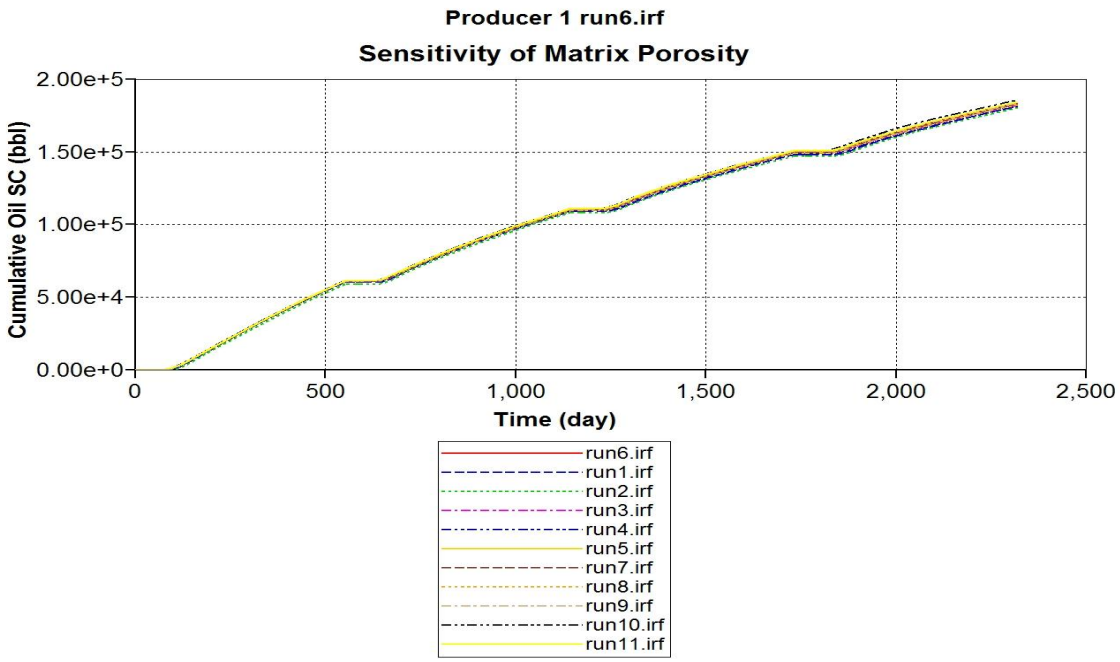

Figure **5-67**: Sensitivity of matrix porosity on cumulative production of oil 1.

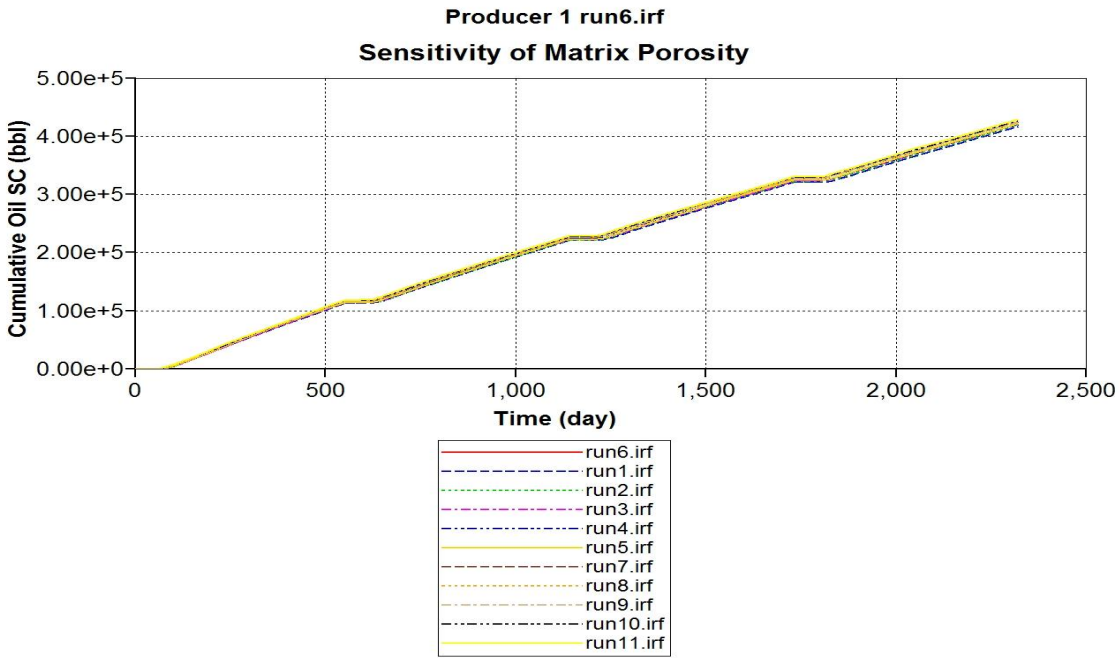

Figure **5-68**: Sensitivity of matrix porosity on cumulative production of oil 2.

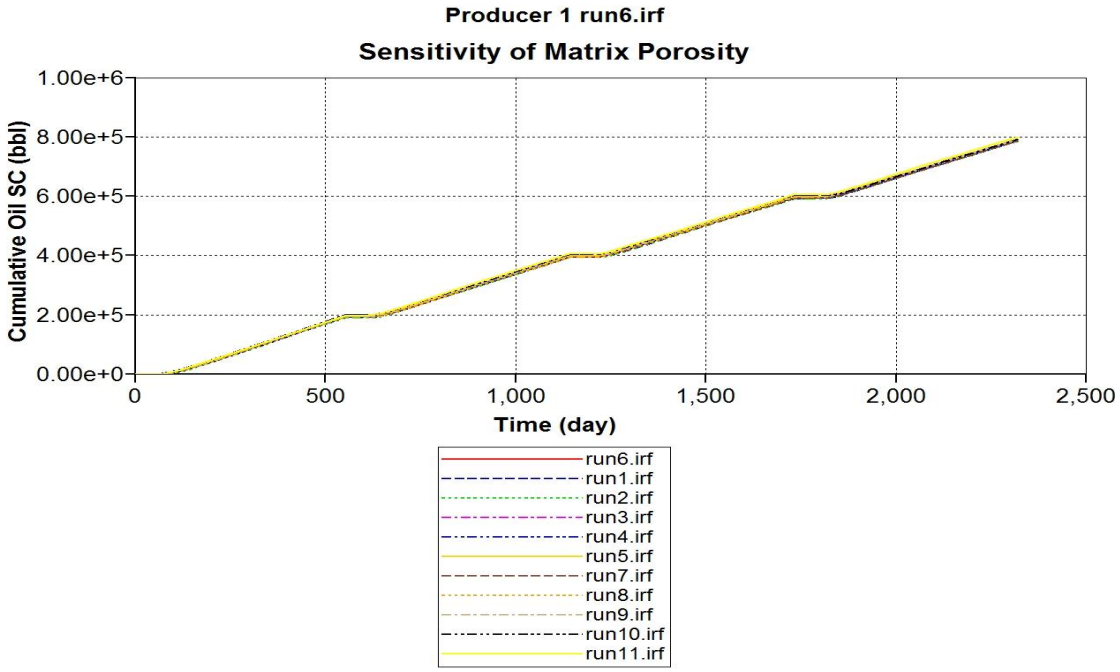

Figure **5-69**: Sensitivity of matrix porosity on cumulative production of oil 3.

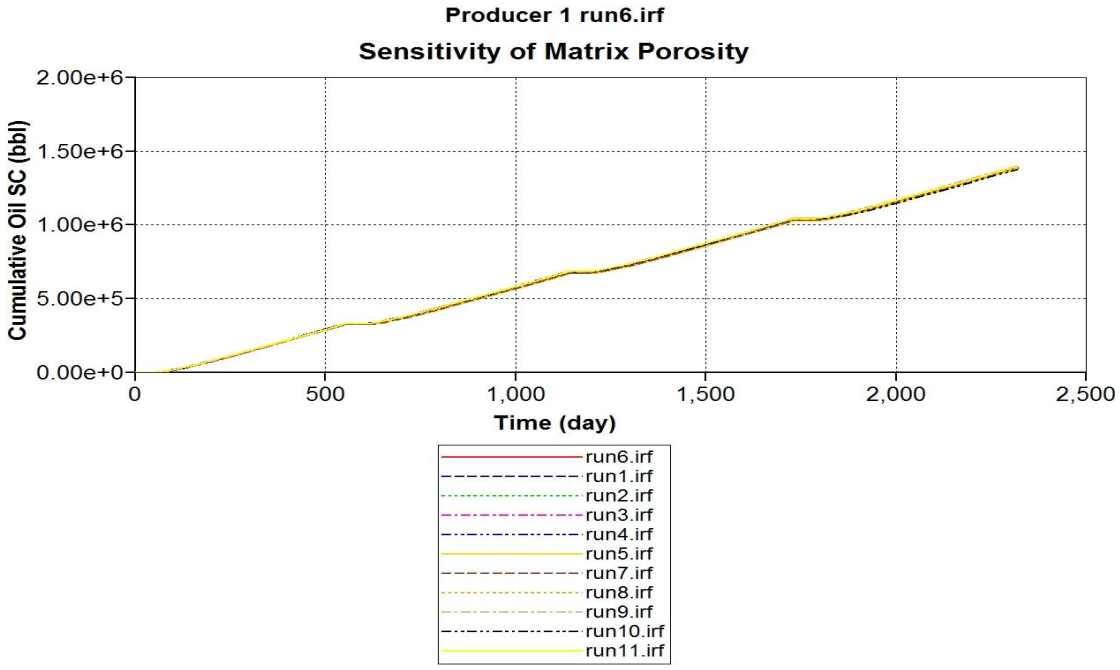

Figure **5-70**: Sensitivity of matrix porosity on cumulative production of oil 4.

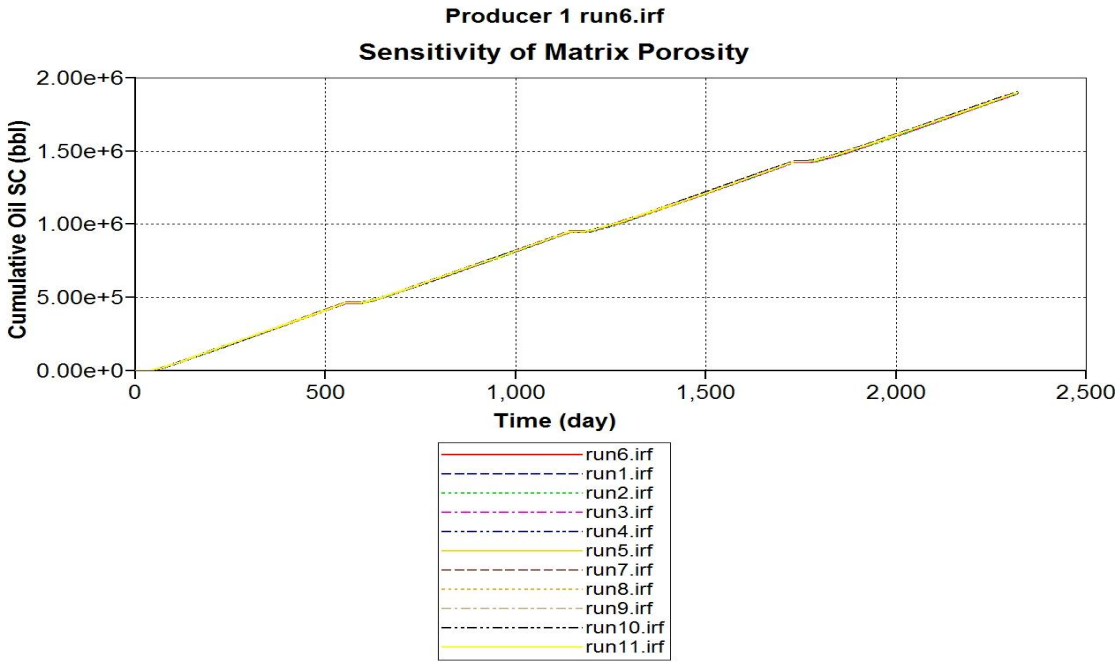

Figure **5-71**: Sensitivity of matrix porosity on cumulative production of oil 5.

It can be observed from plots above that the effect of matrix porosity on cumulative production is negligible. This is true for all the oils.

5.6.11 Sensitivity of Steam Injection Rate (SIR)

Figures **5-72**, **5-73**, **5-74**, **5-75** & **5-76** show the sensitivity of steam injection rate on cumulative production for oils 1, 2, 3, 4 & 5 respectively. In all these figures, run 6 is the base simulation file.

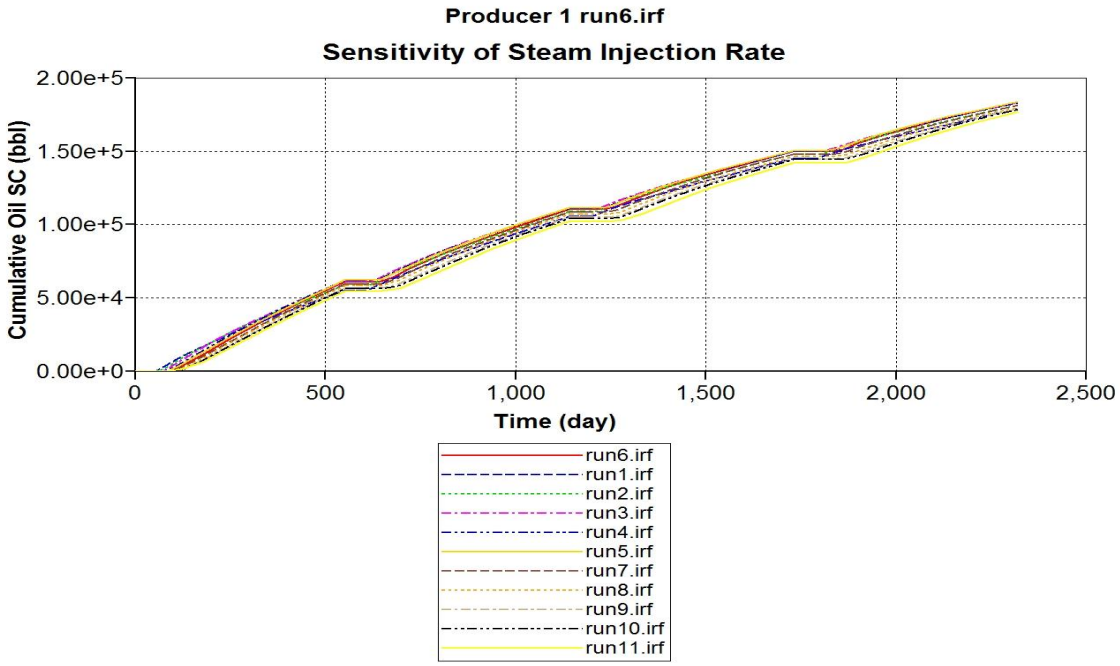

Figure **5-72**: Sensitivity of SIR on cumulative production of oil 1.

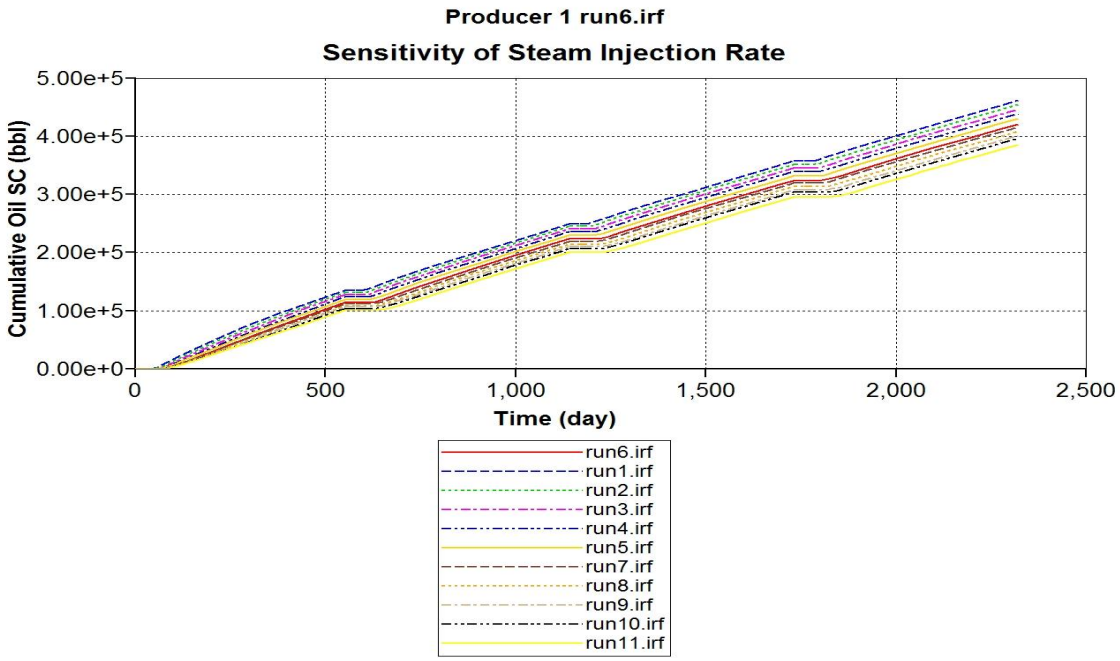

Figure **5-73**: Sensitivity of SIR on cumulative production of oil 2.

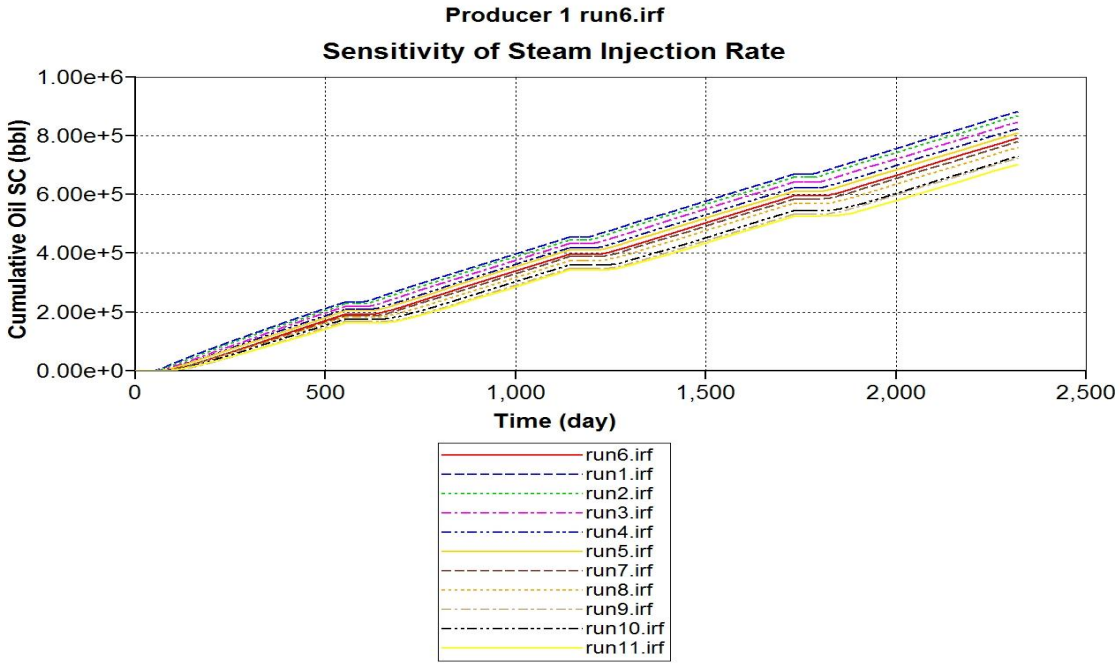

Figure **5-74**: Sensitivity of SIR on cumulative production of oil 3.

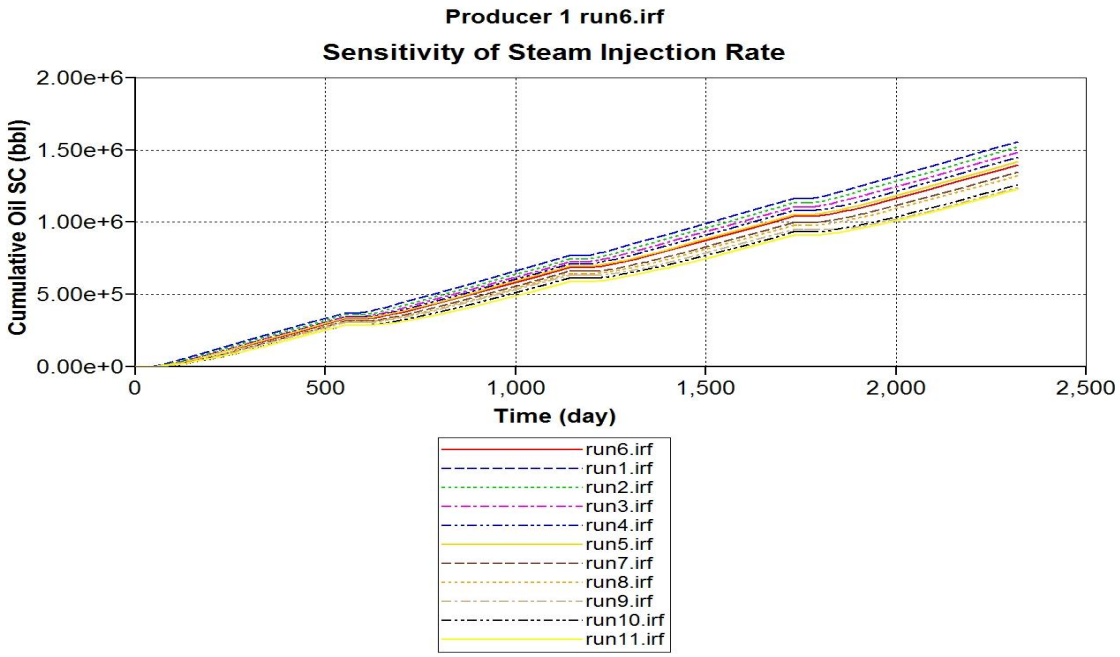

Figure **5-75**: Sensitivity of SIR on cumulative production of oil 4.

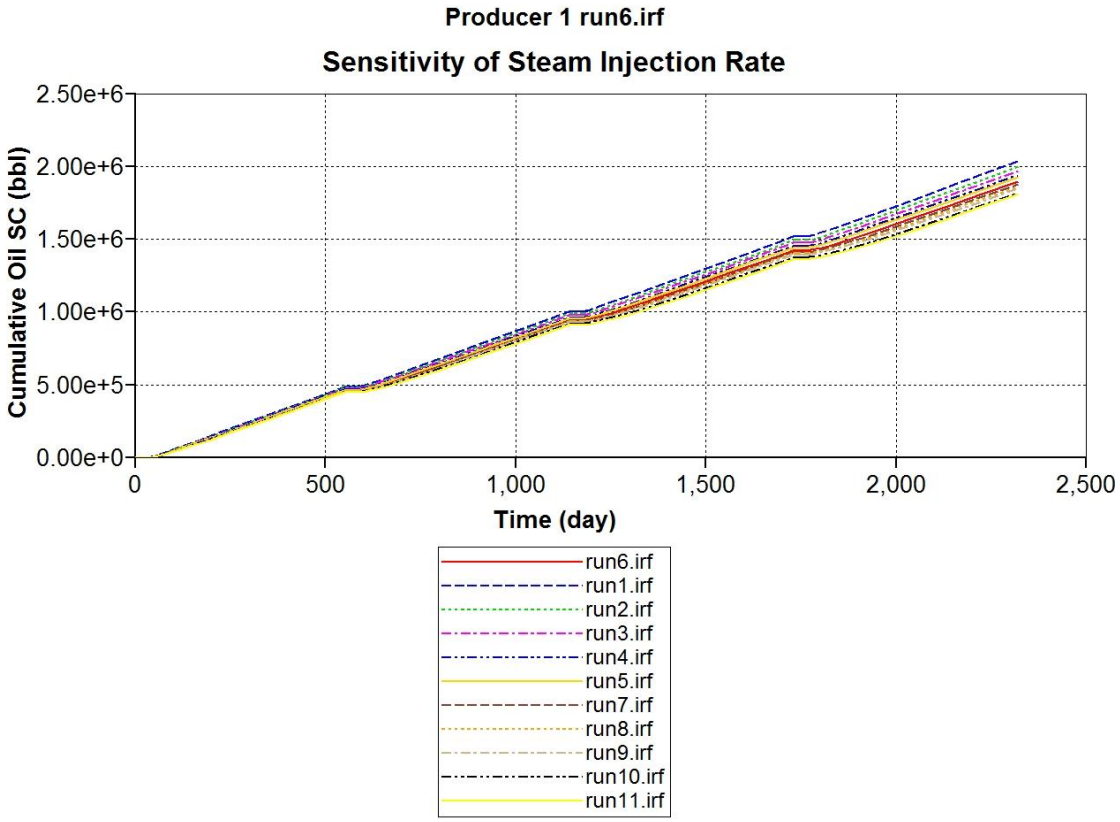

Figure **5-76**: Sensitivity of SIR on cumulative production of oil 5.

It can be observed from the plots above that steam injection has small effect on cumulative production of oil. As we move from oil 1 to oil 5 the effect of steam injection becomes significant. But in all the oils the cumulative production decreases as we inject more steam at same quality and temperature. The possible reason for this could be that as more steam is injected at same quality, temperature and soaking period, more condensed steam is produced along with oil during production period – thereby reducing the cumulative production at the end of four cycles.

5.6.12 Sensitivity of Steam Quality

Figures **5-77**, **5-78**, **5-79**, **5-80** & **5-81** show the sensitivity of steam injection rate on cumulative production for oils 1, 2, 3, 4 & 5 respectively. In all these figures, run 6 is the base simulation file.

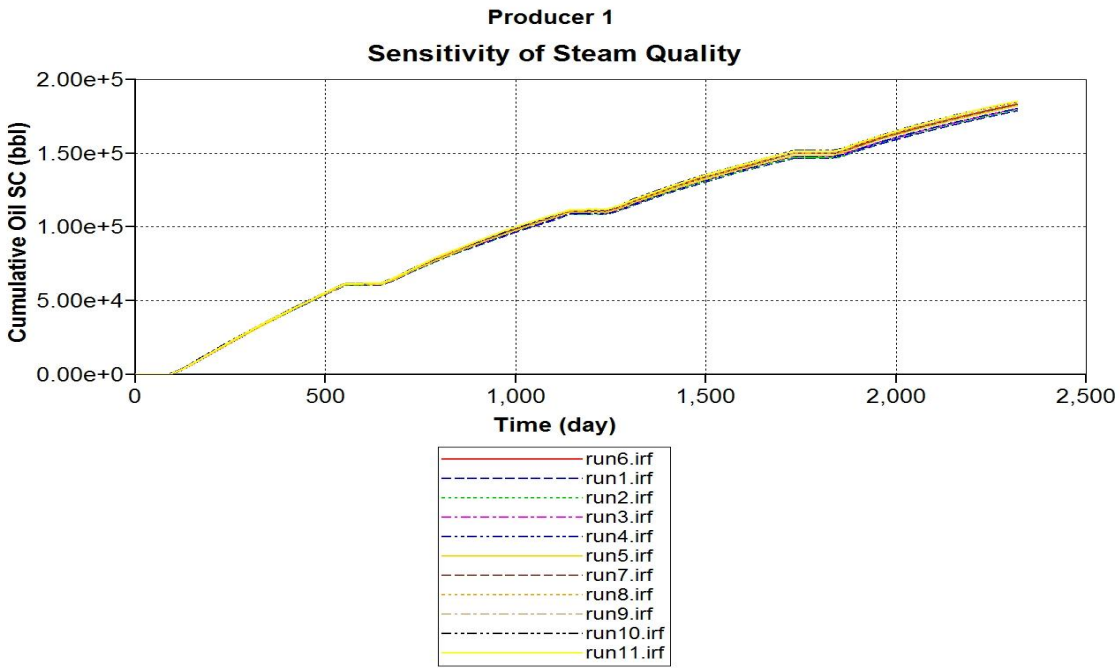

Figure **5-77**: Sensitivity of steam quality on cumulative production of oil 1.

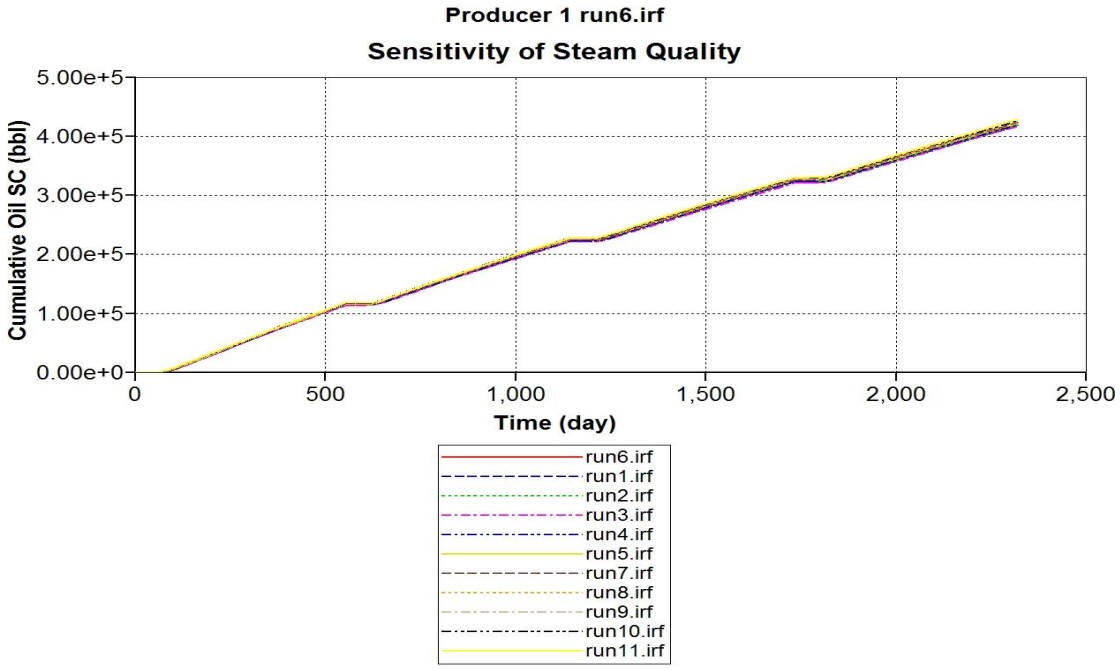

Figure **5-78**: Sensitivity of steam quality on cumulative production of oil 2.

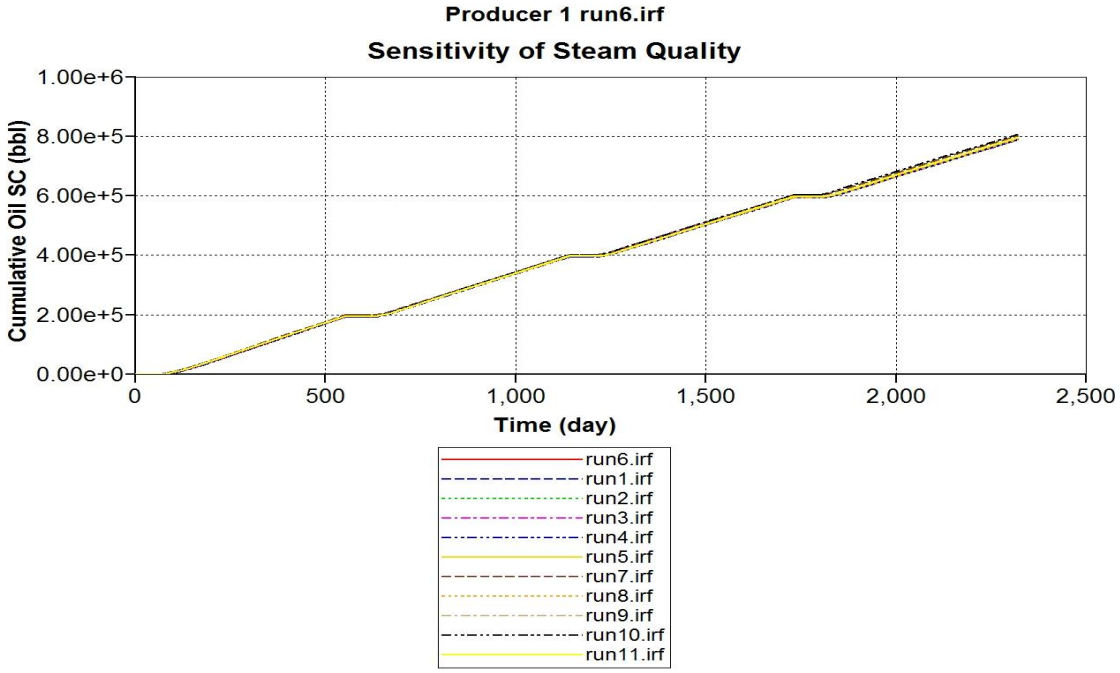

Figure **5-79**: Sensitivity of steam quality on cumulative production of oil 3.

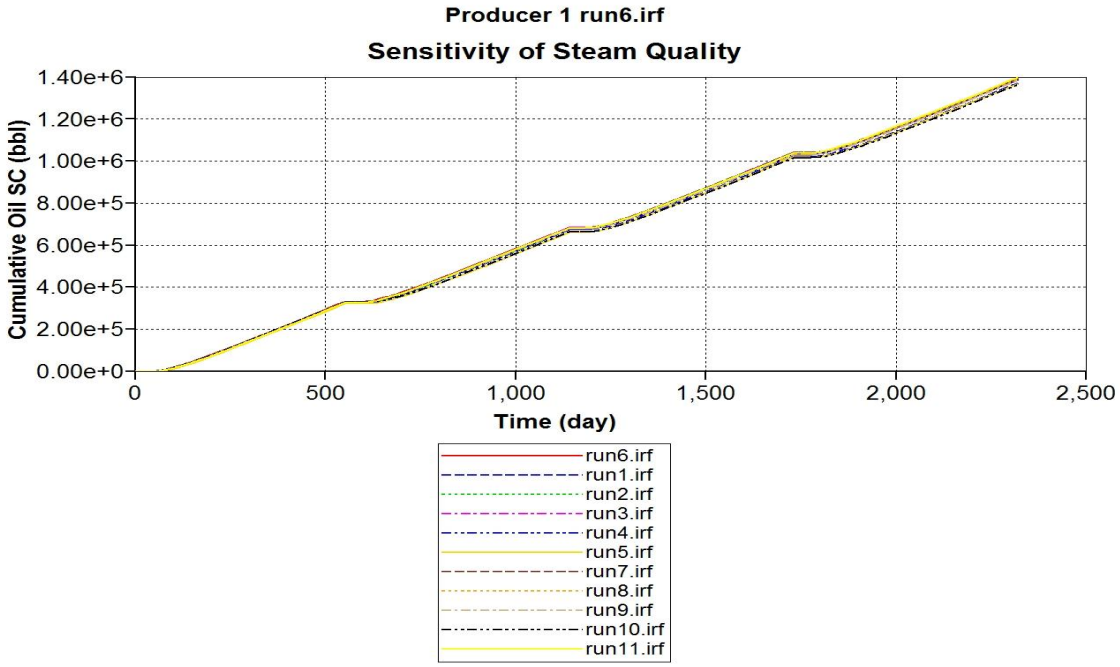

Figure **5-80**: Sensitivity of steam quality on cumulative production of oil 4.

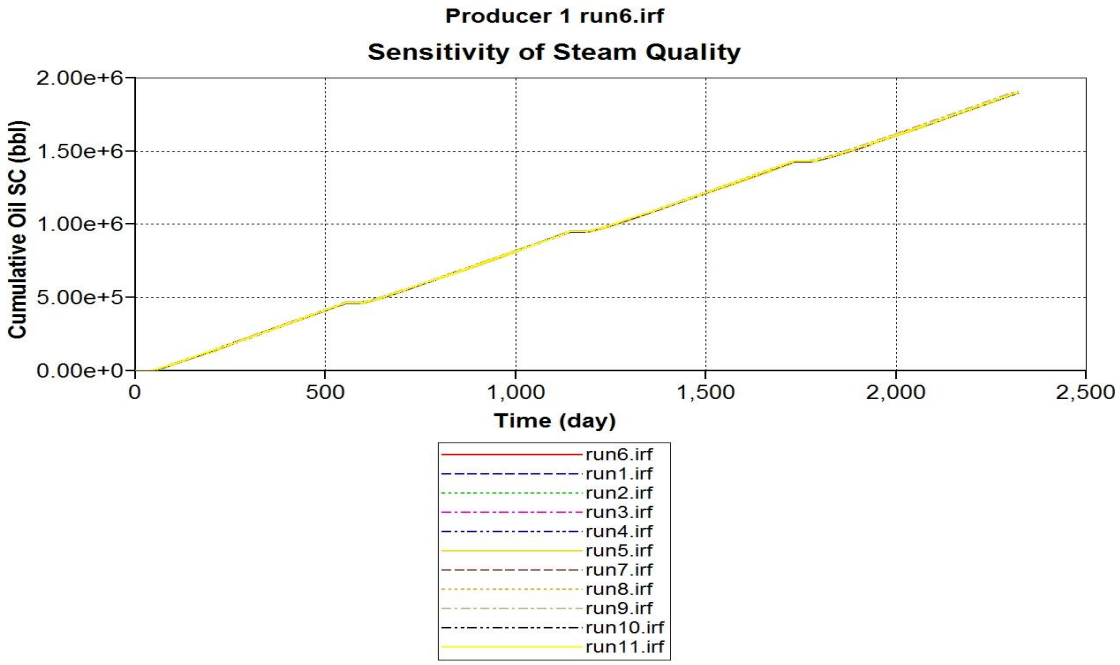

Figure **5-81**: Sensitivity of steam quality on cumulative production of oil 5.

It can be observed from plots above that steam quality has a very small effect on cumulative production of oil. This is true for all the oils in the reservoir. The possible reason for this could be that at steam temperature of 525 F the enthalpy of steam does not vary significantly as the steam quality is varied between 0.7-1.

5.6.13 Sensitivity of Steam Temperature

Figures **5-82**, **5-83**, **5-84**, **5-85** & **5-86** show the sensitivity of steam injection rate on cumulative production for oils 1, 2, 3, 4 & 5 respectively. In all these figures, run 6 is the base simulation file.

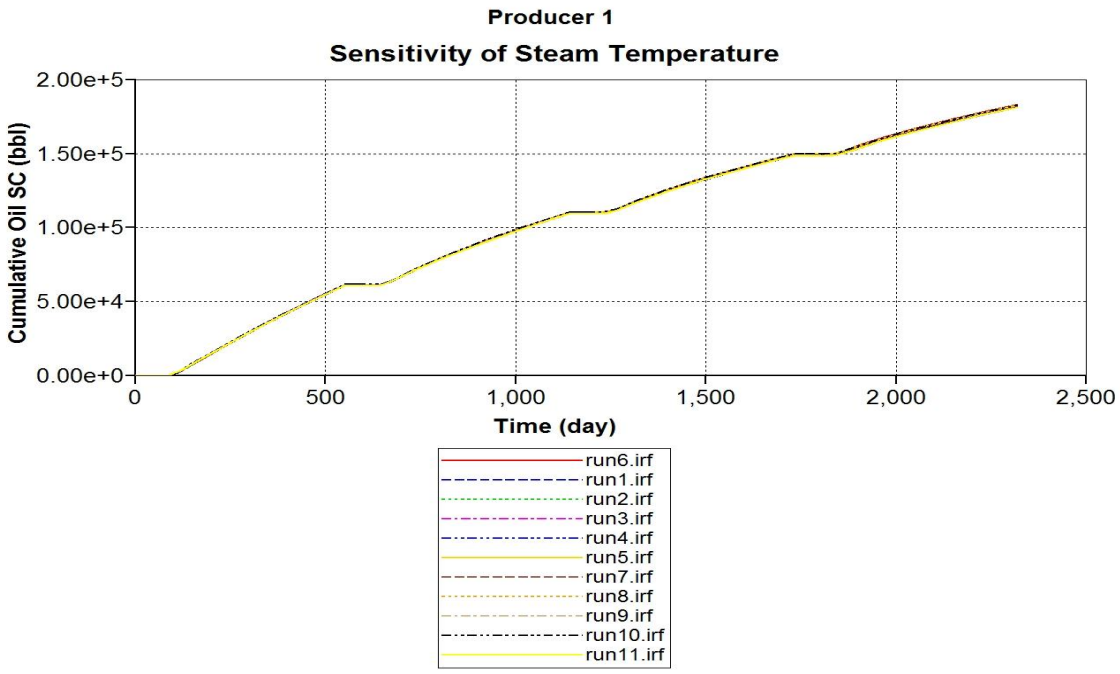

Figure **5-82**: Sensitivity of steam temperature on cumulative production of oil 1.

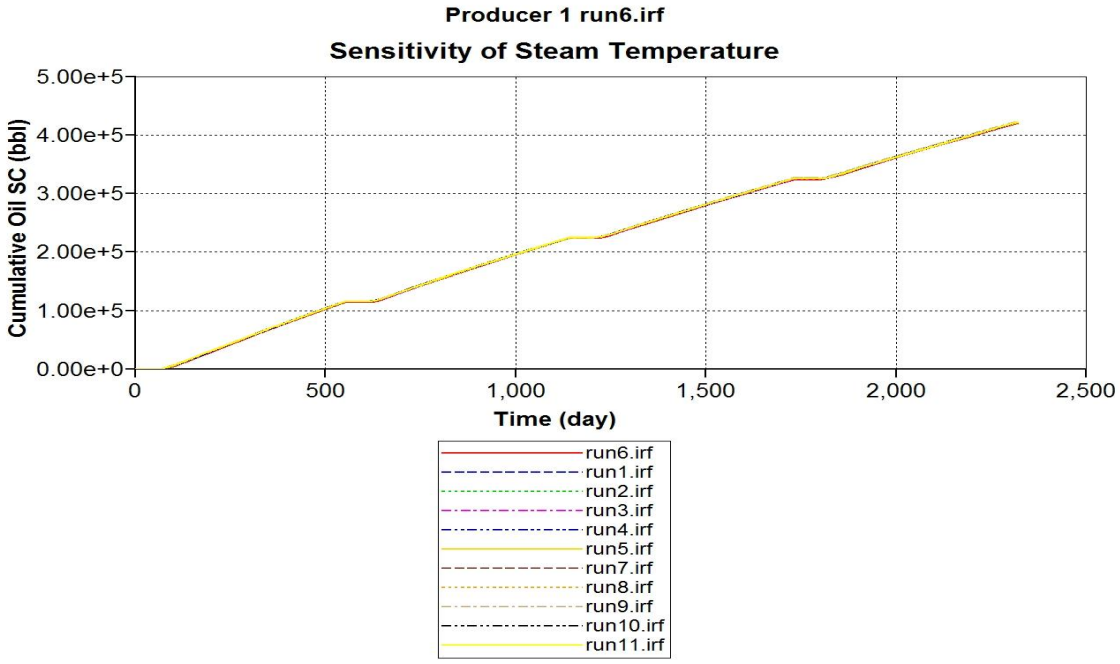

Figure **5-83**: Sensitivity of steam temperature on cumulative production of oil 2.

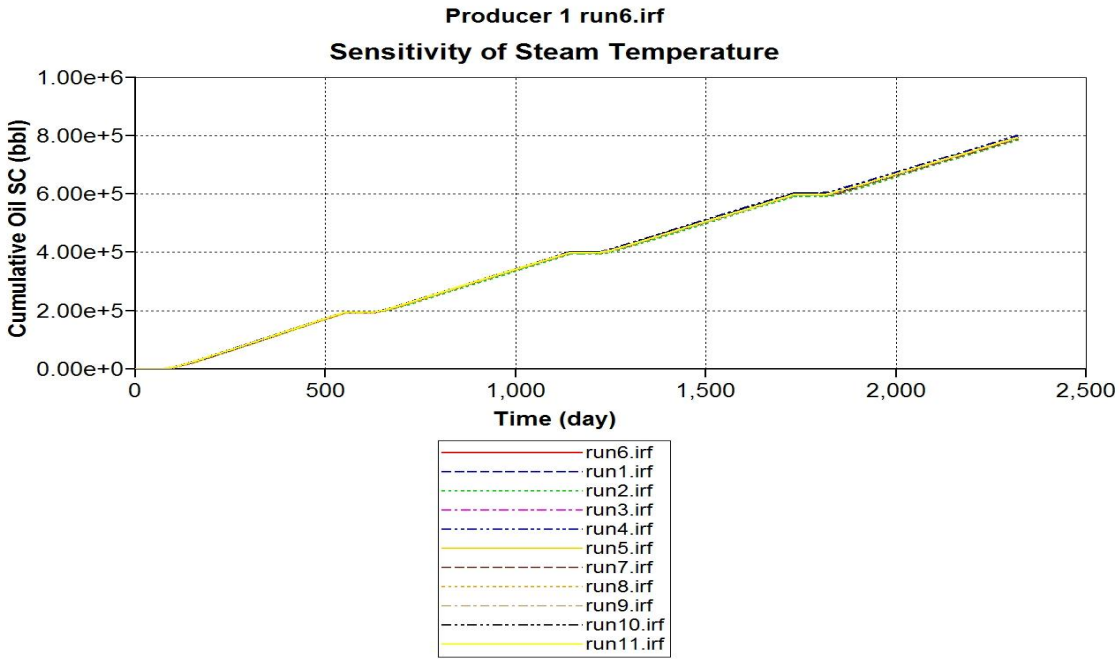

Figure **5-84**: Sensitivity of steam temperature on cumulative production of oil 3.

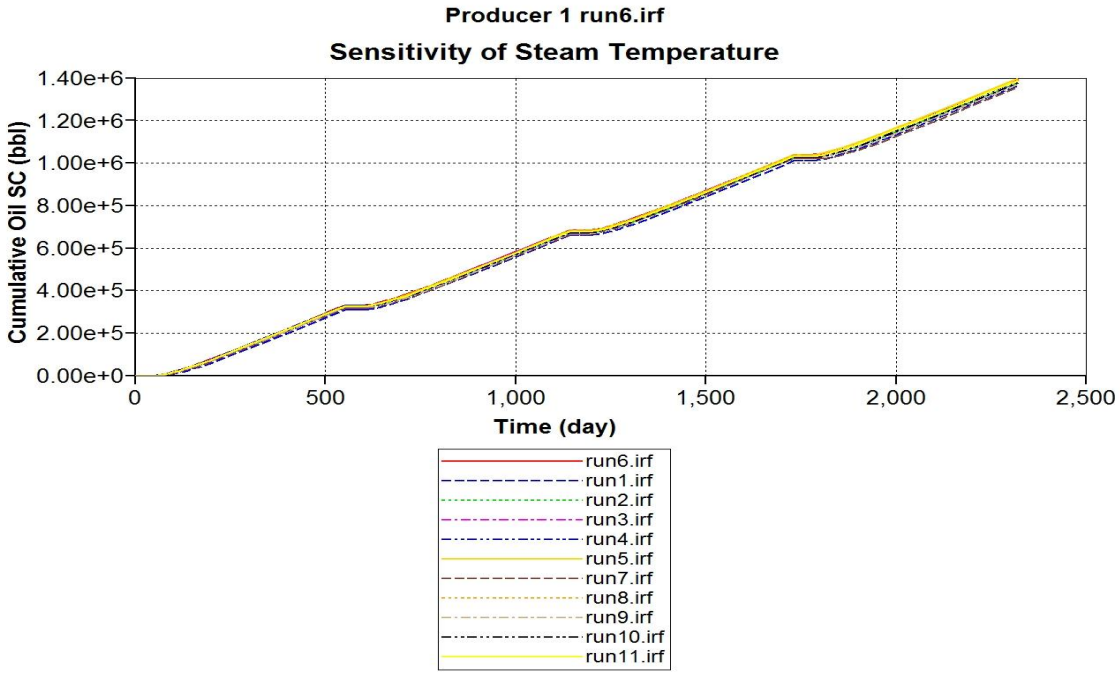

Figure **5-85**: Sensitivity of steam temperature on cumulative production of oil 4.

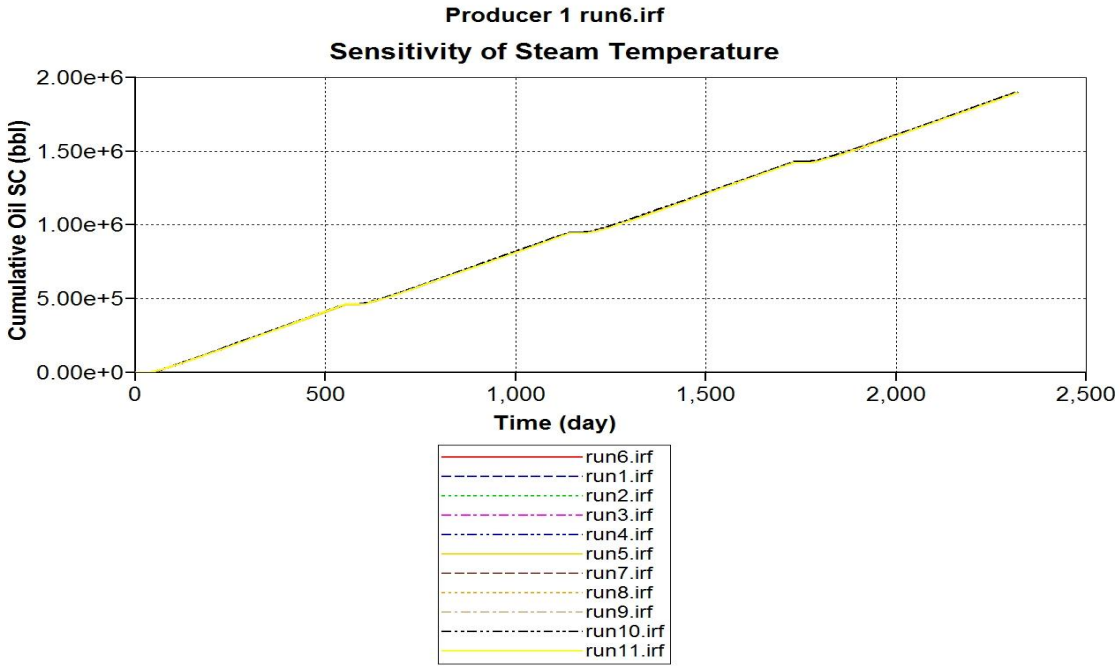

Figure **5-86**: Sensitivity of steam temperature on cumulative production of oil 5.

It can be observed from plots above that steam temperature has almost no effect on cumulative production. This is true for all the oils. The possible reason for this could be that, as the soaking period is constant at 10 days/cycle in this project, there was not sufficient time for the thermal gradients to equalize at higher steam temperatures. Hence we observe similar production profile for all steam temperatures irrespective of the oil.

5.6.14 Sensitivity of Thickness

Figures **5-87**, **5-88**, **5-89**, **5-90** & **5-91** show the sensitivity of steam injection rate on cumulative production for oils 1, 2, 3, 4 & 5 respectively. In all these figures, run 6 is the base simulation file.

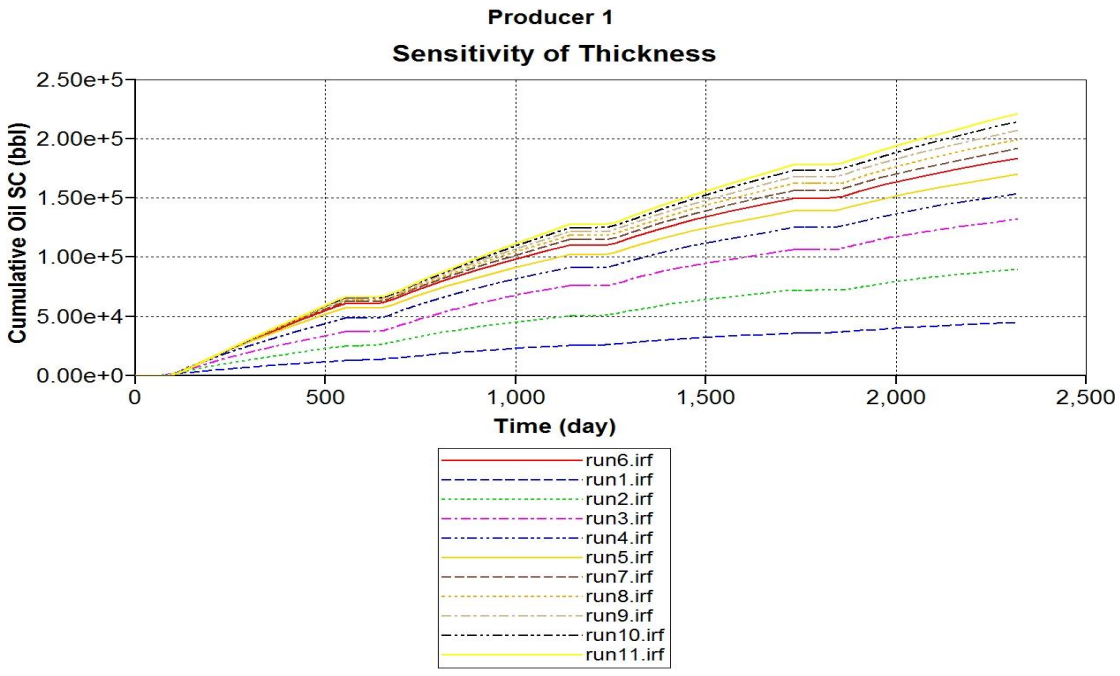

Figure **5-87**: Sensitivity of thickness on cumulative production of oil 1.

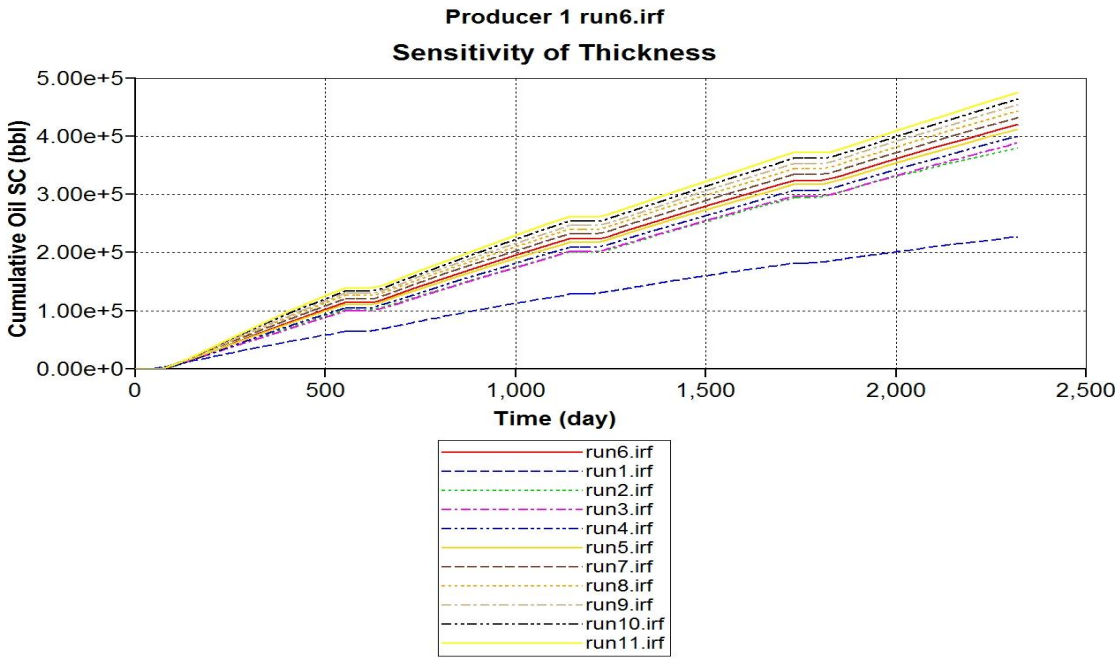

Figure **5-88**: Sensitivity of thickness on cumulative production of oil 2.

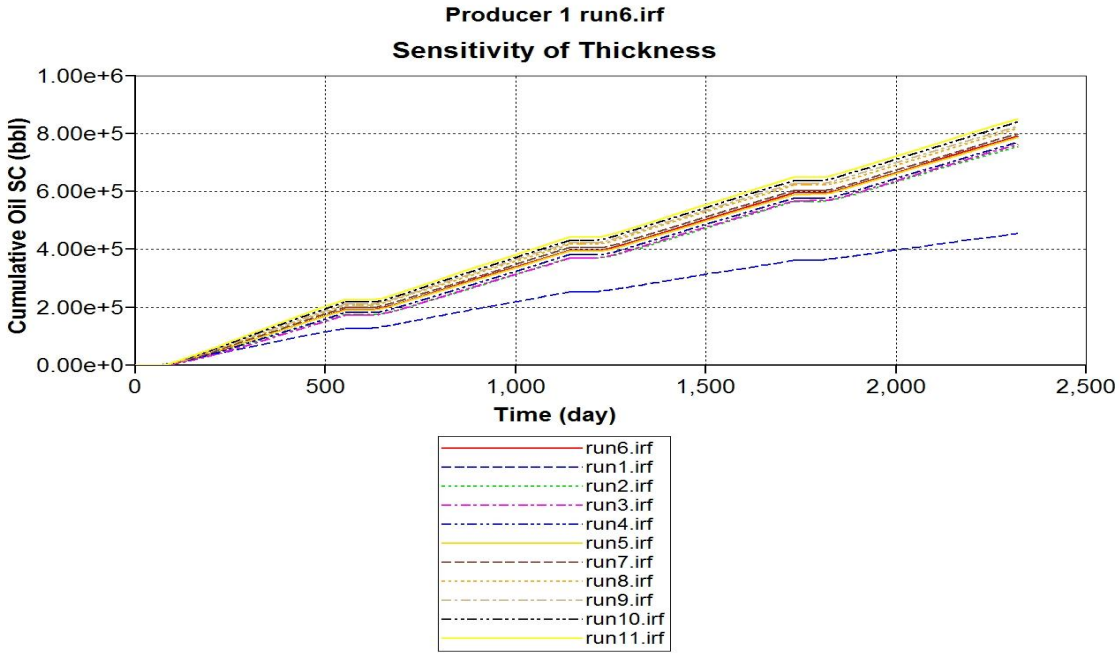

Figure **5-89**: Sensitivity of thickness on cumulative production of oil 3.

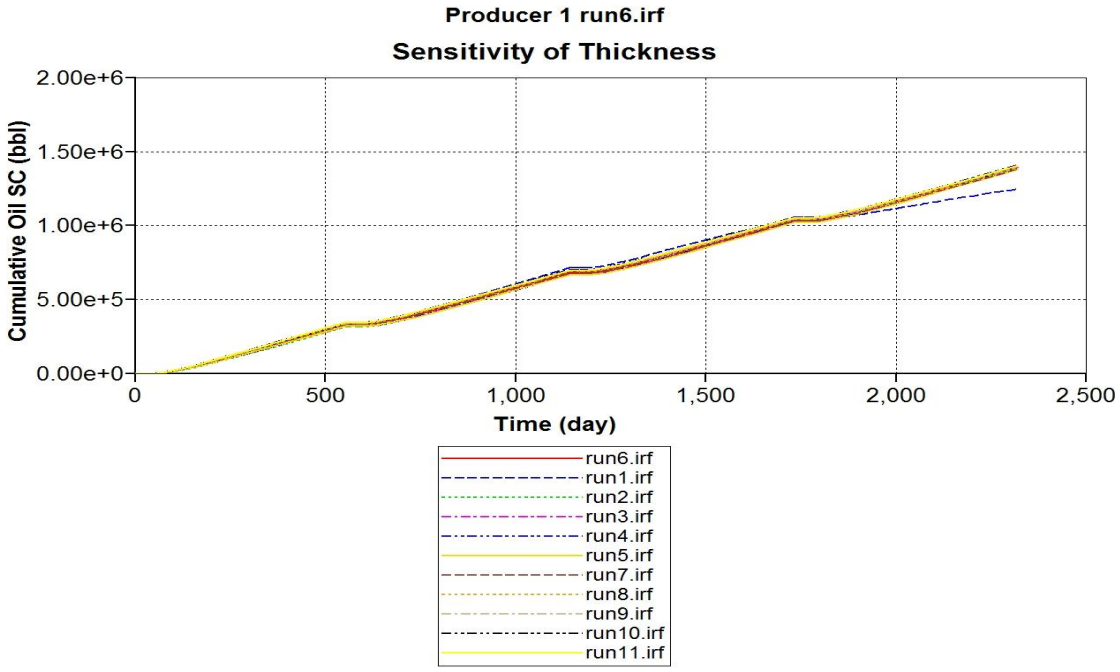

Figure **5-90**: Sensitivity of thickness on cumulative production of oil 4.

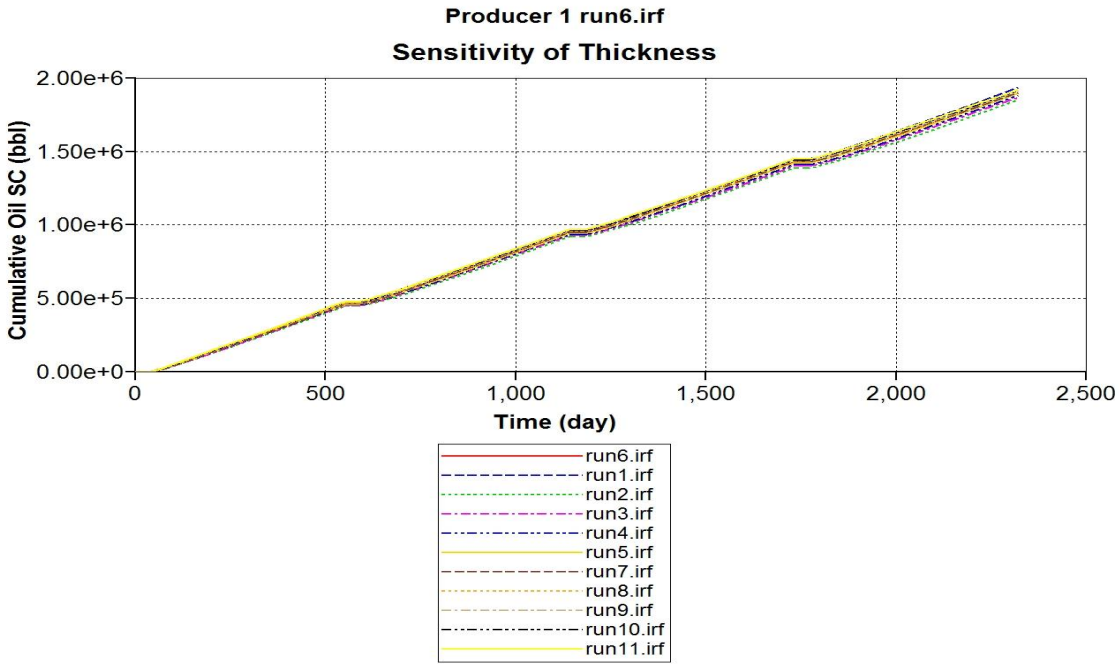

Figure **5-91**: Sensitivity of thickness on cumulative production of oil 5.

It can be observed from plots above that thickness has a significant effect on cumulative production. As the thickness of the reservoir increases, the production increases. This is true for all the oils. Note that for oils 4 and 5 the scale is in million barrels of oil. Hence the curves are not as far apart as in oils 1, 2 and 3. The obvious reason why thickness effects the cumulative production is that, increase in thickness amounts to increase in original oil in place. The second reason is that if we assume heat losses only through overburden and underburden of the reservoir, thick reservoirs lose less heat compared to thin reservoirs. That amounts to more recovery from thick reservoirs under same operating conditions even when the original oil in place is the same. It is a common practice to perform steam injection operations in thick reservoirs and non-thermal EOR operations in thin reservoirs.

5.7 Comparison between commercial simulator and GUI

A GUI was developed to integrate all the five networks under a single window. Appendix A gives a description of working of the GUI. A comparison was made between the GUI and the commercial simulator on time taken to run a sample. On a 64 bit Windows 7 operating system with Intel Core ™ i7-2600 CPU @ 2.4 GHZ and 8 GB RAM, while the commercial simulator took around 2 minutes to run, the GUI took around 5 seconds to report the output.

Chapter 6

Conclusions and Recommendations

6.1 Conclusions

1. Artificial neural networks were successfully developed for five oils under study. As shown in Appendix A, a GUI was developed to integrate all the neural networks under a single window. The GUI thus mimics the commercial reservoir simulator within the assumptions stated above.
2. The comparison of results between the commercial simulator and ANN for all testing samples could not be presented. Only the best and worst predictions were presented in addition to the error frequency of testing points.
3. From sensitivity analysis it can be concluded that certain variables affect the output (cumulative production from each cycle) more than others. These are initial oil saturation (S_{oi}), initial temperature (T_i) and thickness of reservoir (h). The higher the value of these variables the higher is the production from the reservoir.
4. The viscosity of oil plays an important role in production of oil from the reservoirs. The fact that more oil can be recovered from light oil reservoirs compared to heavy oil reservoirs under similar operating conditions can be seen here.
5. It can be concluded that ANN predicts better when the input of testing sample is at middle or at higher end of input range. For inputs at lower end

the prediction is not very good. This is particularly true for some of the more important variables such as S_{oi}, T_i, and h. This can be seen inferred from figures **5-1**, **5-5**, **5-9**, **5-13** and **5-17**.

6. It can be observed that for oils 1 and 2 the production per each cycle is around 10^4-10^5 barrels and the production per each cycle for oils 4 and 5 is of the order of 10^5-10^6 barrels. 10% error of 10^4 barrels is only 1000 barrels while 10% error of 10^6 barrels is around 10^5 barrels. Hence it can be concluded that though the error percentage is higher for high viscosity oils the absolute difference between ANN prediction and result of commercial simulator is low.
7. A comparison of time taken to run the simulation between GUI and the commercial simulator showed that GUI predicts the output faster than the simulator. However, it should be noted that the GUI makes this prediction only for the specific problem stated in this work.
8. Error filter was implemented to improve the result of original artificial neural networks. However, for this problem it was found that the use of error filter did not yield expected results.

6.2 Recommendations

This work can be extended further by removing some of the assumptions made. In this work the number of cycles was fixed to four. Also the injection, soaking and production periods were kept constant. Hence the future work for this project would be to develop an expert system for variable injection, soaking and production periods and also variable number of cycles.

Also in this work a vertical well was used. A lot of current research on cyclic steam injection is being done using horizontal and multilateral wells. Hence this work can be extended by developing an expert system for cyclic steam injection processes using horizontal wells.

Chapter 7

References

- Artun, E., Ertekin, T. and Watson, R. 2008. Optimized Design of Cyclic Pressure Pulsing in a Depleted, Naturally Fractured Reservoir. Paper SPE 117762-MS presented at SPE Eastern Regional/AAPG Eastern Section Joint Meeting, Pittsburgh, Pennsylvania, USA, 11-15 October.
- Ayala, Luis F., Ertekin, T. and Adewumi, M. 2007. Study of Gas/Condensate Reservoir Exploitation Using Neurosimulation. *SPE Res Eval &Eng* **10** (2): 140-149.
- Aziz, K., Ramesh, A.B. and Woo, P.T. 1987. Fourth SPE Comparative Solution Project: Comparison of Steam Injection Simulators. *J. Pet Tech* (December 1987): 1576-1584. SPE-13510.
- Babadagli, T. 2002. Evaluation of EOR methods for heavy-oil recovery in naturally fractured reservoirs. *Journal of Petroleum Science and Engineering* **37** (2003): 25-37.
- Bansal, Y. 2009. Conducting In-Situ Combustion Tube Experiments using Artificial Neural Networks, M.S. Thesis, The Pennsylvania State University, State College, Pennsylvania.
- Boberg, Thomas C. 1988. *Thermal Methods of Oil Recovery.* An Exxon Monograph. USA: John Wiley & Sons, 1, 13.

- Bose, N.K., Liang, P. 1996. *Neural Network Fundamentals with Graphs, Algorithms and Applications.* USA: McGraw-Hill, Inc.
- Briggs, P.J. 1989. A Simulator for the Recovery of Heavy Oil from Naturally Fractured Reservoirs Using Cyclic Steam Injection. Paper SPE 17954 presented at the SPE Middle East Oil Technical Conference and Exhibition, Manama, Bahrain, 11-14 March.
- Browne, A. 1997. *Neural Network Analysis, Architectures and Applications*. Bristol, UK: J W Arrowsmith.
- Chen, W.H., Wasserman, M.L. and Fitzmorris, R.E.1987. A Thermal Simulator for Naturally Fractured Reservoirs. Paper SPE 16008 presented at the Ninth SPE Symposium on Reservoir Simulation, San Antonio, Texas, 1-4 February.
- Doraisamy, H., Ertekin, T. and Grader, A.S. 1998. Key Parameters Controlling the Performance of Neuro-Simulation Applications in Field Development. Paper SPE 51079-MS presented at SPE Eastern Regional Meeting, Pittsburgh, Pennsylvania, 9-11 November.
- Ertekin, T., Abou-Kassem, J.H. and King, G.R. 2001. *Basic Applied Reservoir Simulation.* Richardson, Texas, USA: SPE.
- Fausett, Laurene V. 1994. *Fundamentals of Neural Networks.* Upper Saddle River, New Jersey: Prentice Hall.
- Gilman, J.R., Kazemi, H. 1983. Improvements in Simulation of Naturally Fractured Reservoirs. *SPE J* (August 1983): 695-707. SPE-10511.

- Guler, B., Ertekin, T. and Grader, A.S. 2003. An Artificial Neural Network Based Relative Permeability Predictor. *Journal of Canadian Petroleum Technology* **42** (4): 49-57.
- Kulga, I.B. 2010. Development of an Artificial Neural Network for Hydraulically Fractured Horizontal Wells in Tight Gas Sands, M.S. Thesis, The Pennsylvania State University, State College, Pennsylvania.
- Lake, Larry W. 1989. *Enhanced Oil Recovery*. Englewood Cliffs, New Jersey: Prentice Hall, 1, 451-452.
- Li, M., Astete, E. and Wang, H. 2010. A Simulation Study of a Cyclic Steam Stimulation Pilot in a Deep Carbonate Heavy Oil Reservoir in Oudeh Field, Syria. Paper CSUG/SPE 137603 presented at the Canadian Unconventional Resources & International Petroleum Conference, Calgary, Alberta, Canada, 19-21 October.
- Michael, P. 1982. *Thermal Recovery*. New York, Dallas, USA: SPE of AIME.
- Priddy, Kevin L. and Keller, Paul E. 2005. *Artificial Neural Networks: An Introduction*. Bellingham, Washington USA: SPIE Press.
- Reis, J.C. 1992. An Analysis of Oil Expulsion Mechanisms from Matrix Blocks during Steam Injection in Naturally Fractured Reservoirs. *IN SITU* **16** (1): 43-73.
- Shahin, G.T. Jr. 2006. The Physics of Steam Injection in Fractured Carbonate Reservoirs: Engineering Development Options That Minimize

Risk. Paper SPE 102186 presented at the 2006 Annual Technical Conference and Exhibition, San Antonio, Texas, 24-27 September.

- STARS Advanced Process and Thermal Reservoir Simulator, Version 2008 User Guide. 2008. Calgary, Alberta: CMG.
- Srinivasan, K. and Ertekin, T. 2008. Development and Testing of an Expert System for Coalbed Methane Reservoirs Using Artificial Neural Networks. Paper SPE 119935-MS presented at SPE Eastern Regional/AAPG Eastern Section Joint Meeting, Pittsburgh, Pennsylvania, USA, 11-15 October.

Appendix A

Graphical User Interface (GUI)

The five artificial neural networks developed in this work were integrated into a single window by developing a GUI. As the range of inputs for all the expert systems is same the process of integrating them became relatively simpler. Various snapshots of the GUI are presented in this section.

Figure **A-1** is a snapshot of the GUI when it is opened

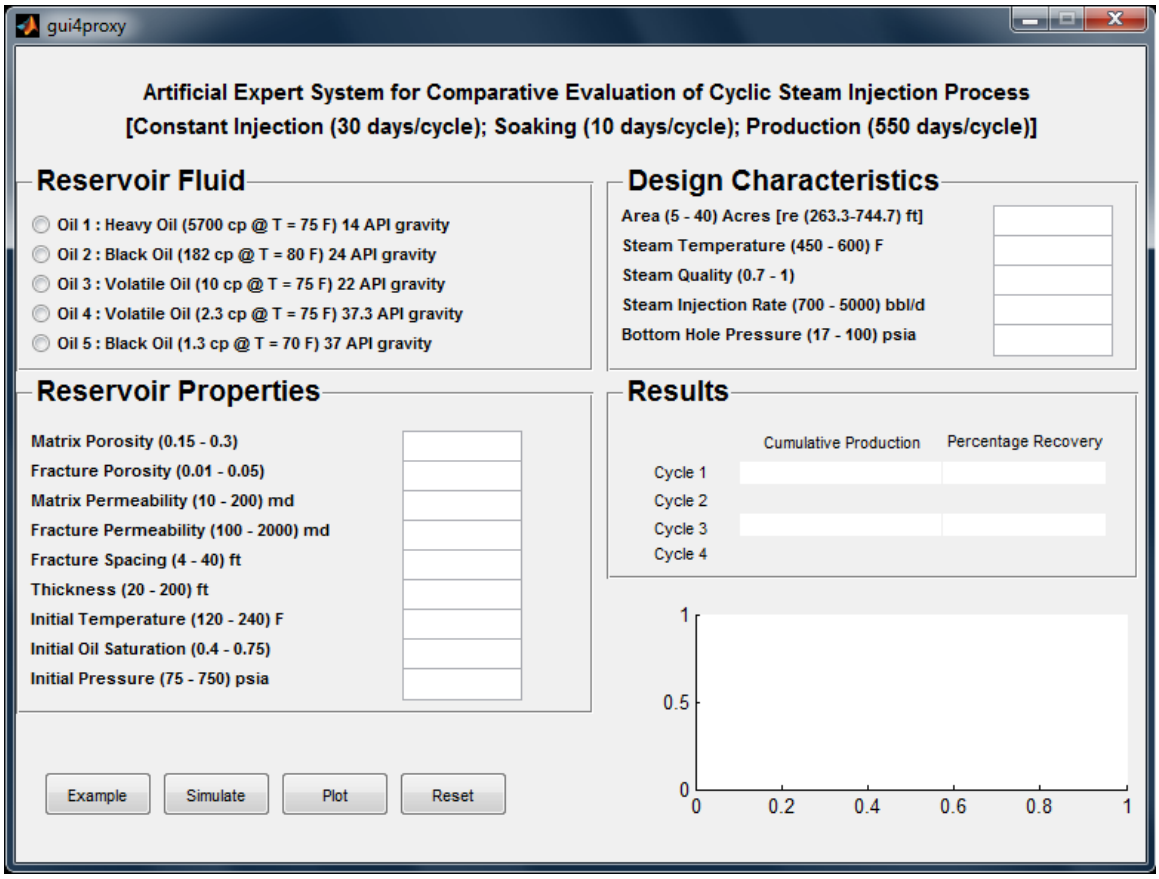

Figure **A-1**: Snapshot of GUI when it is opened.

As shown in Figure **A-1** the user has an option to choose from five different oils. When the user selects a radio button the corresponding oil is selected. Figure **A-2** shows a snapshot of GUI after a radio button is selected.

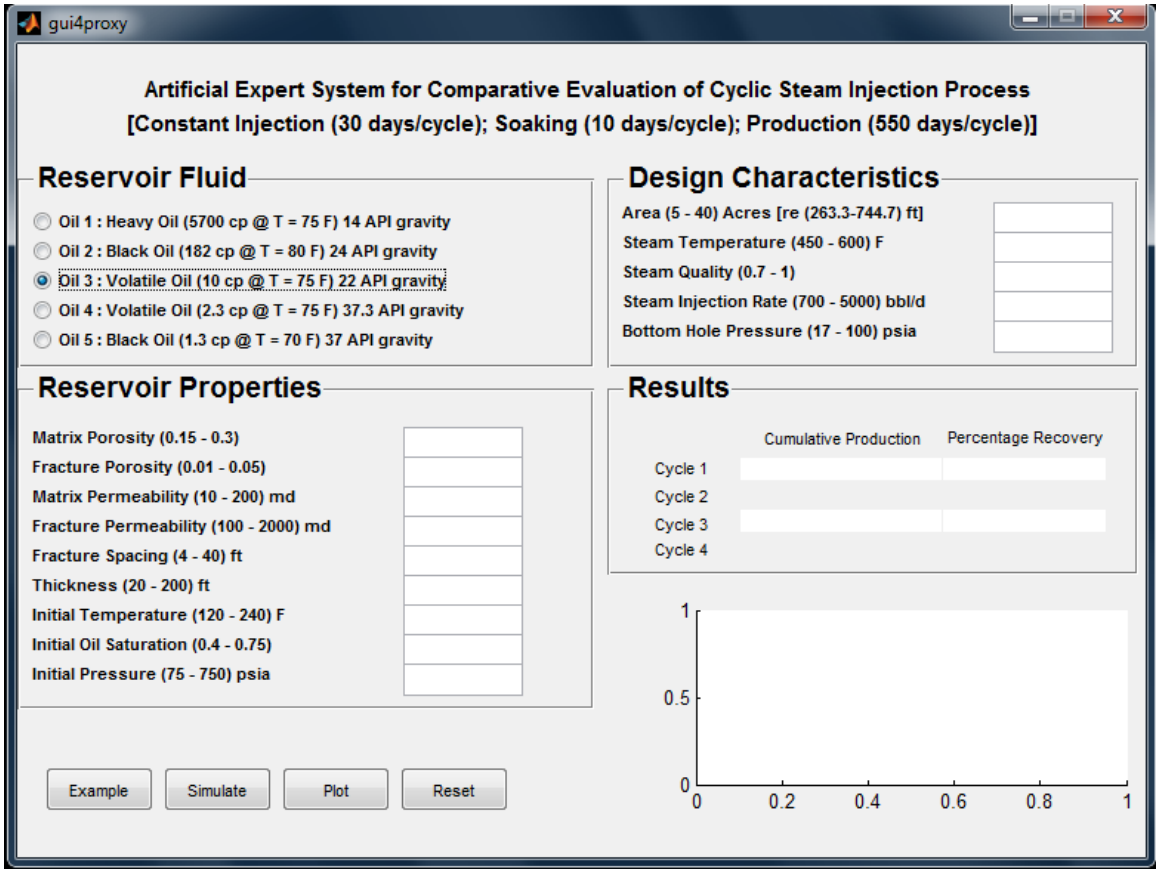

Figure **A-2**: Snapshot of GUI after reservoir fluid is selected.

One can observe that there are four options at the bottom of GUI. The example button loads a valid input sample. A valid input sample is one in which all the reservoir properties and design characteristics are within the range specified in the figure. Figure **A-3** is a snapshot of GUI after Example button is selected.

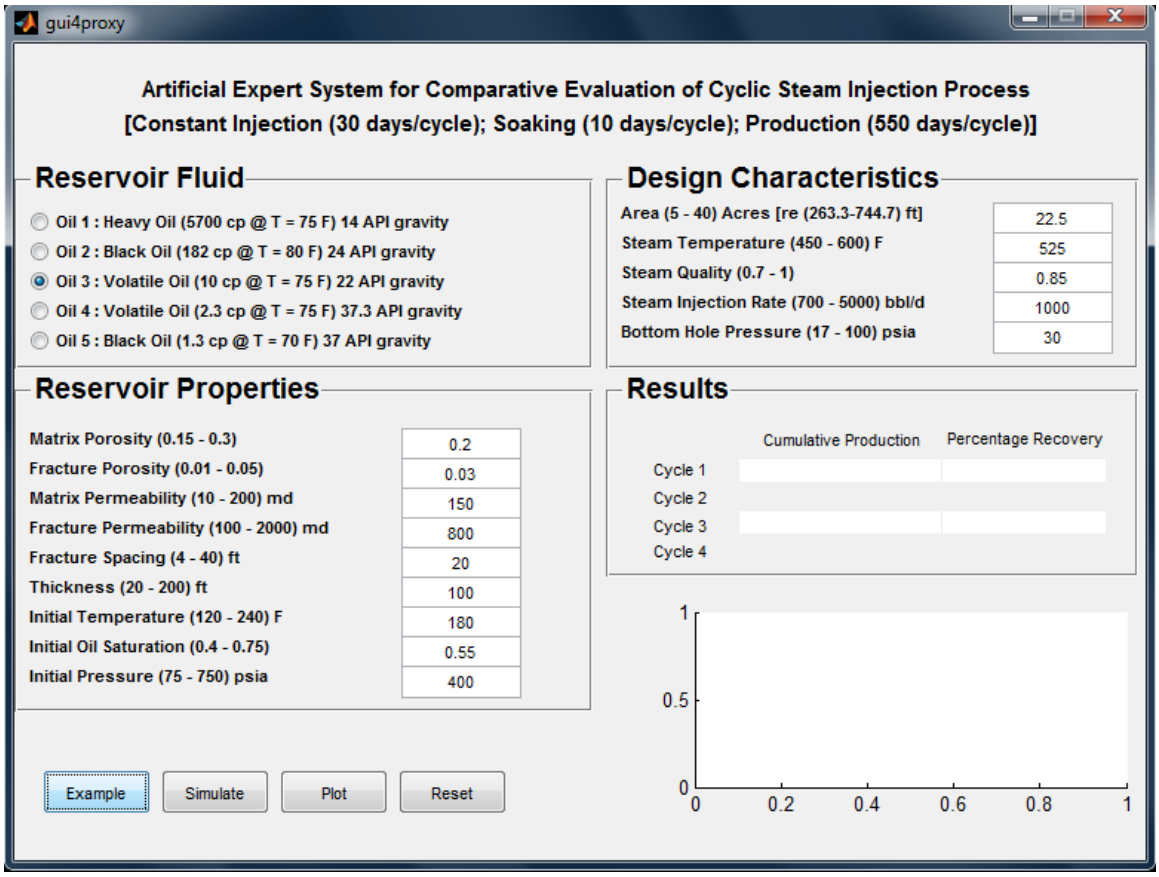

Figure **A-3**: Snapshot of GUI after Example button is selected.

After selecting the Example button, the user has option to change reservoir properties or design characteristics to any other value within the range. In fact the user need not click on Example button and can directly enter a valid input sample. If the user does not enter a property say fracture spacing within the range an error message pops up. Figure **A-4** is a snapshot of the error message window.

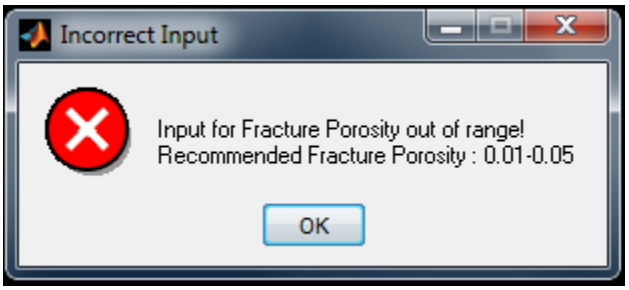

Figure **A-4**: Snapshot of error message when input is out of range.

If the user enters an extreme value of an input say thickness, a warning message pops out. The valid input range for thickness is 20-200 ft. If 20 ft is entered a warning message as shown in Figure **A-5** appears. If other the extreme 200 ft is entered a warning message as shown in Figure **A-6** appears.

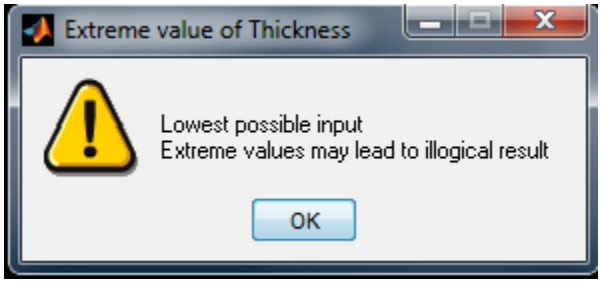

Figure **A-5:** Snapshot of warning message when lowest possible input is chosen.

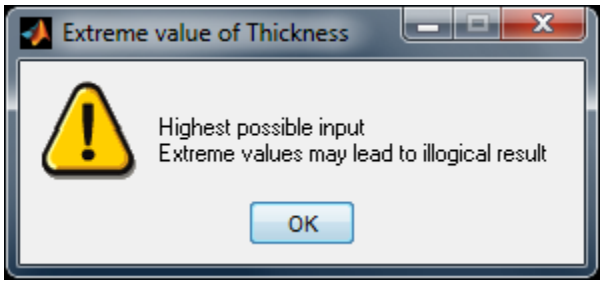

Figure **A-6**: Snapshot of warning message when highest possible input is chosen.

After entering a valid input the user can click on Simulate button. By clicking Simulate button the neural network corresponding to the oil selected is activated and it predicts the output (cumulative production from each cycle). It also predicts the percentage recovery of original oil in place. Figure **A-7** is a snapshot of GUI after Simulate button is selected.

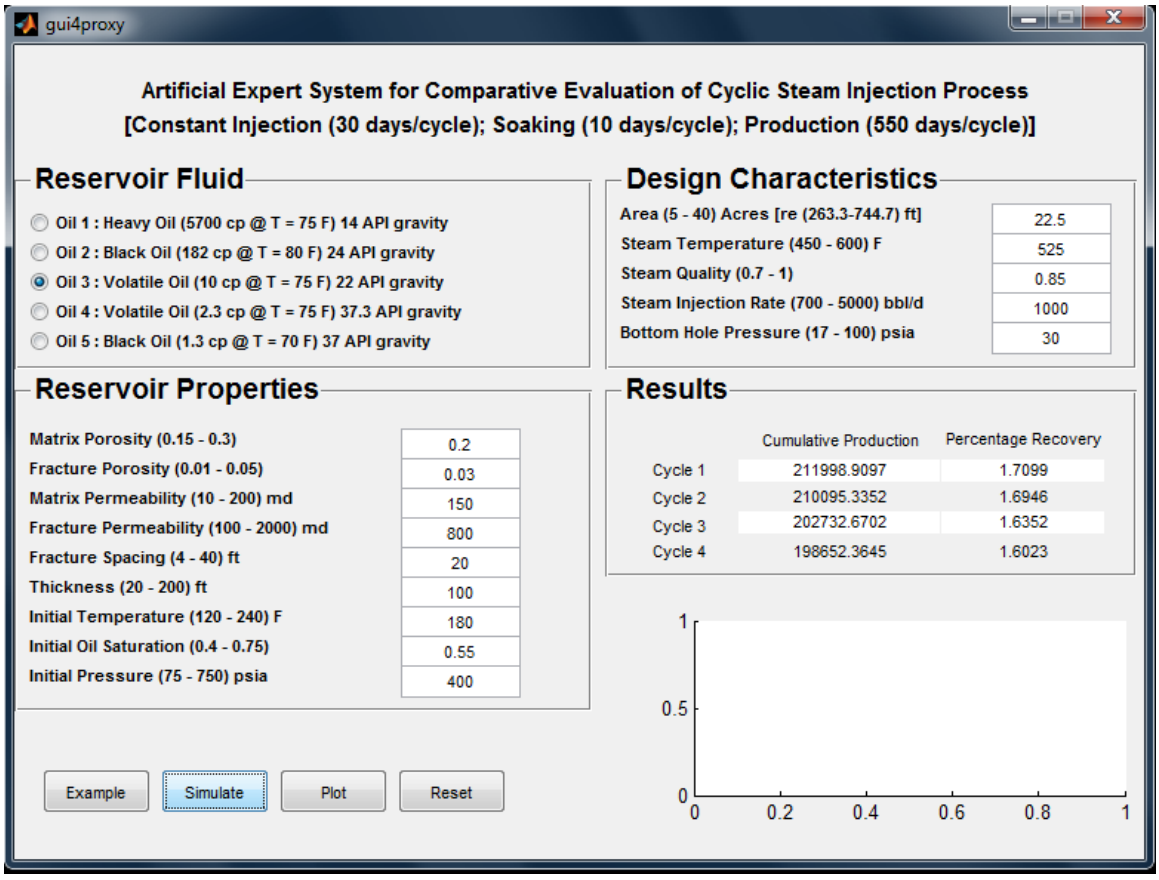

Figure **A-7**: Snapshot of GUI after Simulate button is selected.

The user can plot the cumulative production of each cycle. This can be done by clicking on plot button. After the plot button is selected a bar plot of cumulative production of each cycle is displayed on the GUI. Figure **A-8** is a snapshot of GUI after plot button is selected.

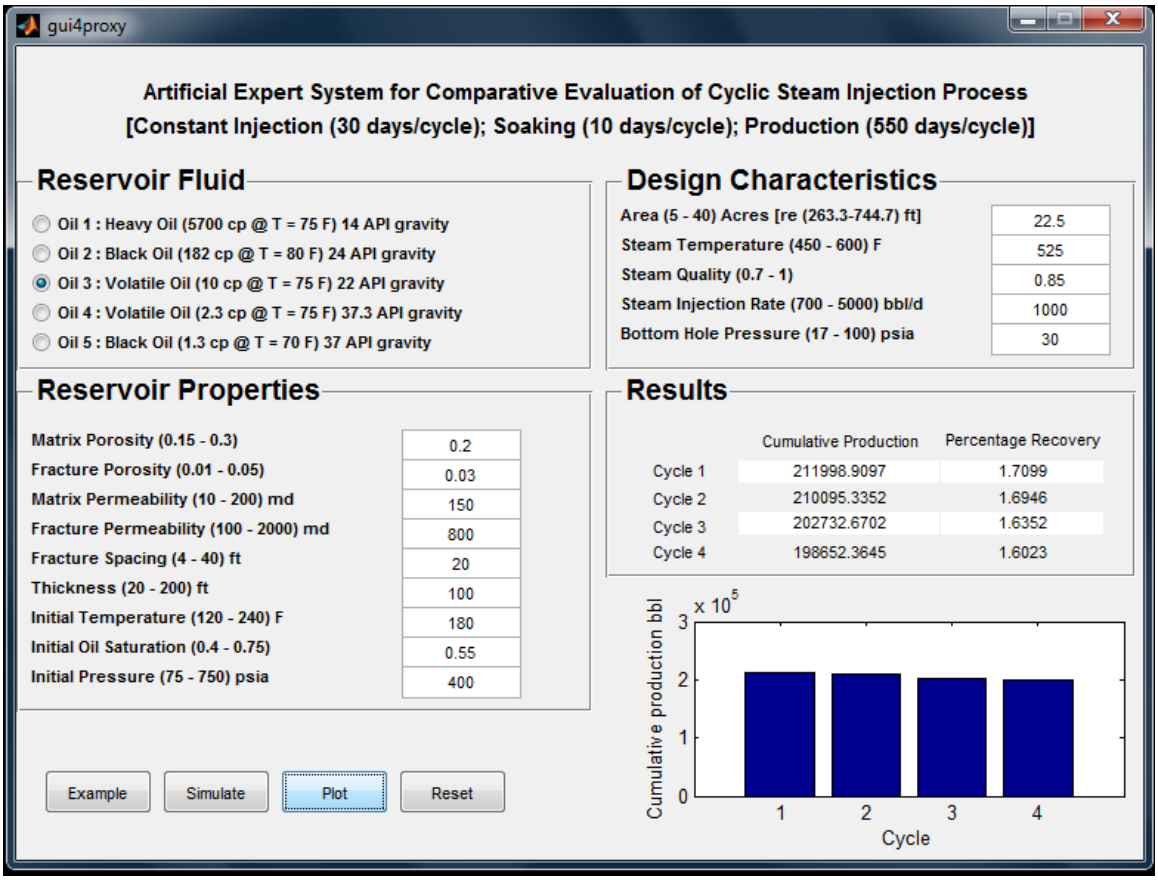

Figure **A-8**: Snapshot of GUI after Plot button is selected.

Finally the user can reset everything by selecting the Reset button. The GUI looks like Figure **A-1** after reset button is selected. All the results and the plot are refreshed.

Appendix B

MATLAB CODE FOR TRAINING ANN

```
clear all
close all
clc
format long

%% load input and output files
load INPUTimp.txt
load prodcycleimp.txt

%% Eigen values
for i=1:length(INPUTimp(1,:));
   A1 = [INPUTimp(5,i) INPUTimp(6,i); INPUTimp(3,i) INPUTimp(4,i)];
   A2 = [INPUTimp(1,i) INPUTimp(10,i); INPUTimp(11,i) INPUTimp(14,i)];
   A3 = [INPUTimp(7,i) INPUTimp(8,i); INPUTimp(12,i) INPUTimp(13,i)];
   A4 = [INPUTimp(11,i) INPUTimp(10,i); INPUTimp(14,i) INPUTimp(9,i)];
   A5 = [INPUTimp(2,i) INPUTimp(4,i); INPUTimp(6,i) INPUTimp(9,i)];

   INPUTimp(m+1,i) = max(eig(A1));
   INPUTimp(m+2,i) = max(eig(A2));
   INPUTimp(m+3,i) = max(eig(A3));
   INPUTimp(m+4,i) = max(eig(A4));
   INPUTimp(m+5,i) = max(eig(A5));

end

%%
P = INPUTimp;
T = prodcycleimp;

[P2,ps2] = removeconstantrows(P);

%normalising the data
[Pn,ps] = mapminmax(P2,-1,1);   % gives all values between -1 & 1
[Tn,ts] = mapminmax(T,-1,1);   % gives all values between -1 & 1

[mi,ni] = size(Pn);
[mo,no] = size(Tn);
```

```
[Pn_train,Pn_val,Pn_test,trainInd,valInd,testInd] = dividerand(Pn,0.80,0.1,0.1);
%Assigns the number of neurons for training, validation&          testing
[Tn_train,Tn_val,Tn_test] = divideind(Tn,trainInd,valInd,testInd);


val.T = Tn_val;
val.P = Pn_val;
test.T = Tn_test;
test.P = Pn_test;

%Initiating network parameters
NNeu0 = 61;
NNeu1 = 47;
NNeu2 = 23;
NNeu3 = 11;
NNeu4 = 9;
net =
newff(Pn,Tn,[NNeu0,NNeu1,NNeu2,NNeu3,NNeu4],{'tansig','tansig','tansig','tansig','pur
elin'},'trainscg','learngdm','msereg');


%setting training parameters for the network

net.trainParam.goal = 0.00005; %accuracy within this range
net.trainParam.epochs = 10000; % number of iteration sets
net.trainParam.show = 1;
net.trainParam.max_fail = 1000;
net.trainParam.mem_reduc = 50; %to reduce memory requirements

%starting training the network
[net,tr] = train(net,Pn_train,Tn_train,[],[],test,val);
plotperf(tr)

%%
%getting data from the trained network
Tn_train_ann = sim(net,Pn_train);
Tn_test_ann = sim(net,Pn_test);
Tn_val_ann = sim(net,Pn_val);


[m_Te,n_Te] = size(Tn_test);
NP_test = 1:n_Te;
%denormalising the data sets obtained
%output reversal
T_train = mapminmax('reverse',Tn_train,ts);
```

```
T_test = mapminmax('reverse',Tn_test,ts);
T_train_ann = mapminmax('reverse',Tn_train_ann,ts);
T_test_ann = mapminmax('reverse',Tn_test_ann,ts);

T_val = mapminmax('reverse',Tn_val,ts);
T_val_ann = mapminmax('reverse',Tn_val_ann,ts);

%input reversal
P_train = mapminmax('reverse',Pn_train,ps);
P_val = mapminmax('reverse',Pn_val,ps);
P_test = mapminmax('reverse',Pn_test,ps);

%% error estimation
% A = abs(T_test-T_test_ann);
A = (T_test-T_test_ann);
B= A./T_test;
error_test = B.*100;
mean(mean(abs(error_test)))
for i=1:size(error_test,1)
   ER(i) = mean(abs(error_test(i,:)));
end

A2 = (T_train-T_train_ann);
B2= A2./T_train;
error_train = B2.*100;
mean(mean(abs(error_train)))
```

Appendix C

MATLAB CODE FOR GENERATING BATCH FILE

```
function runmaker()

clc
clear all
range(1,1) = 5; range(1,2) = 40;              % area (acres)
range(2,1) = 4; range(2,2) = 40;              % fracture spacing (ft)
range(3,1) = 0.15; range(3,2) = 0.30;          % matrix porosity
range(4,1) = 0.01; range(4,2) = 0.05;          % fracture porosity
range(5,1) = 10; range(5,2) = 200;             % matrix permeability (md)
range(6,1) = 100; range(6,2) = 2000;           % fracture permeability (md)
range(7,1) = 450; range(7,2) = 600;            % steam temperature (F)
range(8,1) = 0.7; range(8,2) = 1;              % steam quality
range(9,1) = 20; range(9,2) = 200;             % thickness (ft)
range(10,1) = 120; range(10,2) = 240;          % Initial temperature of reservoir (F)
range(11,1) = 0.4; range(11,2) = 0.75;         % Initial oil saturation
range(12,1) = 700; range(12,2) = 5000;         % Steam Injection Rate (BPD of CWE)
range(13,1) = 17; range(13,2) = 100;           % Bottom Hole Pressure (psia)
range(14,1) = 75; range(14,2) = 750;           % Initial Pressure of formation (psia)
INPUT(1,:) = range(1,1) + (range(1,2)-range(1,1)).*rand(300,1);
INPUT(2,:) = range(2,1) + (range(2,2)-range(2,1)).*rand(300,1);
INPUT(3,:) = range(3,1) + (range(3,2)-range(3,1)).*rand(300,1);
INPUT(4,:) = range(4,1) + (range(4,2)-range(4,1)).*rand(300,1);
INPUT(5,:) = range(5,1) + (range(5,2)-range(5,1)).*rand(300,1);
INPUT(6,:) = range(6,1) + (range(6,2)-range(6,1)).*rand(300,1);
INPUT(7,:) = range(7,1) + (range(7,2)-range(7,1)).*rand(300,1);
INPUT(8,:) = range(8,1) + (range(8,2)-range(8,1)).*rand(300,1);
INPUT(9,:) = range(9,1) + (range(9,2)-range(9,1)).*rand(300,1);
INPUT(10,:) = range(10,1) + (range(10,2)-range(10,1)).*rand(300,1);
INPUT(11,:) = range(11,1) + (range(11,2)-range(11,1)).*rand(300,1);
INPUT(12,:) = range(12,1) + (range(12,2)-range(12,1)).*rand(300,1);
INPUT(13,:) = range(13,1) + (range(13,2)-range(13,1)).*rand(300,1);
INPUT(14,:) = range(14,1) + (range(14,2)-range(14,1)).*rand(300,1);

forCMG='CMGbatch_file.bat';

fidbat=fopen(forCMG,'wt');



for i=1:size(INPUT,2)
```

```
   temp = ['run' num2str(i) '.dat'];
   fid = fopen(temp,'w');
   nb=91;                        % number of radial blocks
   rw=0.3;                       % radius of well
   height=INPUT(9,i)/4;              % height of block
   area=INPUT(1,i);
   re=sqrt(area*43560/pi);
   wi= 2*pi*INPUT(5,i)*height/(log(0.5*3/0.3));
   fprintf(fid,'**  ==============  INPUT/OUTPUT CONTROL
======================\n\n');

fprintf(fid,'RESULTS SIMULATOR STARS\n\n');
fprintf(fid,'*INTERRUPT *STOP\n\n');
fprintf(fid,'*INUNIT *FIELD \n');
fprintf(fid,'*OUTPRN *GRID *PRES *SW *SO *SG *TEMP *Y *X *W *SOLCONC
*OBHLOSS *VISO *VISG\n');
fprintf(fid,'*OUTPRN *WELL *ALL\n');
fprintf(fid,'*WRST 200\n');
fprintf(fid,'*WPRN *GRID 200\n');
fprintf(fid,'*WPRN *ITER 200\n');
fprintf(fid,'OUTSRF SPECIAL BLOCKVAR CCHLOSS 1,1,4\n');
fprintf(fid,'             MATBAL  WELL %s\n','"OIL"');
fprintf(fid,'             MATBAL  WELL %s\n','"Water"');
fprintf(fid,'OUTSRF GRID PRES SG SO TEMP\n\n');
fprintf(fid,'**  ==============  GRID AND RESERVOIR DEFINITION
=================\n\n');
fprintf(fid,'GRID RADIAL 91 1 4 *RW 0.3     \n\n');
fprintf(fid,'KDIR UP\n');
fprintf(fid,'DI IVAR');

for j=1:nb
   alpha=(re/rw)^(1/nb);
   if j==1
   ri(j)=rw*(log(alpha))/(1-1/alpha);
   else
   ri(j)=ri(j-1)*alpha;
   end
   fprintf(fid,' %f',ri(j));
   if rem(j,13)==0
   fprintf(fid,'\n');
   end
end
fprintf(fid,'\nDJ CON 360  **  Full circle\n');
```

```
fprintf(fid,'DK KVAR %f %f %f
%f\n',INPUT(9,i)/4,INPUT(9,i)/4,INPUT(9,i)/4,INPUT(9,i)/4);
fprintf(fid,'NULL MATRIX CON           1\n');
fprintf(fid,'NULL FRACTURE CON         1\n\n');
fprintf(fid,'DUALPOR\n\n');
fprintf(fid,'DIFRAC CON %f\n',INPUT(2,i));
fprintf(fid,'DJFRAC CON %f\n',INPUT(2,i));
fprintf(fid,'DKFRAC CON %f\n',INPUT(2,i));
fprintf(fid,'\nPOR MATRIX CON %f\n',INPUT(3,i));
fprintf(fid,'\nPOR FRACTURE CON %f\n',INPUT(4,i));
fprintf(fid,'\nPERMI MATRIX CON %f\n',INPUT(5,i));
fprintf(fid,'PERMJ MATRIX CON %f\n',INPUT(5,i));
fprintf(fid,'PERMK MATRIX CON %f\n',INPUT(5,i));
fprintf(fid,'\nPERMI FRACTURE CON %f\n',INPUT(6,i));
fprintf(fid,'PERMJ FRACTURE CON %f\n',INPUT(6,i));
fprintf(fid,'PERMK FRACTURE CON %f\n',INPUT(6,i));
fprintf(fid,'\nPINCHOUTARRAY CON  1\n');
fprintf(fid,'\nEND-GRID\n');
fprintf(fid,'\nROCKTYPE 1\n');
fprintf(fid,'\n*CPOR 5e-5\n');
fprintf(fid,'*PRPOR 75\n');
fprintf(fid,'*ROCKCP 35\n');
fprintf(fid,'*THCONR 24\n');
fprintf(fid,'*THCONW 24\n');
fprintf(fid,'*THCONO 24\n');
fprintf(fid,'*THCONG 24\n');
fprintf(fid,'*HLOSSPROP  *OVERBUR 35 24  *UNDERBUR 35 24\n');
fprintf(fid,'\n\n**  ==============  FLUID DEFINITIONS
======================\n\n');
fprintf(fid,'*MODEL 2 2 2   ** Components are water and dead oil.  Most water\n');
fprintf(fid,'               ** properties are defaulted (=0).  Dead oil K values\n');
fprintf(fid,'               ** are zero, and no gas properties are needed.\n');
fprintf(fid,'*COMPNAME      %s    %s\n','"Water"','"OIL"');
fprintf(fid,'**             -----    -------\n');
fprintf(fid,'    *CMM        18.02      600\n');
fprintf(fid,'    *PCRIT      3206.2     0        ** These four properties\n');
fprintf(fid,'    *TCRIT      705.4      0        ** are for the gas phase.\n');
fprintf(fid,'    *AVG        1.13e-5    0        ** The dead oil component does\n');
fprintf(fid,'    *BVG        1.075      0        ** not appear in the gas phase.\n');
fprintf(fid,'\n     *MOLDEN     0       0.10113\n');
fprintf(fid,'    *CP         0       5.e-6\n');
fprintf(fid,'    *CT1        0       3.8e-4\n');
fprintf(fid,'    *CPL1       0       300\n');
fprintf(fid,'\n*VISCTABLE\n');
fprintf(fid,'**      Temp\n');
```

```
fprintf(fid,'         75     0        5780\n');
fprintf(fid,'        100     0        1380\n');
fprintf(fid,'        150     0         187\n');
fprintf(fid,'        200     0          47\n');
fprintf(fid,'        250     0         17.4\n');
fprintf(fid,'        300     0          8.5\n');
fprintf(fid,'        350     0          5.2\n');
fprintf(fid,'        500     0          2.5\n');
fprintf(fid,'        700     0          2.5\n');
fprintf(fid,'\n*PRSR 14.7\n');
fprintf(fid,'*TEMR 60\n');
fprintf(fid,'*PSURF 14.7\n');
fprintf(fid,'*TSURF 60\n');
fprintf(fid,'\n**  ==============  ROCK-FLUID PROPERTIES
======================\n');
fprintf(fid,'\n*ROCKFLUID\n');
fprintf(fid,'RPT 1\n');
fprintf(fid,'\n*SWT   **  Water-oil relative permeabilities\n');
fprintf(fid,'\n**   Sw        Krw        Krow\n');
fprintf(fid,'**  ----     --------    -------\n');
fprintf(fid,'    0.25     0.0        0.4\n');
fprintf(fid,'    0.30     0.0002     0.3361\n');
fprintf(fid,'    0.35     0.001134   0.2777\n');
fprintf(fid,'    0.40     0.003125   0.225\n');
fprintf(fid,'    0.45     0.00641    0.17777\n');
fprintf(fid,'    0.50     0.01112    0.1361\n');
fprintf(fid,'    0.55     0.01768    0.1\n');
fprintf(fid,'    0.60     0.02598    0.0694\n');
fprintf(fid,'    0.65     0.03628    0.0444\n');
fprintf(fid,'    0.70     0.04871    0.025\n');
fprintf(fid,'    0.75     0.06339    0.01111\n');
fprintf(fid,'    0.80     0.08045    0.00277\n');
fprintf(fid,'    0.85     0.1        0.0\n');
fprintf(fid,'\n*SLT   **  Liquid-gas relative permeabilities\n');
fprintf(fid,'\n**   Sl        Krg        Krog\n');
fprintf(fid,'**  ----     -------    -------\n');
fprintf(fid,'    0.25     0.2        0.0\n');
fprintf(fid,'    0.35     0.15813    0.0\n');
fprintf(fid,'    0.37     0.15016    0.000379\n');
fprintf(fid,'    0.40     0.13846    0.002367\n');
fprintf(fid,'    0.42     0.13084    0.004639\n');
fprintf(fid,'    0.45     0.11968    0.009467\n');
fprintf(fid,'    0.47     0.11243    0.013633\n');
fprintf(fid,'    0.50     0.10184    0.021302\n');
fprintf(fid,'    0.52     0.09498    0.027361\n');
```

```
fprintf(fid,'   0.55    0.08498    0.037870\n');
fprintf(fid,'   0.57    0.07853    0.045822\n');
fprintf(fid,'   0.60    0.06917    0.05917\n');
fprintf(fid,'   0.62    0.06316    0.06901\n');
fprintf(fid,'   0.65    0.05449    0.08520\n');
fprintf(fid,'   0.67    0.04895    0.09694\n');
fprintf(fid,'   0.70    0.04102    0.11597\n');
fprintf(fid,'   0.72    0.03600    0.12961\n');
fprintf(fid,'   0.75    0.02889    0.15147\n');
fprintf(fid,'   0.77    0.02445    0.16700\n');
fprintf(fid,'   0.80    0.01827    0.19171\n');
fprintf(fid,'   0.82    0.01450    0.20913\n');
fprintf(fid,'   0.85    0.00942    0.23668\n');
fprintf(fid,'   0.87    0.00646    0.25600\n');
fprintf(fid,'   0.90    0.00279    0.28639\n');
fprintf(fid,'   0.94    0.0        0.32956\n');
fprintf(fid,'   1.00    0.0        0.4\n');
fprintf(fid,'\n**  ==============  INITIAL CONDITIONS
======================\n');
fprintf(fid,'\n*INITIAL\n');
fprintf(fid,'\n** Automatic static vertical equilibrium\n');
fprintf(fid,'VERTICAL DEPTH_AVE\n');
fprintf(fid,'REFPRES %f\n',INPUT(14,i));
fprintf(fid,'REFBLOCK 1 1 4\n');
fprintf(fid,'TEMP MATRIX CON         %f\n',INPUT(10,i));
fprintf(fid,'TEMP FRACTURE CON       %f\n',INPUT(10,i));
fprintf(fid,'SW MATRIX CON        %f\n',1-INPUT(11,i));
fprintf(fid,'SW FRACTURE CON        %f\n',1-INPUT(11,i));
fprintf(fid,'\n\n**  ==============  NUMERICAL CONTROL
======================\n');
fprintf(fid,'\n*NUMERICAL   ** All these can be defaulted.  The definitions\n');
fprintf(fid,'              ** here match the previous data.\n');
fprintf(fid,'\n*SDEGREE GAUSS\n');
fprintf(fid,'*DTMAX 90\n');
fprintf(fid,'\n*NORM     *PRESS 200  *SATUR 0.2   *TEMP 180  *Y 0.2   *X 0.2\n');
fprintf(fid,'\n*RUN\n\n');
fprintf(fid,'**  ==============  RECURRENT DATA
======================\n\n');
fprintf(fid,'**    The injection and production phases of the single cycling well\n');
fprintf(fid,'**  will be treated as two distinct wells which are in the same\n');
fprintf(fid,'**  location but are never active at the same time.  In the well data\n');
fprintf(fid,'**  below, both wells are defined immediately, but the producer is\n');
fprintf(fid,'**  shut in, to be activated for the drawdown.\n');
fprintf(fid,'\n\n*DATE 2011 2 1\n');
fprintf(fid,'\n   *DTWELL .02\n');
```

```
fprintf(fid,'**    *WELL 1 %s *VERT 1 1\n','"Injector 1"');
fprintf(fid,'WELL  %s\n','"Injector 1"');
fprintf(fid,'   *INJECTOR *MOBWEIGHT %s\n','"Injector 1"');
fprintf(fid,'   *INCOMP WATER  1.0  0.0\n');
fprintf(fid,'   *TINJW %f\n',INPUT(7,i));
fprintf(fid,'   QUAL %f\n',INPUT(8,i));
fprintf(fid,'   *OPERATE     *BHP   1550    \n');
fprintf(fid,'   *OPERATE *MAX *STW   %f      \n',INPUT(12,i));
fprintf(fid,'PERF  WI  %s\n','"Injector 1"');
fprintf(fid,'**$ UBA    wi      Status  Connection\n');
fprintf(fid,'    1 1 4  %f  OPEN    FLOW-FROM  %s  REFLAYER\n',wi,'"SURFACE"');
fprintf(fid,'    1 1 3  %f  OPEN    FLOW-FROM  1\n',wi);
fprintf(fid,'    1 1 2  %f  OPEN    FLOW-FROM  1\n',wi);
fprintf(fid,'    1 1 1  %f  OPEN    FLOW-FROM  1\n',wi);
fprintf(fid,'\n**    *WELL 2 %s *VERT 1 1\n','"Producer 1"');
fprintf(fid,'WELL  %s\n','"Producer 1"');
fprintf(fid,'   *PRODUCER %s\n','"Producer 1"');
fprintf(fid,'   *OPERATE     *STL    1000    \n');
fprintf(fid,'   *OPERATE *MIN *BHP    %f      \n',INPUT(13,i));
fprintf(fid,'\n**$         rad  geofac  wfrac  skin\n');
fprintf(fid,'GEOMETRY  K  0.3  0.5  1.  0\n');
fprintf(fid,'PERF  GEO  %s\n','"Producer 1"');
fprintf(fid,'**$ UBA    ff  Status  Connection\n');
fprintf(fid,'    1 1 4  1.  OPEN    FLOW-TO  %s  REFLAYER\n','"SURFACE"');
fprintf(fid,'    1 1 3  1.  OPEN    FLOW-TO  1\n');
fprintf(fid,'    1 1 2  1.  OPEN    FLOW-TO  2\n');
fprintf(fid,'    1 1 1  1.  OPEN    FLOW-TO  3\n');
fprintf(fid,'   ** Cycle No. 1  -  Injection\n');
fprintf(fid,'\n   *SHUTIN %s   ** Shut in producer\n','"Producer 1"');
fprintf(fid,'OUTSRF GRID PRES SG TEMP\n');
fprintf(fid,'\n*TIME 30\n');
fprintf(fid,'\n   *DTWELL 7\n');
fprintf(fid,'   ** Cycle No. 1  -  Soak\n');
fprintf(fid,'\n   *SHUTIN %s   ** Shut in injector\n','"Injector 1"');
fprintf(fid,'OUTSRF GRID SG TEMP\n');
fprintf(fid,'\n*TIME 40\n');
fprintf(fid,'\n   *DTWELL 1\n');
fprintf(fid,'   ** Cycle No. 1  -  Production\n');
fprintf(fid,'   *OPEN %s   ** Turn on producer\n','"Producer 1"');
fprintf(fid,'OUTSRF GRID PRES\n');
fprintf(fid,'\n*TIME 550\n');
fprintf(fid,'\n   *DTWELL .01\n');
fprintf(fid,'\n   ** Cycle No. 2  -  Injection\n');
fprintf(fid,'   *SHUTIN %s   ** Shut in producer\n','"Producer 1"');
fprintf(fid,'   *OPEN %s     ** Turn on injector\n','"Injector 1"');
```

```
fprintf(fid,'OUTSRF GRID NONE\n');
fprintf(fid,'\n*TIME 580\n');
fprintf(fid,'\n   *DTWELL 7\n');
fprintf(fid,'\n   ** Cycle No. 2  -  Soak\n');
fprintf(fid,'   *SHUTIN %s   ** Shut in injector\n','"Injector 1"');
fprintf(fid,'\n*TIME 590\n');
fprintf(fid,'   *DTWELL .5\n');
fprintf(fid,'\n   ** Cycle No. 2  -  Production\n');
fprintf(fid,'  *OPEN %s    ** Turn on producer\n','"Producer 1"');
fprintf(fid,'\n*TIME 1140\n');
fprintf(fid,'\n   *DTWELL .002\n');
fprintf(fid,'\n   ** Cycle No. 3  -  Injection\n');
fprintf(fid,'\n   *SHUTIN %s    ** Shut in producer\n','"Producer 1"');
fprintf(fid,'   *OPEN %s      ** Turn on injector\n','"Injector 1"');
fprintf(fid,'OUTSRF GRID SG TEMP\n');
fprintf(fid,'\n*TIME 1170\n');
fprintf(fid,'\n   *DTWELL 7\n');
fprintf(fid,'   ** Cycle No. 3  -  Soak\n');
fprintf(fid,'\n   *SHUTIN %s   ** Shut in injector\n','"Injector 1"');
fprintf(fid,'OUTSRF GRID SG TEMP\n');
fprintf(fid,'\n*TIME 1180\n');
fprintf(fid,'\n   *DTWELL 1\n');
fprintf(fid,'   ** Cycle No. 3  -  Production\n');
fprintf(fid,'   *OPEN %s   ** Turn on producer\n','"Producer 1"');
fprintf(fid,'OUTSRF GRID SO\n');
fprintf(fid,'\n*TIME 1730\n');
fprintf(fid,'\n   *DTWELL .02\n');
fprintf(fid,'\n   ** Cycle No. 4  -  Injection\n');
fprintf(fid,'   *SHUTIN %s   ** Shut in producer\n','"Producer 1"');
fprintf(fid,'   *OPEN %s     ** Turn on injector\n','"Injector 1"');
fprintf(fid,'OUTSRF GRID SG TEMP\n');
fprintf(fid,'\n*TIME 1760\n');
fprintf(fid,'\n   *DTWELL 7\n');
fprintf(fid,'\n   ** Cycle No. 4  -  Soak\n');
fprintf(fid,'   *SHUTIN %s   ** Shut in injector\n','"Injector 1"');
fprintf(fid,'\n*TIME 1770\n');
fprintf(fid,'   *DTWELL 1\n');
fprintf(fid,'\n   ** Cycle No. 4  -  Production\n');
fprintf(fid,'  *OPEN %s    ** Turn on producer\n','"Producer 1"');
fprintf(fid,'OUTSRF GRID SO \n');
fprintf(fid,'\n*TIME 2320\n');
fprintf(fid,'STOP\n');

fclose(fid);
%      temp = ['check' num2str(i) '.dat'];
```

```
    fprintf(fidbat,'%s','call "C:\Program Files
(x86)\CMG\STARS\2009.11\Win_x64\EXE\st200911.exe" -f run');
    fprintf(fidbat,num2str(i));
    fprintf(fidbat,'%s\n','.dat');
end

fclose(fidbat);
```